CHARACTERIZATION OF HEPARAN SULFATE-PROTEIN INTERACTIONS FOR SYNTHETIC HEPARIN DESIGN

Elizabeth Pempe Chappell

A dissertation submitted to the faculty of the University of North Carolina at Chapel Hill in partial fulfillment of the requirements for the degree of Doctor of Philosophy in the Department of Pharmaceutical Sciences (Chemical Biology and Medicinal Chemistry).

Chapel Hill
2013

Approved by:

Jian Liu, Ph.D.

Gowthami Arepally, M.D.

Edward Harris, Ph.D.

Michael Jarstfer, Ph.D.

Andrew Lee, Ph.D.

ABSTRACT

ELIZABETH PEMPE CHAPPELL: Characterization of heparan sulfate-protein interactions for synthetic heparin design
(Under the direction of Jian Liu, Ph.D.)

Heparin is a widely prescribed anticoagulant that has been in clinical use for over 70 years. It is a natural product and a special form of heparan sulfate, a heterogeneous polysaccharide that is expressed as a proteoglycan on the surface of all animal tissues. In recent years, the development of a chemoenzymatic method to synthesize specific heparan sulfate polysaccharides and oligosaccharides has enabled studies of the structure-based interactions between negatively charged heparan sulfate and its protein binding partners.

A synthetic version of heparin and its low-molecular-weight derivatives could have several advantages over the drugs that are currently available. First, a synthetic drug would evade the historically contaminated porcine intestine supply chain from which heparin is currently derived. In addition, the structure of the drug could be tailored for improved safety and efficacy and to meet the needs of different patient populations. In this dissertation, we sought to characterize structure-function relationships of heparan sulfate with several goals: to reduce binding to platelet factor 4, an initiating step in heparin-induced thrombocytopenia; to identify the structure required for binding to Stabilin receptors, which clear heparins via the liver rather than the kidneys; and to create a heparan sulfate structure that has optimum bioavailability and activity against factors of the coagulation cascade. Through biochemical, cell-based and *in vivo* assays, we determined that PF4 binding was decreased by Sulf-2 treatment and by limiting the oligosaccharide length, that a 3-*O*-sulfated 10-mer is required for robust Stabilin binding, that a 19-mer will confer anti-IIa activity and that oligosaccharides as short as a 6-mer are bioavailable through subcutaneous injection.

ACKNOWLEDGEMENTS

Several people were involved in the completion of this work, and many others supported me throughout my years of research. I am grateful and fortunate to have these people in my life.

Thanks to Tom, my husband, who convinced me that I was capable of doing a Ph.D., who supported me throughout every step of graduate school and who gave me a full life and so much happiness outside of the university.

Thanks to my family (Treats, Pempes, Chappells, Evanses and Cederholms), who inspire me to be capable, interesting, grounded and loving through their example.

Thank you to my labmates in the Liu laboratory: Sherket, Courtney, Heather, Ryan, Justin, Yongmei, Zhou, Sheng, Kai, Lan, Renpeng, Joyce, Susan, T, Tim and Chunhui. I have learned from each of them and have enjoyed their company every day that I was in the lab. Special thanks to Joyce Chandarajoti and Danielle Cook for their scientific help, laughter and endless moral support.

Finally, a sincere thank you to my advisor, Jian, who has been an exceptional mentor. He has spent countless hours training me, tackling experimental problems with me and pushing my critical thinking. Any scientific success in my future will be due largely to his generosity and guidance.

TABLE OF CONTENTS

LIST OF TABLES

Table

LIST OF FIGURES

Figure

LIST OF ABBREVIATIONS

ΔUA	$\Delta^{4,5}$-unsaturated uronic acid
2-OST	2-*O*-sulfotransferase
3-OST	3-*O*-sulfotransferase
6-OST	6-*O*-sulfotransferase
AnMan	anhydromannitol
AT	antithrombin
ATP	adenosine triphosphate
BSA	bovine serum albumin
C_5-epi	C_5-epimerase
CHO	Chinese hamster ovary
CM	conditioned medium
ConA	concanavalin A
CS	chondroitin sulfate
DEAE	diethylaminoethyl
DMEM	Dulbecco's Modified Eagle Medium
ESI-MS	electrospray ionization mass spectrometry
Ext	exostosin
EV	empty vector
FBS	fetal bovine serum
GlcA	glucuronic acid
GlcN	glucosamine
HARE	hyaluronic acid receptor for endocytosis
HIT	heparin-induced thrombocytopenia

HPLC	high-performance liquid chromatography
HS	heparan sulfate
HUVEC	human umbilical vein endothelial cells
IACUC	Institutional Animal Care and Use Committee
IdoA	iduronic acid
IPTG	isopropyl β-D-1-thiogalactopyranoside
KfiA	*N*-acetylglucosaminyltransferase from *E. coli* K5
LMWH	low-molecular-weight heparin
MES	2-(*N*-morpholino)ethanesulfonic acid
NDST	*N*-deacteylase/*N*-sulfotransferase
NST	*N*-sulfotransferase
PAMN	polyamine
PAPS	3'-phosphoadenosine 5'-phosphosulfate
PBS	phosphate-buffered saline
PF4	platelet factor 4
pmHS2	heparosan synthase-2 from *P. multocida*
pnp	*para*-nitrophenol
SDS-PAGE	sodium dodecyl sulfate polyacrylamide gel electrophoresis
SNAC	sodium *N*-[8-(2-hydroxybenzoyl)amino]caprylate
Stab	Stabilin
Sulf	6-*O*-endosulfatase
TBST	Tris-buffered saline with Tween-20
TEV	tobacco etch virus
TFA	trifluoroacetic acid
UDP	uridine diphosphate
UFH	unfractionated heparin

VEGF	vascular endothelial growth factor
VTE	venous thromboembolism

CHAPTER I

INTRODUCTION

Heparan sulfate

Heparan sulfate (HS) is a widely expressed carbohydrate. As the body's most negatively charged molecule, it interacts with numerous proteins to regulate many biological functions relevant to human health and disease. These functions range from embryonic development and coagulation to inflammation and cancer metastasis. Heparan sulfate is part of the glycosaminoglycan family, the members of which contain long unbranched carbohydrates made up of repeating disaccharide units. Other members include keratan sulfate, dermatan sulfate, hyaluronan and chondroitin sulfate [1].

Heparan sulfate structure

The bioactivity of HS is dependent on its structure, namely the location of electronegative sulfo groups along its backbone and the presence of iduronic acid (IdoA), glucuronic acid (GlcA) and glucosamine (GlcN) residues (Fig. 1.1). HS exists on the surface of animal cells and within the extracellular matrix as a proteoglycan consisting of long carbohydrate chains attached to a core protein. Cell surface HS proteoglycans include syndecans and glypicans; perlecan and agrin are the primary extracellular examples [2-4]. The HS chains are composed of repeating disaccharide units of uronic acid and glucosamine. The uronic acid is present as either glucuronic or iduronic acid and can be sulfated at the -OH on carbon 2 (2-*O*-sulfation). The glucosamine can be 6-*O*- and 3-*O*-

sulfated, and its amine group can be acetylated, sulfated or unsubstituted (Fig. 1.1). The biological functions of HS proteoglycans are dominated by the HS side chains.

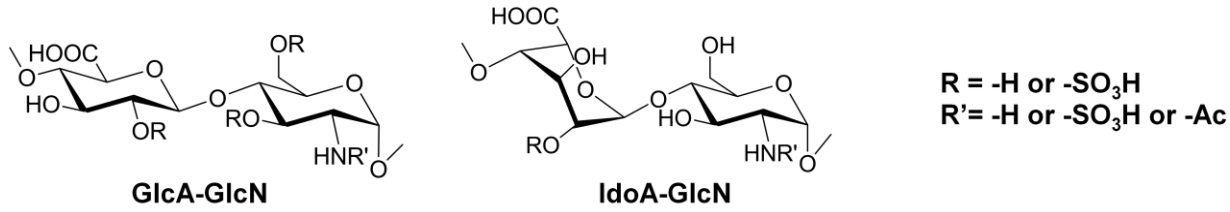

Figure 1.1. Chemical structure of the disaccharides present in HS. GlcA, glucuronic acid; IdoA, iduronic acid; GlcN, glucosamine.

This broad structural variation in the location of negative groups, in addition to variation in length and glycosidic bond position, allows HS to interact with different binding protein partners to display many biological functions. Although nonspecific ionic interactions between HS and proteins exist, the binding of HS to proteins can be specific. Thus, the preparation of unique HS chains with defined sulfation patterns and length is highly desirable, as they allow researchers to investigate the substrate specificity of HS-protein interactions and provide numerous therapeutic opportunities.

HS biosynthetic enzymes

HS biosynthesis occurs in the Golgi apparatus and is carried out by a series of enzymes (Figure 1.2). The synthesis of HS has two main components: chain elongation and modification of the individual sugars. *In vivo*, the HS chain is elongated by the Exostosin genes, Ext1 and Ext2 [5]. This process can be mimicked *in vitro* by two bacterial glycosyltransferases: *N*-acetylglucosaminyl transferase from the *E. coli* K5 strain, known as

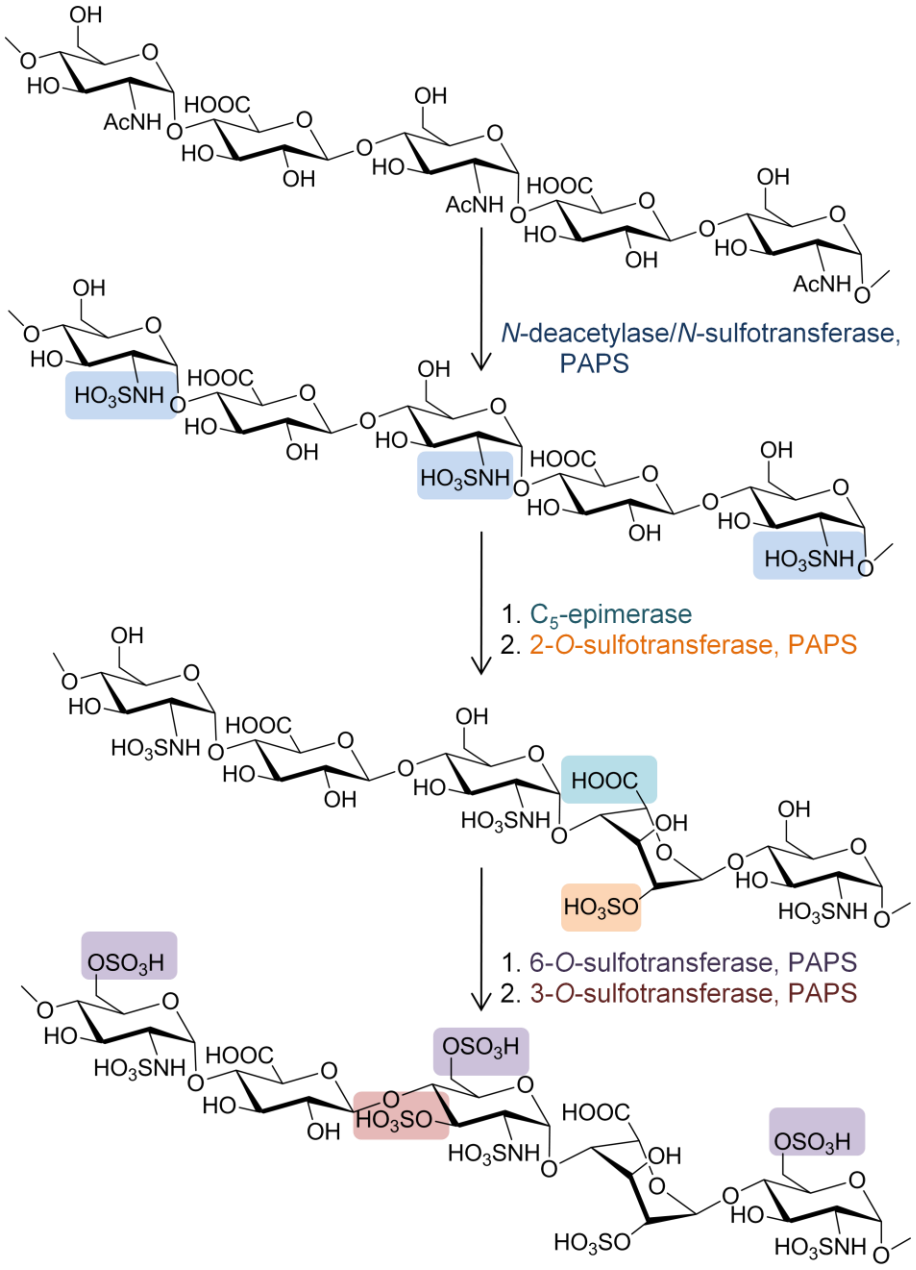

Figure 1.2. Enzyme reactions in the synthesis of heparan sulfate. *N*-deacetylase/*N*-sulfotransferase replaces *N*-acetyl groups with *N*-sulfo groups. C_5-epimerase converts glucuronic acid to iduronic acid. 2-*O*-, 6-*O*- and 3-*O*-sulfotransferase add sulfation at their respective positions.

KfiA [6], and heparosan synthase-2 from *Pasteurella multocida*, or pmHS2 [7]. In laboratory syntheses, KfiA and pmHS2 are incubated with uridine 5'-diphospho-*N*-trifluoroacetylglucosamine (UDP-NTFA) and UDP-GlcA, respectively; with each cycle of incubation, the oligosaccharide is elongated by one sugar unit [8]. GlcNTFA is used because it is easily chemically deacetylated to $GlcNH_2$ for later *N*-sulfation.

The *N*-deacetylase/*N*-sulfotransferase (NDST) enzyme is the first to modify an intact HS chain during biosynthesis, and its action is believed to direct the location of all subsequent sulfation reactions [9]. The 325-aa C-terminal region (constituting the *N*-sulfotransferase domain) of NDST is commonly expressed and used for HS synthesis *in vitro* following chemical deacetylation [10], although recent studies have focused on expression of the entire NDST enzyme [11]. Sulfation reactions are carried out by incubating HS with a sulfotransferase and 3'-phosphoadenosine 5'-phosphosulfate (PAPS), a natural sulfate donor.

Characterization of NDST-1 by Sheng et al. uncovered a unique substrate specificity for this enzyme [12]. Treatment of a synthetic dodecasaccharide substrate with NDST-1 produced a variety of *N*-sulfated products containing clusters of GlcNS, suggesting that NDST-1 binds to HS at a random position, converts consecutive GlcNAc to GlcNS from the non-reducing to reducing end, then releases the substrate when it is five sugars away from the reducing end. There are a total of four isoforms of NDST; NDST-2, which is highly expressed in mast cells, is proposed to be involved in the synthesis of highly-sulfated heparin but not HS [13]. This was principally confirmed by the absence of heparin in mast cells from NDST-2 knockout mice [14]. The *N*-deacetylase and *N*-sulfotransferase activities of NDST-2 through -4 have been investigated, but their use in HS synthesis specifically has not been fully explored [15].

After *N*-sulfation, C_5-epimerase (C_5-epi) converts some D-glucuronic acid residues to L-iduronic acid by altering the configuration of carbon 5 [16]. C_5-epimerase was recently

shown to exhibit a biphasic catalytic mode: depending on the substitution groups of the surrounding saccharide residues, the epimerization reaction is either reversible or irreversible. Using structurally defined oligosaccharides, Sheng et al. identified that C_5-epi will act on a GlcA residue if the residue immediately upstream (towards the non-reducing end) is a GlcNS residue. If the residue three sugars upstream is GlcNS, $GlcNH_2$ or not present, the reaction is reversible; if it is GlcNAc, the reaction is irreversible (Figure 1.3A) [17]. This finding will enable researchers to "lock" IdoA sugars in place and synthesize pure HS oligosaccharides containing IdoA during *in vitro* synthesis.

A series of *O*-sulfotransferases then sulfate their respective positions on HS. Heparan sulfate 2-*O*-sulfotransferase (2-OST) catalyzes the transfer of an $-OSO_3H$ group from PAPS to IdoA or GlcA. It is present in one isoform and has approximately five-fold greater affinity for IdoA than for GlcA [18], although mutational analyses have suggested that the preference for IdoA over GlcA can be controlled through site-specific mutations [19].

6-OST sulfates both GlcNAc and GlcNS to form GlcNAc6S and GlcNS6S, respectively. 6-OST isoforms, of which there are three, appear to sulfate the same substrates [20]; however, placement of 6-*O*-sulfo groups in oligosaccharides can be controlled somewhat by the enzymatic reaction time and by elongating oligosaccharides already containing 6-*O*-sulfated glucosamine [21]. A combination of 6-OST-1 and -3 was demonstrated to prefer GlcNAc residues close to the reducing end of oligosaccharide substrates, but placement of a single 6-*O*-sulfo group in an oligosaccharide remains a challenge [21, 22].

3-OST adds a sulfo group to the 3-OH position of GlcN residues and is present in seven isoforms. In endogenous HS, 3-*O*-sulfation is a relatively rare modification, sulfating only a small component of disaccharides [23]. However, the presence of 3-*O*-sulfation is critical for multiple types of HS activity, including binding to antithrombin, gD (a herpes simplex virus type 1 entry receptor) and Stabilin-1/2 (heparin clearance receptors) [24, 25].

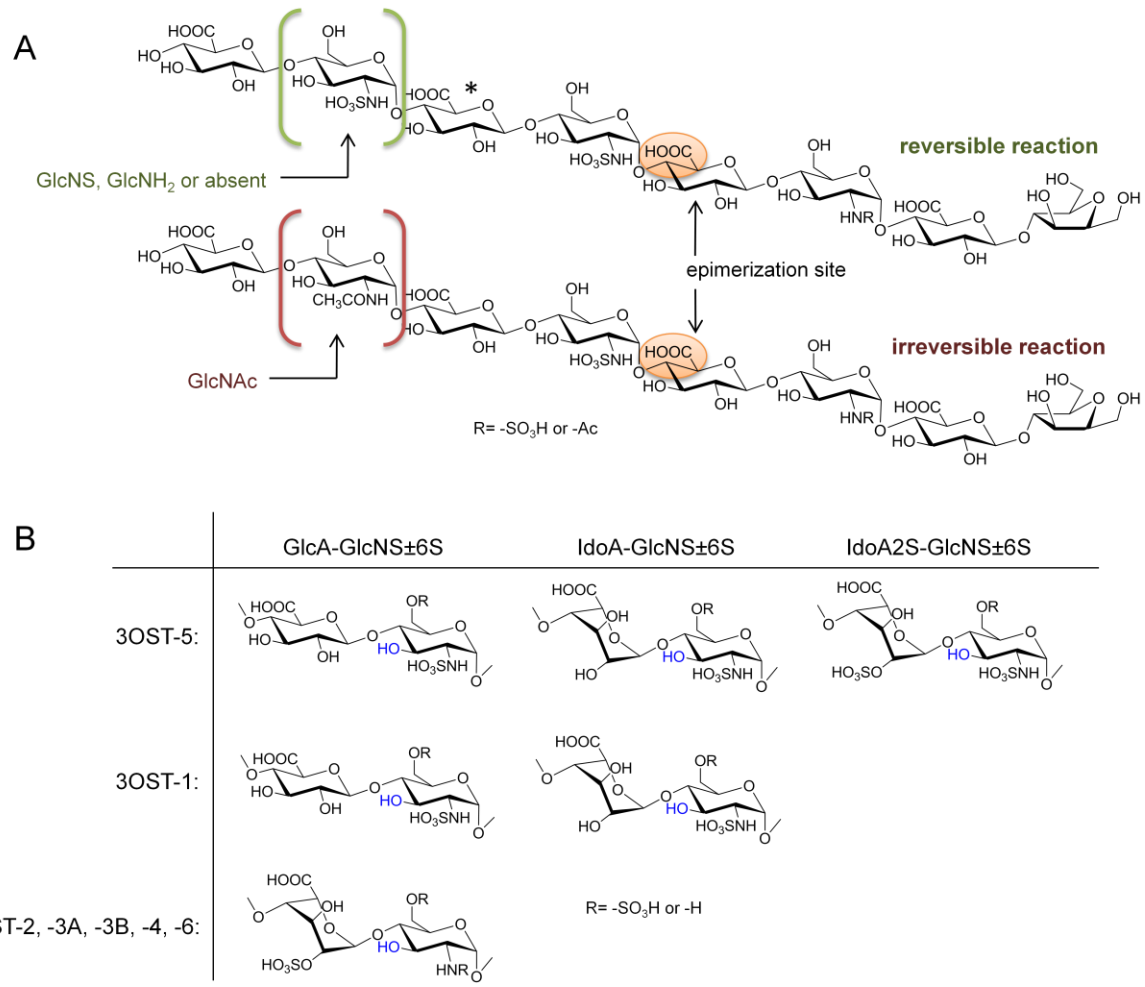

Figure 1.3. Substrate recognition of C_5-epimerase and 3OST. **A.** The epimerization reaction of C_5-epi is reversible or irreversible depending on the GlcN three sugars towards the nonreducing end of the glucuronic acid to be modified. The asterisk indicates a GlcA that could be epimerized if the sugar to the immediate left is GlcNS. **B.** Substrates of the seven 3OST isoforms. The position that will carry the 3-*O*-sulfo group is shown in blue.

The 3-OST isoforms exhibit greater than 60% homology in their sulfotransferase domains [9], and the substrate recognition of the 3-OSTs generally falls into one of three types, depending on the sugar linked to the non-reducing side of the glucosamine to be modified. 3-OST-1 will transfer a sulfo group to a GlcNS that is linked to a GlcA or IdoA at the non-reducing end. 3-OST-5 sulfates a GlcNS that is linked to an IdoA2S, GlcA or IdoA.

The remaining 3OSTs (-2, -3A, -3B, -4 and -6) will sulfate a GlcNS or $GlcNH_2$ linked to an IdoA2S at the non-reducing end (Figure 1.3B). These different substrate specificities allow placement of 3-*O*-sulfo groups in specific locations depending on the identity of the neighboring residue. Based on their ease of production in *E. coli*, 3-OST-1, -3 and -5 are most commonly used in chemoenzymatic syntheses; 3-OST-3 and -5 will produce HS that binds to gD [24]. A complete list of the enzymes used in HS synthesis is given in Table 1.1.

Heparin vs. HS

Heparin and HS have very similar structures; however, heparin refers to a special form of HS that has more sulfo groups and a higher level of iduronic acid residues. Heparan sulfate is produced by virtually all cells in species ranging from simple invertebrates to humans [23]. Heparin, on the other hand, is produced by mast cells and is present only in some tissues of select members of the animal kingdom. Interesting examples include the observations that rabbit tissues do not contain heparin [26] and that chicken skin contains relatively high levels of heparin [27].

Heparan sulfate proteoglycans appeared early in metazoan evolution, and their common structural motifs are conserved in modern organisms [23]. Uncharacterized proteoglycans have been identified in ancient multicellular organisms such as *Hydra* [28], and lower organisms such as Drosophila and *C. elegans* contain homologs of syndecan, glypican and perlecan [29]. The essential role of HS proteoglycans (and heparins) in the development and physiology of living organisms is supported by their prevalence throughout the animal kingdom.

Heparan sulfate is commonly made up of two domains, one composed of *N*-acetylated and *N*-sulfated disaccharides containing glucuronic acid and one composed of more highly sulfated disaccharides containing iduronic acid [26]. Mammalian heparan

Enzymes	Abbreviated Names	Enzymatic function	Expression system
N-deacetylase/*N*-sulfotransferase -1	NDST-1	Converts a GlcNAc to a GlcNS residue	*E. coli* ([30]), *S. cerevisiae* ([11])
N-deacetylase/*N*-sulfotransferase -2	NDST-2	Similar to NDST-1, but prone to synthesize a long cluster of GlcA-GlcNS repeating domains	*E. coli* ([31]), insect cells ([32])
N-deacetylase/*N*-sulfotransferase -3	NDST-3	Similar to NDST-1	
N-deacetylase/*N*-sulfotransferase -4	NDST-4	Similar to NDST-1	
N-sulfotransferase[1]	NST	Converts a $GlcNH_2$ to a GlcNS residue	*E. coli* ([30]), *K. lactis* ([33])
C_5-epimerase	C_5-epi	Converts a GlcA to an IdoA residue	*E. coli* ([34]), insect cells ([35])
2-*O*-sulfotransferase	2-OST	Introduces a sulfo group to the 2-OH position of an IdoA or a GlcA residue	*E. coli* ([36]), *K. lactis* ([33]), insect cells ([32])
6-*O*-sulfotransferase 1	6-OST-1	Introduces a sulfo group to the 6-OH position of a GlcNS or a GlcNAc residue	*E. coli* ([36]), *K. lactis* ([33]), insect cells ([32])
6-*O*-sulfotransferase 2	6-OST-2	Same as 6-OST-1	insect cells ([32])
6-*O*-sulfotransferase 3	6-OST-3	Same as 6-OST-1	*E. coli* ([37]), *K. lactis* ([33])
3-*O*-sulfotransferase 1	3-OST-1	Introduces a sulfo group to the 3-OH position of a GlcNS±6S residue that is linked to a GlcA (or an IdoA) on the nonreducing end	*E. coli* ([38]), *K. lactis* ([33]), insect cells ([39])
3-*O*-sulfotransferase 2	3-OST-2	Introduces a sulfo group to the 3-OH position of a GlcNS±6S residue that is linked to an IdoA2S on the nonreducing end	insect cells ([40])
3-O-sulfotransferase 3A	3-OST-3A	Introduces a sulfo group to the 3-OH position of a GlcNS±6S residue that is linked to an IdoA2S on the nonreducing end	*E. coli* ([41]), insect cells ([42])
3-O-sulfotransferase 3B	3-OST-3B	Same as 3-OST-3A	insect cells ([40])
3-O-sulfotransferase 4	3-OST-4	Same as 3-OST-3A	insect cells ([40])
3-O-sulfotransferase 5	3-OST-5	Has both 3-OST-1 and 3-OST-3A substrate specificities	*E. coli* ([43]), insect cells ([44])
3-O-sulfotransferase 6	3-OST-6	Same as 3-OST-3A	
pmHS2[A]	from *P. multocida*	Transfers a GlcA and a GlcNAc (or a GlcNTFA) residue to the backbone	*E. coli* ([7])
KfiA[B]	from *E. coli*	Transfers a GlcNAc (or a GlcNTFA) residue to the backbone	*E. coli* ([6])

[a] *N*-sulfotransferase is a protein that is composed of the *N*-sulfotransferase domain of NDST-1. NST is an unnatural protein, and it is used in the chemoenzymatic synthesis to convert a $GlcNH_2$ residue to a GlcNS residue.

[b] Both pmHS2 and KfiA are bacteria enzymes, not HS biosynthetic enzymes. However, they are used for building the backbone structure of HS during chemoenzymatic synthesis.

Table 1.1. List of HS biosynthetic enzymes.

sulfates from many different sources have been found to contain these domains in addition to a short linker that is positioned between the domains [45]. Heparan sulfate is ubiquitous in invertebrates as well; a survey of 23 invertebrates from 13 different phyla identified heparan sulfate in all of the species studied [46]. Studies in crustaceans and mollusks have characterized heparan sulfate in various tissues and found that the concentration of heparan sulfate is directly proportional to the salinity of the habitat [26].

There is much greater variation in the distribution of heparin, both among different organisms and within the tissues of a given species. In mammals, heparin is generally found in tissues that are in direct contact with the external environment, such as the skin, intestines and lungs, but it has low prevalence in the brain, muscle and kidneys of most species [26]. Several mollusks have been shown to contain heparin-like polysaccharides that possess anticoagulant activity [47, 48], but heparin is not present in all invertebrates. Like HS, heparin is understood to be comprised primarily of two different regions: a highly sulfated region that is subject to degradation by heparinase and a lowly sulfated region that is susceptible to heparitinase II, and the length and quantities of these regions depend on the species of origin and the specific tissue [26]. For example, bovine lung heparin is rich in the heparinase-cleavable region, while bovine intestinal heparin and mollusk heparins contain more of the heparitinase II-cleavable region [49, 50]. The roles of heparan sulfate and heparin appear to be the same in vertebrates and invertebrates.

Current anticoagulant therapies

Anticoagulants prevent the formation of blood clots by interfering with the blood coagulation cascade. Commonly used anticoagulants include vitamin K antagonists, thrombin inhibitors (both direct and indirect) and factor Xa inhibitors. Heparin drugs function as indirect (antithrombin-mediated) thrombin and Xa inhibitors, and they are typically

classified as unfractionated heparin, low-molecular-weight heparin or synthetic pentasaccharides.

Warfarin, the primary vitamin K antagonist, is a synthetic derivative of a natural product of plant and fungal origin, dicumarol [51]. It functions by inhibiting the biosynthesis of vitamin K-dependent procoagulant factors II (also called prothrombin), VII, IX and X [52]. It is given orally, and due to the long half-lives of some of these factors, it can take several days for it to reach its full antithrombotic effect. Warfarin is a mixture of *R* and *S* enantiomers (which are both active, but to different degrees) [53], and it is influenced by drug interactions and diet, especially the intake of vitamin K-rich greens. Thus, warfarin drugs require close monitoring and can cause bleeding complications [52]. Available reversal agents include vitamin K, fresh frozen plasma and bypassing agents such as prothrombin complex concentrates or recombinant factor VIIa. Warfarin is most typically administered for thrombosis treatment or prophylaxis.

Full-length unfractionated heparin (UFH) is isolated as a mixture from animal mast cells, primarily porcine intestine. It was discovered in 1916, before the establishment of the Food and Drug Administration, and it is one of the oldest drugs still in clinical use [54]. Heparin is a potent activator of antithrombin, a protein that inhibits factors Xa and IIa to prevent the downstream formation of fibrin clots (Fig. 1.4). Its inexpensive production, short half-life and reversibility with protamine make UFH an advantageous drug for surgery and for handling blood in laboratory settings. It also has certain drawbacks, including an unreliable supply chain, side effects such as heparin-induced thrombocyptopenia (HIT) and dosing difficulties due to its heterogeneous nature. Its short (30- to 60-min) half-life and intravenous administration route limit its clinical use to in-patient procedures, and it must be monitored using activated partial thromboplastin time [52].

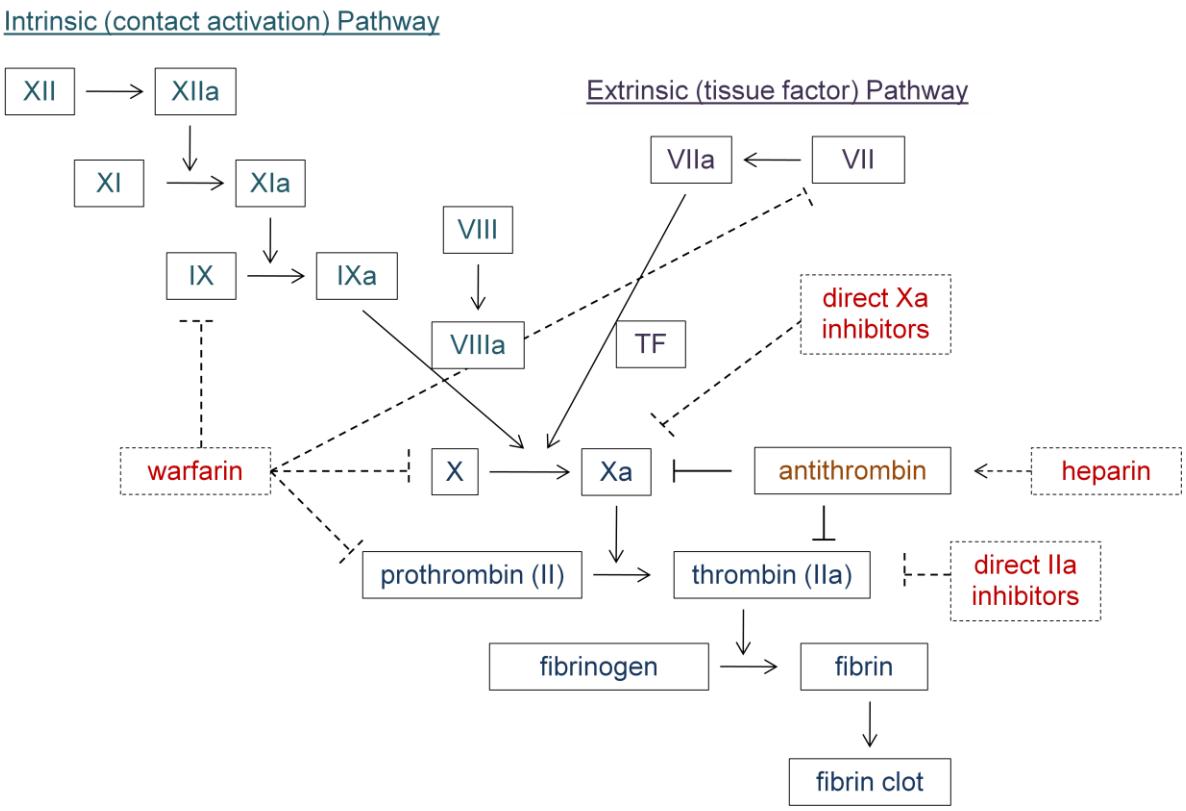

Figure 1.4. Interaction of anticoagulant drugs with the coagulation cascade. Coagulation is initiated by the intrinsic or extrinsic pathway. The two pathways converge on the activation of factor X to Xa and result in the formation of fibrin clots. Target sites for current anticoagulant drugs are shown in red.

Low-molecular-weight heparin (LMWH) drugs, such as enoxaparin (Lovenox), are a mixture of products from depolymerized UFH. The average length is about 15 saccharide units, compared to 40 for UFH. LMWH inhibits IIa to a lesser extent than UFH, as not all components of the mixture are long enough to form an antithrombin:Xa:IIa complex. It tends to be safer than UFH, having a lower incidence of HIT, and its longer half-life and subcutaneous dosing make it more appropriate for venous thromboembolism prophylaxis and treatment. Its more predictable anticoagulant effect also means that fixed or weight-based dosing is possible without routine laboratory monitoring [52]. At least a fraction of

LMWH is cleared by the kidneys, so anti-Xa monitoring is recommended for patients with renal impairment as well as for elderly, pregnant or obese patients.

The shortest and most recently developed heparin drugs, such as fondaparinux (Arixtra), are analogs of the antithrombin-binding heparin pentasaccharide. They inhibit Xa and do not have anti-IIa activity. Arixtra is produced through a lengthy chemical synthesis and, unlike UFH and LWMH, it is a pure compound, not a mixture. Like LMWH, it is dosed subcutaneously. Arixtra has a half-life of approximately 17 hours, allows for unmonitored once-daily dosing and is currently approved for deep vein thrombosis and pulmonary embolism [55]. A hypermethylated version of fondaparinux known as idraparinux was developed in the late 1990s [56]. It has a 30-fold higher affinity for antithrombin than Arixtra, and its 120-hour half-life permits once-weekly administration [55]. Like Arixtra, it does not have an antidote. However, a biotinylated version of idraparinux was developed, and its anti-Xa activity is effectively reversed by avidin [57]. Both fondaparinux and idraparinux do not bind to PF4 and do not show evidence of causing heparin-induced thrombocytopenia. Despite these promising developments, idraparinux was associated with an increased risk of major hemorrhage in clinical trials [58], and it was withdrawn from further development.

Thrombin, or factor IIa, is a serine protease that is central to hemostasis. Direct thrombin inhibitors function independently of antithrombin and do not bind PF4 [52]. The drugs lepirudin, desirudin and bivalirudin are derivatives of hirudin, a naturally occurring peptide found in the salivary glands of medicinal leeches, and they are approved for thrombosis with HIT, postsurgical VTE and unstable angina, respectively [52]. Argatroban is a reversible small-molecule direct thrombin binder that is also approved for HIT. Dabigatran (given as an oral prodrug, dabigatran etexilate), is a small-molecule competitive direct thrombin inhibitor that is approved for deep vein thrombosis [52]. It was shown to be equal to enoxaparin in terms of safety and efficacy in reducing DVT after hip replacement surgery [59].

Direct Xa inhibitors have the advantage of bypassing intermediary molecules like antithrombin, which may result in more consistent anticoagulation. Razaxaban and apixaban are both oral small-molecule direct Xa inhibitors developed by Bristol-Myers Squibb. Razaxaban was abandoned in favor of apixaban due to its better safety profile, and apixaban (Eliquis) was FDA-approved in December 2012. Rivaroxaban is another FDA-approved Xa inhibitor; it is also a small molecule developed by Bayer that can be given in once-daily oral doses. Of all oral anticoagulants, rivaroxaban has been evaluated the most extensively and in largest patient populations [55]. It has a half-life that is considerably shorter than other oral Xa inhibitors (about 5 to 9 hours) [52], and it has a low risk of drug-drug interactions [60]. Although they have many promising characteristics, a disadvantage of the oral Xa inhibitors is their lack of a reversal agent.

Selective direct inhibitors of factors IXa and XIa are also in development, but they have yet to complete clinical trials [55].

Strategies for improved heparin drugs

Although unfractionated, low-molecular-weight and pentasaccharide heparin drugs are presently available, there is a need for more advanced heparins that suit the requirements of distinct patient populations. As long as binding to antithrombin is maintained, the structure of heparin can be rationally designed to allow for optimal interactions with other molecules and desirable pharmacological properties.

A primary consideration in the administration of a drug is its bioavailability and delivery route, and the ease of administration is a major factor in patient compliance and acceptability. An oral heparin would be an improved anticoagulant for long-term therapy, such as the prevention of thrombosis [61], but its high molecular weight and negative charge density limit its oral bioavailability [62]. Several efforts have been made to synthesize orally available heparins. To counteract the poor delivery of anionic heparin across the mucosal

gastrointestinal lining, penetration enhancers such as SNAC (sodium *N*-[8-(2-hydroxybenzoyl)amino]caprylate) have been administered with heparin, with promising results [63]. Other approaches include novel drug delivery systems, such as nanoparticles, lipid conjugates and enteric coatings [64-66]. Despite experimental successes, no oral heparin formulations have reached the market. A more relevant issue for rational synthesis of the heparin carbohydrate chain would be to focus on structures that were bioavailable via subcutaneous injection (like Arixtra and LMWHs) rather than intravenously. Although unfractionated heparin can be administered subcutaneously, its bioavailability is reduced to about 30% (compared to nearly 100% for LMWH), so much higher doses are required [67, 68]. Thus, heparins of reduced molecular weight are likely to have high subcutaneous bioavailability.

After administration, side effects of heparin drugs come into consideration. For many drugs, unwanted side effects can be avoided by modifying the structure of the active compound, but the heterogeneous nature of the heparin polysaccharide chain negates this approach, even when dealing with fragmented low-molecular-weight heparins [69]. Bleeding is the most common side effect of heparin therapy; major bleeding occurs in 4 to 5% of patients receiving unfractionated heparin [70, 71]. Other complications include heparin-induced thrombocytopenia and, less commonly, osteoporosis, eosinophilia, skin reactions, alopecia (hair loss), liver dysfunction and hyperkalemia (elevated blood potassium) [72]. There is also an acute anaphylactic reaction that occurs within 5 to 10 minutes after commencing intravenous heparin bolus therapy; it includes the abrupt onset of chills and fever, tachycardia, diaphoresis and nausea, with possible hypertension, chest pain and amnesia [73]. This reaction is consistent with an immunoglobulin E-stimulated response [72]. The development and use of homogeneous heparin compounds could prevent many of these unwanted effects: first, because the dosing and anticoagulation would be much more

predictable, and second, because the compounds could be designed to avoid interaction with immunogenic molecules.

For certain heparin applications, particularly surgery, the availability of an antidote is imperative. Additionally, unstopped hemorrhaging as a result of heparin therapy can lead to long-term debilitating diseases and may be life threatening [74]. Protamine sulfate can be used to reverse unfractionated heparin, although heparin rebound is a concern, but it is ineffective with low-molecular-weight heparin and Arixtra [75]. Excessive bleeding due to Arixtra, although rare, can be very difficult to manage because of its long half-life [76]. It has been successfully managed with fresh frozen plasma and prothrombin complex concentrates [75], but the only systematically evaluated reversal for pentasaccharide heparins is the use of recombinant FVIIa [76]; however, the use of rFVIIa for hemorrhage is still controversial [77]. Novel heparin drugs would ideally be reversible by protamine to evade life-threatening bleeding episodes.

Finally, the metabolic route and rate by which heparin is cleared from the body can make it ideal or dangerous depending on the patient population. Long-acting heparins suit patients that require long-term therapy, and short-acting heparins better treat those undergoing surgery or at risk for anticoagulant complications. In addition, clearance by the liver is preferred over kidney clearance, as many patients have kidney impairment that results in the accumulation of short heparins like Arixtra [78]. Although length is known to be a determining factor, the structure of heparin required for liver clearance has not been previously described. Taking the aforementioned considerations into account, we sought to determine the structure-function relationships of synthesized heparins with the goal of designing heparins that had improved safety, administration, clearance and reversibility profiles to the existing drugs.

Statement of Problem

Heparin has been widely used for decades, but it has several limitations as a drug. Unfractionated heparin has contamination issues due to its sourcing and causes side effects like heparin-induced thrombocytopenia. Low-molecular-weight heparin can cause severe bleeding due to its structural heterogeneity. Pentasaccharides like Arixtra are unsafe for kidney impaired patients due to their renal clearance route [79]. The goals of this dissertation were to characterize the protein interactions underlying some of these drawbacks and to propose improved heparin structures.

Recent advances in heparan sulfate synthesis using a chemoenzymatic approach have enabled the production of novel molecules with desired sulfation patterns and lengths (for a review, see [80]). First, this synthetic approach was used to investigate methods to reduce binding between heparan sulfate and PF4, an interaction that initiates heparin-induced thrombocytopenia. In addition, we sought to characterize the structural requirements for binding to Stabilin receptors, which were recently identified as heparin clearance receptors [81]. We hypothesized that heparan sulfate structures with robust binding to Stabilins would be cleared by the liver and cleared more quickly than non-binding ones. During these studies, bioavailability and affinity for coagulation factors (Xa and IIa) were also investigated. The results of these studies should provide insight into the mechanisms underlying heparin's properties in the body and also suggest meaningful strategies for the development of improved heparin drugs.

CHAPTER II

MATERIALS AND METHODS

Expression of HS biosynthetic enzymes

Several enzymes were used for HS synthesis, including NST, C_5-epi, 2-OST, 6-OST-1, 6-OST-3, 3-OST-1, 3OST-5, KfiA, and pmHS2. All enzymes were expressed in *E. coli* and purified by appropriate affinity chromatography as described previously [82].

Preparation of ^{35}S-labeled polysaccharides

Radiolabeled polysaccharide substrates were prepared using approximately 1 µg heparosan, a capsular polysaccharide isolated from the *E. coli* K5 strain, as a starting material [83]. Other substrates were prepared from bovine kidney heparan sulfate. The starting materials were modified with 5-10 µg of C_5-epi, NST, 6OST-1/3, 2OST, 3OST-1 and 3OST-5 enzymes in sequential 200-µL reactions containing approximately 1 x 10^6 cpm [^{35}S]PAPS and 10 nmol unlabeled PAPS in 50 mM MES (pH 7) and 0.5% triton X-100. The enzymatic reactions were incubated at 37°C for 60 min, heat inactivated and purified using a DEAE column [83].

Expression of recombinant Sulf-2 in CHO cells

A plasmid consisting of a full-length cDNA encoding human Sulf-2 was purchased from Open Biosystem (Clone ID #7969293). The gene was cloned into a pcDNA3.1A mammalian expression vector (from Invitrogen) using XhoI/HindIII sites to obtain a Sulf-2 expression

plasmid designated as pcDNA3.1A-myc/His-HSulf-2. Wild-type CHO cells were transiently transfected with the expression plasmid pcDNA3.1A-*myc*/His-HSulf-2 or an empty pcDNA3.1A vector according to a standard protocol. Briefly, CHO cells were seeded in 6-well plates in F-12 media supplemented with 10% fetal bovine serum (FBS) and were maintained in a 5% CO_2 humidified incubator at 37°C. When the cells reached 90-95% confluence, they were transfected using Lipofectamine 2000 reagent (Invitrogen) and Opti-MEM Reduced Serum Media (Invitrogen) according to the manufacturer's protocol. After 4-6 h, the medium was replaced with F-12 media containing 10% FBS. The conditioned medium was collected after 48-72 h of incubation and centrifuged at 4,000 rpm for 15 minutes to remove cellular debris.

Western blotting

Sulf-2 and EV-transfected cells were collected using trypsin and washed with PBS. Cells were lysed with 1.5 M sucrose, 1% triton X-100 and 1 mM PMSF. Sulf-2 and EV CM and lysates were separated by 12% SDS-PAGE and visualized with an anti-myc primary antibody (Cell Signaling Technology) and the SuperSignal detection system (Thermo Scientific).

Sulf-2 enzymatic assay

A 100-µL reaction containing ^{35}S-labeled substrate, 50 mM MES (pH 6.5), 10 mM $CaCl_2$, 0.1% triton X-100 and 50 µL Sulf-2 enzyme was incubated overnight at 37°C. Polysaccharide substrates were purified using Quick Spin Columns for radiolabeled DNA purification (Roche). Columns were centrifuged at 1100 x *g* for 2 min to remove the column buffer, then placed into a fresh collection tube and loaded with 50 µL of reaction mixture. After centrifugation for 4 min at 1100 x *g*, the eluate was collected and the amount of ^{35}S-labeled polysaccharide was quantified using a scintillation counter.

Analysis of synthetic polysaccharides

To determine the structural compositions of radiolabeled substrates, disaccharide analyses were performed using heparin lyase digestion. Polysaccharide substrates were incubated overnight with a mixture of heparin lysase I, II and III (0.1 mg/mL each) in 200 µL of 50 mM sodium phosphate (pH 7) at 37°C. The reaction was terminated by boiling at 100°C for 5 min and was loaded onto a Bio-Gel P-2 column (Bio Rad) to isolate disaccharides. These disaccharides were analyzed using reverse-phase ion-pairing HPLC [31].

Preparation of ^{35}S-labeled HS from CHO cells

A T-75 flask of wild-type CHO cells was grown to confluence in F-12 media supplemented with 10% FBS. The cells were then incubated with 1 mL of 1.0 mCi/mL sodium [^{35}S]sulfate (Perkin Elmer) for 6 h at 37°C with 5% CO_2. Two hundred microliters of a pronase stock solution containing 1 mg/mL Pronase (Sigma), 240 mM NaAcO (pH 6.5) and 1.92 M NaCl was added to the cells, and the flask was incubated overnight at 37°C. The pronase-digested sample was centrifuged at 10,000 rpm for 15 min and filtered using a 0.45-µm filter, then purified using a DEAE-Sepharcel column (Sigma), which was equilibrated using a buffer containing 20 mM NaAcO (pH 5) and 150 mM NaCl. The [^{35}S]HS was eluted from the column with 1 M NaCl in 20 mM NaAcO and was dialyzed overnight against 50 mM ammonium bicarbonate using a 14,000 MWCO membrane, then dried. The sample was reconstituted in 1 mL water, and 10 µL of a solution containing 10 N NaOH and 0.89 M sodium borohydride was added to break the linkage between the core protein and HS. It was incubated at 46°C for 16 h. The sample was also treated with 20 U/mL chondroitinase ABC (Sigma) to remove chondroitin sulfate before use.

Preparation of 3OST-1-treated [^{35}S]HS

To 3-*O*-sulfate [^{35}S]HS using unlabeled PAPS for affinity co-electrophoresis, approximately 100,000 cpm of [^{35}S]HS was added to a 50-µL reaction containing 0.05 ng 3OST-1, 10 mM $MnCl_2$, 5 mM $MgCl_2$, 75 ug/mL protamine chloride, 0.4 mg/mL chondroitin sulfate, 0.12 mg/mL BSA, 1% triton X-100 and 0.5 mM PAPS. The reaction was incubated at 37°C for 20 min, inactivated at 80°C for 10 min, then diluted with 60 µL H_2O and centrifuged at 2000 x *g* for 10 min. Substrates used for antithrombin binding studies were then isolated using a concanavalin A-Sepharose column (Sigma).

Preparation of mPF4

The full-length murine PF4 cDNA was obtained from Open Biosystems (Clone ID: 582960). The heparin-binding domain of PF4 (Ala^{33}-Ser^{105}) was cloned into a PET32 vector (Novagen) using NcoI and HindIII sites to give a plasmid named as PF4-PET32/TEV. In this plasmid, a tobacco etch virus protease (TEV) cleavage hexapeptide sequence, EQLYFQG, was constructed between thioredoxin and PF4. The design permitted cleavage of the thioredoxin-PF4 fusion protein to release PF4. The resultant recombinant PF4 protein has five extra amino acid residues (GSRHG) at the *N*-terminus. A bacterial strain, BL21(DE3)-RIL/pRK793, expressing TEV protease was a generous gift from Dr. Lars Pedersen (National Institute of Environmental Health Sciences).

The PF4-PET32/TEV plasmid was introduced into BL21 cells, and the cells were grown in LB medium containing 50 µg/mL carbenicillin and induced with IPTG. The cells were pelleted, lysed in 25 mM Tris, 500 mM NaCl and 300 mM imidazole (pH 7.5) and purified using a nickel column. The fractions containing protein were collected and incubated overnight with TEV protease (1:25 w/w ratio of TEV:PF4). After TEV cleavage, the PF4 was dialyzed against 20 mM Tris and 250 mM NaCl (pH 8) and was purified with a heparin column, which was eluted with 250 mM to 2000 mM NaCl gradient in 20 mM Tris (pH 8).

The purity of PF4 was greater than 90% as determined by NuPAGE 12% Bis-Tris Gel (Invitrogen). PF4 was eluted as a protein with a MW of 30 kDa on a Sephadex G75 column, suggesting that PF4 is present in a tetrameric form that was consistent with a previous report [84]. The concentration of PF4 was determined by amino acid compositional analysis.

Dot blot assay for PF4 binding

A dot blot assay was used to determine the binding affinities of HS to PF4. ^{35}S-labeled HS (approximately 6,000 cpm) was incubated with 0-15 µg/mL PF4 for 30 min at 37°C in 130 mM NaCl, 50 mM Tris (pH 7) buffer (for the [^{35}S]HS polysaccharide studies) or in 250 mM NaCl, 50 mM Tris (pH 7.3) buffer (for the oligosaccharide studies) to allow complex formation. The mixture was then spotted onto a nitrocellulose membrane (GE Healthcare), which binds to proteins nonspecifically, allowing the capture of PF4-[^{35}S]HS complexes. The membrane wells were washed with buffer, then excised, and the bound radioactivity was quantified using a scintillation counter.

Affinity co-electrophoresis

Affinity co-electrophoresis gels were prepared using a standard protocol [85] with lanes containing 0-1.41 µM PF4 or 0-3.2 µM AT and approximately 50,000 cpm [^{35}S]HS per gel. Gels were run for 2 (AT) or 2.5 (PF4) hours and the bands were imaged using a Storm 860 phosphorimager (Molecular Dynamics) and ImageQuant TL v2005 software (GE Healthcare Life Sciences). K_d values were determined by plotting R/[protein] vs. R, where R = (Mo – M)/Mo; Mo = the mobility of free HS and M = the mobility of HS at each protein concentration. The slope is equal to $-1/K_d$.

AT binding assay

To quantify the binding of Sulf-2-treated and untreated HS to AT, 3OST-1-labeled substrates were incubated with 0.1 mg/mL AT, and the complex of AT and HS was captured using concanavalin A-Sepharose beads (Sigma). For this experiment, the AT-binding [^{35}S]HS was prepared by incubating HS from bovine kidney with the 3OST-1 enzyme and [^{35}S]PAPS.

Preparation of enzyme cofactors

A sulfo donor, 3'-phosphoadenosine 5'-phophosulfate (PAPS), was prepared using adenosine phosphokinase and ATP-sulfurylase [82]. The preparation of UDP-GlcNTFA was started from glucosamine (Sigma), which was first converted to GlcNTFA by reacting with *S*-ethyl trifluorothioacetate (Sigma-Aldrich) following the protocol described previously [82]. The resultant GlcNTFA was converted to GlcNTFA-1-phosphate using *N*-acetylhexosamine 1-kinase [86]. The plasmid expressing *N*-acetylhexoamine 1-kinase was a generous gift from Prof. Peng Wang (Georgia State University), and the expression of the enzyme was carried out in *E. coli* as reported [86]. The UDP-GlcNTFA synthesis was completed by transforming GlcNTFA-1-phosphate using glucosamine-1-phosphate acetyltransferase/*N*-acetylglucosamine-1-phosphate uridyltransferase (GlmU) as described [82]. The resultant UDP-GlcNTFA was then ready for the elongation reaction using KfiA.

Preparation of oligosaccharide backbone

A disaccharide (GlcA-AnMan) was prepared from heparosan as described [82]. The disaccharide was then elongated to N-TFA oligosaccharides by repetitive exposure to KfiA, pmHS2, UDP-GlcNTFA and UDP-GlcA as shown in Fig 1. Briefly, the disaccharide (20 mg), KfiA (30 μg/mL) and UDP-GlcNTFA (500 μM) were mixed in 120 mL of 50 mM Tris buffer. The reaction was incubated at room temperature overnight. The completion of the reaction

was monitored by the disappearance of UDP-GlcNTFA using a silica-based polyamine HPLC column (PAMN-HPLC, Waters). Once the reaction was completed, pmHS2 (30 μg/mL) and UDP-GlcA (750 μM) were added, and the reaction was incubated for another 24 hours at room temperature. The resultant product was a tetrasaccharide, which was purified by a Biogel P-2 column (0.75 × 200 cm) that was equilibrated with 0.1 M ammonium bicarbonate at a flow rate of 6 mL/h. The fractions were then subjected to ESI-MS analysis. The fractions containing the tetrasaccharide were pooled. The procedures for synthesizing the N-TFA pentadecasaccharide (15-mer), N-TFA heptadecasaccharide (17-mer), N-TFA nonadecasaccharide (19-mer) and N-TFA henicosasaccharide (21-mer) were essentially the same completed by repeating the above cycle with the designated times.

When the backbone was elongated beyond octasaccharide, a special method was employed to deplete the UDP-GlcNTFA and UDP-GlcNAc prior to the further elongation by pmHS2. If unreacted UDP-GlcNTFA of UDP-GlcNAc was present in the GlcA elongation step involving pmHS2, an uncontrolled elongation occurred, resulting in a mixture. It is, therefore, especially important to avoid the formation of mixtures when the synthesis reached octasaccharide and beyond because the P-2 column cannot separate oligosaccharides larger than octasaccharides. To this end, disaccharide (GlcA-AnMan) was added to the reaction to exhaust the residue UDP-GlcNTFA and GlcNAc at the reaction, and the resultant trisaccharide was removed by the P-2 column.

N-detrifluoroacetylation

Oligosaccharide backbones (1 to 2 mg) were resuspended in a solution (20 mL) containing CH_3OH, H_2O and $(C_2H_5)_3N$ (v/v/v = 2:2:1). The reaction was incubated at 50°C overnight. The samples were dried and reconstituted in H_2O to recover de-*N*-trifluoroacetylated oligosaccharides.

N-sulfation of oligosaccharides

N-sulfation of oligosaccharide was carried out by incubating the oligosaccharide substrates with NST and PAPS. The reaction mixture typically contained 1-2 mg de-*N*-trifluoroacetylated oligosaccharide, 500 µM PAPS, 50 mM MES, pH 7.0 and 1 mg of NST in a total volume of 15 mL. The reaction mixture was incubated at 37°C overnight.

Sulfation and epimerization modifications of oligosaccharide backbones

The conversion of *N*-sulfo oligosaccharides to final products involved three steps, including C_5-epimerization/2-*O*-sulfation, 6-*O*-sulfation and 3-*O*-sulfation. *N*-sulfo oligosaccharides (1-2 mg) were incubated with a reaction mixture containing 50 mM MES, pH 7.0, 0.03 mg/mL C_5-epi and 2 mM $CaCl_2$ in a total volume of 40 mL. After incubating 30 min at 37°C, 2-OST (0.03 mg/mL) and 200 µM PAPS were added, and the reaction was incubated overnight at 37°C. The products were purified by a DEAE column described previously (14). For 6-*O*-sulfation, the substrate was incubated with a reaction mixture containing 50 mM MES, pH 7.0, and 500 µM PAPS overnight at 37°C in the presence of 6-OST-1 (0.03 mg/mL) and 6-OST-3 (0.03 mg/mL) in a total volume of 20 mL overnight at 37°C. The products were purified by a DEAE column. For 3-O-sulfation, the reaction mixture contained 3-OST-1 (0.03 mg/mL), 10 mM $MnCl_2$, 5 mM $MgCl_2$, and PAPS 500 µM in a total volume of 20 mL overnight at 37°C.

Mass spectrometric analysis of oligosaccharides

The analyses were performed with a Thermo LCQ-Deca. The nonsulfated oligosaccharide (1 µL) eluted from BioGel P-2 was directly diluted in 200 µL of 9:1 MeOH/H_2O. A syringe pump (Harvard Apparatus) was used to introduce the sample via direct infusion (35 µL /min). Experiments were carried out in negative ionization mode with the electrospray source

set to 5 KV and 275°C. Sulfated oligosaccharide (1 µL) was diluted in a different working solution containing 200 µL of 70% acetonitrile and 10 mM imidazole. Experiments for sulfated oligosaccharides were carried out in negative ionization mode with the electrospray source set to 2 KV and 200°C. The automatic gain control was set to 1 X 10^7 for full scan MS. The MS data were acquired and processed using Xcalibur 1.3.

Inhibition of the activities of factor Xa and IIa

Assays were based on a previously published method [87, 88]. Briefly, factor Xa (Enzyme Research Laboratories, South Bend, IN) and thrombin (Sigma) were diluted at 80 nM and 100 nM, respectively, with PBS containing 1 mg/mL BSA. Human AT (Cutter Biological) was diluted with PBS containing 1 mg/mL BSA to give a stock solution at the concentration of 0.4 µM. The chromogenic substrates, S-2765 (for factor Xa assay) and S-2238 (for factor IIa assay) were prepared at 1.3 mM and 1.5 mM in water. The synthesized oligosaccharides or heparin was dissolved in PBS at various concentrations (1 to 30 nM). The reaction mixture, which consisted of 70 µL of AT stock solution and 15 µL of the sample solution, was incubated at room temperature for 2 min. Factor Xa or thrombin (10 µL) was added. After incubation at room temperature for 4 min, 30 µL of S-2765 or S-2238 was added. The initial reaction rates as a function of concentration were used to calculate the IC_{50} values. The absorbance of the reaction mixture was measured at 405 nm continuously for 10 min. The absorbance values were plotted against the reaction time. The initial reaction rates as a function of concentration were used to calculate the IC_{50} values.

The neutralization effect of PF4 on anti-Xa activity

HS oligosaccharides were incubated in a 96-well plate with 70 µL BSA (1 mg/mL in PBS), 10 µL AT (0.2 mg/mL in PBS) and 0-16 µL PF4 (0.45 mg/mL) for two minutes at room temperature. Ten microliters of Xa was then added, and after four minutes, 30 µL of chromogenic substrate S-2765 (1 mg/mL) was added to initiate the color change reaction. Sequential absorbance readings at 405 nm were started immediately using an ELx808 plate reader (BioTek). The rate of increased absorbance relative to the rate of a control sample was used to define Xa activity. Quantities of oligosaccharides showing approximately 8% Xa activity in the absence of PF4 were used.

HPLC analysis of oligosaccharides

Both DEAE-HPLC and polyamine-based anion exchange (PAMN)-HPLC were used to determine the purity of the oligosaccharides. The elution conditions for the HPLC analysis are described in the literature [82].

Nitrous acid-degraded disaccharide analysis of ^{35}S-labeled oligosaccharides

The ^{35}S-labeled compound was deacetylated and degraded with nitrous acid at pH 4.5, then at pH 1.5, followed by reduction with sodium borohydride as described by Shively and colleagues [89]. The resultant ^{35}S-labeled disaccharides were resolved by a C_{18} reverse-phase column (0.46 × 25 cm) (Vydac) under reverse-phase ion pairing HPLC conditions. The identities of the disaccharides were determined by coeluting with appropriate ^{35}S-labeled disaccharide standards.

Materials, solutions and buffers for Flp-In 293-based assays

Heparin (or unfractionated heparin) was from Sigma (St. Louis, MO). Fondaparinux (Arixtra®) was purchased from a local pharmacy. Flp-In 293 cells, serum, and high glucose Dulbecco's Modified Eagle Medium (DMEM) were from Gibco, Hygromycin B, Zeocin, and glutamine were from Invitrogen/Gibco (Carlsbad, CA). Western blot analysis was completed by either colorimetric or chemiluminescence detection of blotted protein. Anti-V5 antibodies and resins were from Bethyl Laboratories (Montgomery, TX). Other materials, reagents and kits were obtained as described recently [90]. Tris-buffered saline with Tween-20 (TBST) contains 20 mM Tris-HCl, pH 7.0, 150 mM NaCl, and 0.1% Tween-20. TBST/BSA is TBST with 1.0% (w/v) bovine serum albumin (BSA). Phosphate buffered saline (PBS) contains 137 mM NaCl, 8 mM Na_2HPO_4, 1.5 mM KH_2PO_4, 2.7 mM KCl, pH 7.2. Hank's buffered saline solution (HBSS) contains 5 mM KCl, 0.4 mM KH_2PO_4, 0.8 mM $MgSO_4$, 137 mM NaCl, 0.3 mM Na_2HPO_4, 5.5 mM glucose, 1.26 mM $CaCl_2$, 0.5 mM $MgCl_2$, and 28 μM phenol red; at the time of use, 3.5 g/100 mL of $NaHCO_3$ was added and the pH was adjusted to 7.2 with HCl. Endocytosis Medium contains DMEM supplemented with 0.05% BSA.

Preparation of ^{35}S-labeled HS constructs for Stabilin binding studies

A total of 27 HS constructs were prepared using a chemoenzymatic approach published previously [91, 92]. Constructs **14** through **23** are polysaccharide constructs differing in sulfation types and IdoA content, while construct **24** through **36** are oligosaccharide constructs ranging from hepta- to nonadeca-saccharides (Table 4.1). A representative structure of a decasaccharide (**28b**) is shown in Fig. 4.10. For the synthesis of polysaccharide constructs (**14** through **23**), *N*-sulfo heparosan was used as a starting material and incubated with appropriate enzymes and the sulfo donor 3'-phosphoadenosine 5'-phosphosulfate (PAPS) [91]. The polysaccharide products were analyzed by disaccharide

analysis to confirm the anticipated sulfations [93]. To prepare the oligosaccharide constructs (**24** through **36**), both elongation and modification steps were involved. During the elongation step, a disaccharide starting material (GlcA-AnMan) was first elongated to the desirable size with KfiA (*N*-acetyl glucosaminyl transferase of *E. coli* K5 strain) and pmHS2 (*Pasteurella multocida* heparosan synthase 2) in the presence of UDP-GlcA and UDP-GlcNAc or UDP-GlcNTFA. The elongated products were confirmed by electrospray ionization mass spectrometry (ESI-MS). The oligosaccharides were then converted to *N*-sulfo oligosaccharides by treating with triethylamine followed by *N*-sulfotransferase modification. The products were demonstrated to have the anticipated molecular size and purity by ESI-MS.

The oligosaccharides were then modified by C_5-epimerase (C5-epi), 2-*O*-sulfotransferase (2-OST), 6-*O*-sulfotransferase 1 and 3 (6-OST-1 and 6-OST-3) and 3-*O*-sulfotransferase 1(3-OST-1). After the modifications, a mixture of oligosaccharides with different levels of sulfation was obtained as determined by DEAE (diethylaminoethyl)-HPLC. To introduce a ^{35}S-label to the polysaccharides or oligosaccharides, [^{35}S]PAPS replaced unlabeled PAPS. 3-*O*-[^{35}S]sulfated heparin was prepared by incubating heparin with 3-OST-5 enzyme and [^{35}S]PAPS, and the product was purified by DEAE chromatography.

The procedures for preparing the *N*-sulfo heparosan, PAPS and [^{35}S]PAPS, UDP-GlcNTFA and disaccharide (GlcA-AnMan) starting materials are described elsewhere [82, 91, 94]. The enzymes used for the synthesis, including KfiA, pmHS2, NST, C_5-epi, 2-OST, 6-OST-1, 6-OST-3 and 3-OST-1, were expressed in *E. coli* as described previously [92].

Stabilin expression plasmids

The cDNA for human Stab1 (a kind gift of J. Kzhyshkowska, University of Heidelberg) and Stab2/315-HARE were ligated into the MCS of the pcDNA5/FRT/V5-6xHIS-TOPO vector. The Stab2/190-HARE cDNA encoding the C-terminal 1416 aa is cloned in pSecTag/FRT/V5-6xHIS-TOPO, which provides a secretion signal for the 190-HARE protein [95]. Plasmids encoding the secreted ecto-domain were generated by single primer deletion mutagenesis [96] in which the transmembrane and cytoplasmic domain encoding regions were deleted, and the resulting plasmids were then used to create stable cells which secreted properly folded and functional ecto-domains in the medium. The ecto-domains comprised amino acids M1-P2475 for Stab1, M1-T2458 for Stabilin-2/315-HARE, and S1136-V2453 for Stab2/190-HARE.

Endocytosis assays

Stably transfected cells expressing Stab-1 or Stab-2 receptors or only Hygromycin B resistant (empty vector, EV) were plated in 24-well dishes and grown in DMEM with 8% FBS and 50 µg/mL Hygromycin B for at least 2 days prior to the experiments. The cells were incubated at 37˚C for 3 h with fresh Endocytosis Medium supplemented with labeled ^{35}S-HS constructs (2.0 x 10^4 cpm/mL). For those experiments utilizing AT, the ^{35}S-HS constructs were pre-incubated with AT (0.2 mg/mL) for 30 min prior to diluting ten-fold in endocytosis medium. Specific binding or endocytosis was assessed in the presence of excess unlabeled heparin (0.1 mg/mL) to determine background cpm (counts per minute) values. These values were subtracted from all data points to determine specific ^{35}S-HS endocytosis. At the termination times, cells were washed three times with ice-cold Hank's buffered saline

solution, lysed in 0.3 N NaOH, and radioactivity and protein content were determined and expressed as cpm/µg protein ± standard deviation of the mean. ^{35}S radioactivity of all samples was measured by a Beckman-Coulter LS6500 scintillation counter. Non-specific binding/background radiation levels were consistently between 16 and 20 cpm for all experiments.

Direct ectodomain binding assays

To assess direct protein-HS binding, ecto-domains of each receptor were expressed and secreted in stable cell lines. The ecto-domains were immunoprecipitated with a goat anti-V5 resin (Bethyl labs), washed with TBS and then incubated with 4.0×10^5 cpm of each ^{35}S-HS construct for 1.5 h under rotation. The resin was centrifuged, washed 3 times with TBS, then placed in scintillation fluid and quantified by a Beckman-Coulter LS6500 scintillation counter. The amount of protein on the resin was quantified by separation with 5% SDS-PAGE, blotted, probed with rabbit anti-V5 antibody (Bethyl labs), and images were captured on film.

Assessment of liver clearance

All animal procedures were approved by the IACUC of the University of Nebraska under the Association for Assessment and Accreditation of Laboratory Animal Care (AAALAC) guidelines. BALB/c mice were placed under general anesthesia (isoflurane) on a warming platform during the entire procedure. Once unconsciousness was confirmed, the mice were injected via the lateral tail vein using a 27G x 1/2 needle with 0.053 µCi ^{35}S-labeled HS construct. The radiolabeled material was allowed to circulate for 10 min, followed by abdominal exposure and severance of the descending aorta abdominalis for bleed out. The liver was collected, briefly washed to get rid of residual blood, cut into smaller (~0.1 g)

pieces, weighed and then homogenized with a PowerGen 125 (Fisher) tissue homogenizer in 0.75 mL 1% NP-40. Homogenized tissue was then spun at 12,000 x g for 2 min to clear out insoluble material, and supernatants were mixed with 4 mL scintillation fluid and counted.

Synthesis of pure pnp-tagged oligosaccharides

Oligosaccharides were elongated from a 1-*O*-(*para*-nitrophenyl) glucuronide (GlcA-pnp) monosaccharide (Sigma) using KfiA and pmHS2. The oligosaccharides were modified using 2OST, C5-epi, 6OSTs and 3OST-1. Controlled additions of GlcNAc and GlcNTFA sugars in the backbone to prepare a GlcNTFA-GlcA-GlcNS-GlcA-GlcNS pentasaccharide region allowed exploitation of the irreversible reaction mode of C5-epi on the underlined GlcA. This IdoA was then 2-*O*-sulfated. Next, the GlcNTFA was converted to a GlcNS and another GlcNTFA-GlcA was added to the nonreducing end so that the next GlcA could be converted to IdoA2S. Subsequent cycles prepared pure oligosaccharides that contained repeating GlcNS6S-IdoA2s regions. The reactions were purified using a C_{18} column (0.75 × 20 cm, Biotage), and the product was identified by its absorbance at 310 nm and later by mass spectroscopy.

Protamine reversibility assays

Quanitities of HS oligosaccharides that displayed 90% inhibition of factor Xa were incubated in a standard chromogenic anti-Xa assay with human serum and 0-2.6 µg/mL protamine. Anti-Xa activity was measured by the decrease in the rate of absorbance at 405 nm compared to a control sample without heparin.

Clearance profile of anti-Xa activity in rats

Male Sprague-Dawley rats were dosed with amounts of Lovenox or Arixtra having equivalent anti-Xa activity: 2.27 mg/kg for Lovenox and 0.2 mg/kg for Arixtra. The drugs were diluted in saline and injected subcutaneously at a volume of approximately 100 µL. Blood (approximately 50 µL) was collected from unanesthetized rats at set time intervals by the tail clip method, then spun down to isolate plasma. The plasma was subjected to anti-Xa activity assays. All rat procedures were approved by the UNC IACUC.

Anti-Xa activity in mice

Male BALB/c mice from Charles River Laboratories were injected subcutaneously with 100 nmoles of oligosaccharide per kg body weight. The oligosaccharides were diluted in saline and the injection volume was approximately 100 µL. Thirty minutes after injection, the mice were sacrificed with a CO_2 chamber and approximately 0.5 mL of blood was immediately drawn by cardiac puncture. The blood samples were centrifuged to obtain plasma, which was used for analysis of anti-Xa activity. Plasma from mice injected with saline was used as a control.

CHAPTER III

REDUCTION OF PLATELET FACTOR 4 BINDING TO HEPARAN SULFATE

One of the most dangerous side effects associated with the use of heparin is heparin-induced thrombocytopenia, or HIT. HIT results in platelet degradation and a prothrombotic state and occurs in up to 5% of patients receiving unfractionated heparin [97]. HIT is initiated by the formation of HS-platelet factor 4 complexes that are recognized by platelet-activating antibodies to invoke an immune response [98]. Thus, decreased binding between HS and PF4 could prevent the formation of these complexes and the likelihood of HIT.

Platelet factor 4 (PF4) belongs to the CXC family of chemoattractant chemokines. The interaction between HS and PF4 is mediated by negatively charged sulfo groups on the HS backbone interacting with positively charged residues on the PF4 protein, which is released from alpha-granules upon vascular injury [99]. However, little is known about the specific HS sulfation patterns and length required for this interaction. Based on a preliminary examination of HS-PF4 binding in our laboratory, we hypothesized that the removal of 6-*O*-sulfation should reduce the binding of HS to PF4. Sulf-2, a 6-*O*-endosulfatase, is known to remove these negatively charged 6-*O*-sulfo groups from HS, and its role in mediating HS-PF4 binding was investigated. The substrate specificity of Sulf-2 was also explored.

The Sulfs are known to have endosulfatase activity and remove 6-*O*-sulfo groups from HS [100, 101]. Two Sulf enzymes (Sulf-1 and Sulf-2) have been identified, cloned and expressed in several cell lines [100-104]. The two Sulfs appear to be functionally redundant and have varied roles in cell signaling, development and cancer. The Sulfs

promote some signaling pathways, such as Wnts [100, 105, 106], bone morphogenic protein [107] and glial cell-derived neurotrophic factor [108] while inhibiting others, such as fibroblast growth factor-2 [109, 110] and transforming growth factor-β [111]. Gene knockdown [100] and knock-out studies [108, 112-114] have shown the importance of Sulfs in development; these mice show aberrant growth, muscle innervation, skeletal tissue, and lung development. In cancer, Sulfs are believed to possess both pro-oncogenic [115-117] and tumor suppressing [110, 118, 119] activities. Overexpression of Sulf-2 in particular was recently found to promote carcinogenesis in non-small-cell lung carcinomas, pancreatic cancer and hepatocellular carcinoma [120, 121]. Sulf-2 also regulates receptor tyrosine kinase pathways and tumor growth in glioblastoma [122], making it an attractive target for cancer therapy.

The Sulfs are understood to cleave 6-*O*-sulfo groups from trisulfated (*N*-, 2-*O*- and 6-*O*-sulfated) disaccharides [101]. However, the extent of their substrate specificity and their ability to recognize other disaccharides is not well understood, largely due to the fact that polysaccharides with defined sulfation types were unavailable. In previous studies, only substrates containing this trisulfated motif have been used to test Sulf-2 activity [101, 123]. Utilizing our ability to control the sulfation types in HS polysaccharides using biosynthetic enzymes [37], we enzymatically synthesized ^{35}S-labeled polysaccharides that allowed us to test Sulf-2's ability to recognize other disaccharide motifs. In addition, we investigated the effect of Sulf-2 treatment on the ability of HS to bind to antithrombin (AT) and PF4. Binding to antithrombin is what confers anticoagulant activity to HS: when heparin binds antithrombin, it induces a conformational change that increases antithrombin's affinity for proteases in the blood coagulation cascade, including factors Xa and IIa. This inhibits the downstream production of fibrin and fibrous clots.

In addition to the distribution of negative charges, we hypothesized that the size of HS contributes to its PF4 binding affinity. We investigated the relationship between the

length of HS oligosaccharides and their interaction with PF4 and coagulation factors. An AT-binding pentasaccharide sequence is sufficient for anti-Xa activity, but if the HS chain is long enough, it is capable of forming a ternary complex with antithrombin and factor IIa (also called thrombin). The ratio between factor IIa and Xa activity is an important component of heparin drugs: activity against both coagulation factors is preferred, as it is expected to infer more reliable anticoagulation. Previous studies indicated that to obtain anti-IIa activity, a heparin fragment of approximately 5,000 Da (roughly an 18-mer) was necessary [124]. Our group prepared a set of oligosaccharides ranging from a 15- to 21-mer to investigate the minimum length requirement for anti-IIa activity, and the PF4 binding capabilities of these oligosaccharides were tested. This information could be useful in designing heparins with a high anti-IIa/-Xa ratio and reduced PF4 binding.

Substrate specificity of Sulf-2

The Sulf-2 enzyme was transiently expressed in CHO cells to obtain the Sulf-2 protein for the substrate specificity study. The recombinant Sulf-2 enzyme was detected in both the cell lysate and in the conditioned medium, as measured by western blot analysis (Fig. 3.1D). The recombinant Sulf-2 enzyme was harvested from the conditioned medium of transfected CHO cells. To test the activity of the crude protein, [^{35}S]HS isolated from CHO cells that had been metabolically labeled with sodium [^{35}S]sulfate was subjected to Sulf-2 treatment. The resultant HS was digested with heparin lyases to disaccharides for disaccharide compositional analyses. The HPLC chromatograms of the disaccharide analysis of Sulf-2-treated, empty vector-treated and untreated [^{35}S]HS samples (Fig. 3.1) show a clear decrease in the trisulfated ΔUA2S-GlcNS6S peak in the Sulf-2-treated sample with an increase of the corresponding free [^{35}S]sulfate and ΔUA2S-GlcNS peaks. This suggested that the enzyme was indeed active, and it could remove 6-*O*-sulfo groups located on UA2S-GlcNS6S disaccharides as described in previously published reports [101, 123].

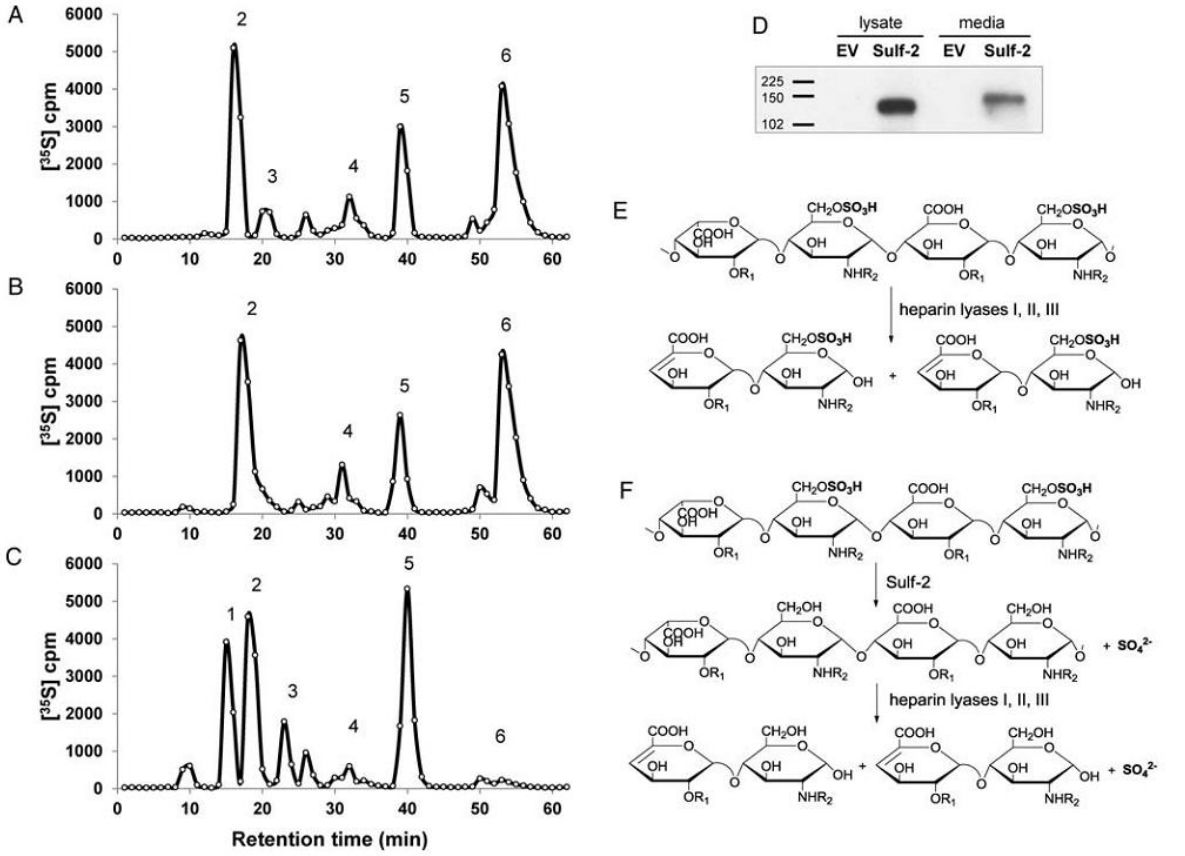

Figure 3.1. Disaccharide composition of Sulf-2-treated and untreated [^{35}S]HS. [^{35}S]HS from CHO cells was digested with heparin lyases and analyzed by RPIP-HPLC. **A.** Disaccharide composition of untreated [^{35}S]HS. Peak 2, ΔUA-GlcNS; peak 3, ΔUA-GlcNac6S; peak 4, ΔUA-GlcNS6S; peak 5, ΔUA2S-GlcNS; peak 6, ΔUA2S-GlcNS6S. **B.** Disaccharide composition of EV-treated [^{35}S]HS. Peak 2, ΔUA-GlcNS; peak 4, ΔUA-GlcNS6S; peak 5, ΔUA2S-GlcNS; peak 6, ΔUA2S-GlcNS6S. **C.** Disaccharide composition of Sulf-2-treated [^{35}S]HS. Peak 1, free sulfate; peak 2, ΔUA-GlcNS; peak 3, ΔUA-GlcNac6S; peak 4, ΔUA-GlcNS6S; peak 5, ΔUA2S-GlcNS; peak 6, ΔUA2S-GlcNS6S. **D.** Western blot showing presence of the Sulf-2 protein. Cell lysates (30 µg) and CM were separated on 12% SDS-PAGE, blotted to nitrocellulose and probed with anti-myc antibody. EV, empty vector-tranfected cells. **E.** Lyase degradation products of [^{35}S]HS. R_1=H/SO_3H, R_2=H/SO_3H/Ac. **F.** Lyase degradation products of Sulf-2-treated [^{35}S]HS. R_1=H/SO_3H, R_2=H/SO_3H/Ac. Cleavable groups are shown in bold.

Having determined that Sulf-2 was active, we sought to determine with greater detail which polysaccharide substrates could function as substrates for the enzyme. To this end, a series of polysaccharides carrying different sulfation types with or without IdoA were prepared using an enzymatic approach, as demonstrated in Fig. 3.2. A ^{35}S-label was strategically introduced to a specific site by a sulfotransferase, facilitating the identification of which sulfo groups were removed by Sulf-2. For example, construct **1**, IdoA2S-[6-*O*-^{35}S]GlcNS6S, carried the 6-*O*-[^{35}S]sulfo group at the *N*,6-*O*-sulfo glucosamine (GlcNS6S) unit. Thus, a release of [^{35}S]sulfo groups from construct **1** after Sulf-2 treatment unambiguously indicated that a 6-*O*-desulfation reaction occurred. Construct **1** was prepared by incubating deacetylated heparosan with unlabeled PAPS and NST, 2OST and C_5-epi in subsequent steps. This compound was ^{35}S-labeled at the 6-*O* position using [^{35}S]PAPS and 6OST. The rest of the constructs (**2-9**) were prepared in a similar fashion using recombinant enzymes, as shown in the synthetic scheme (Fig. 3.2). The structure of each substrate was confirmed by disaccharide analysis as described previously [125].

A disaccharide analysis of the Sulf-2-treated substrate was also performed for each construct. The HPLC analysis of untreated and Sulf-2 treated construct **1** is shown as an example in Fig. 3.3. The presence of the trisulfated peak, ΔUA2S-GlcNS6S, is nearly completely eliminated by treatment with the Sulf-2 enzyme. The reduction of this peak is balanced by the appearance of a large free sulfate peak in the treated sample. In addition, there is a partial decrease in the ΔUA-GlcNS6S peak that contributed to the free sulfate peak.

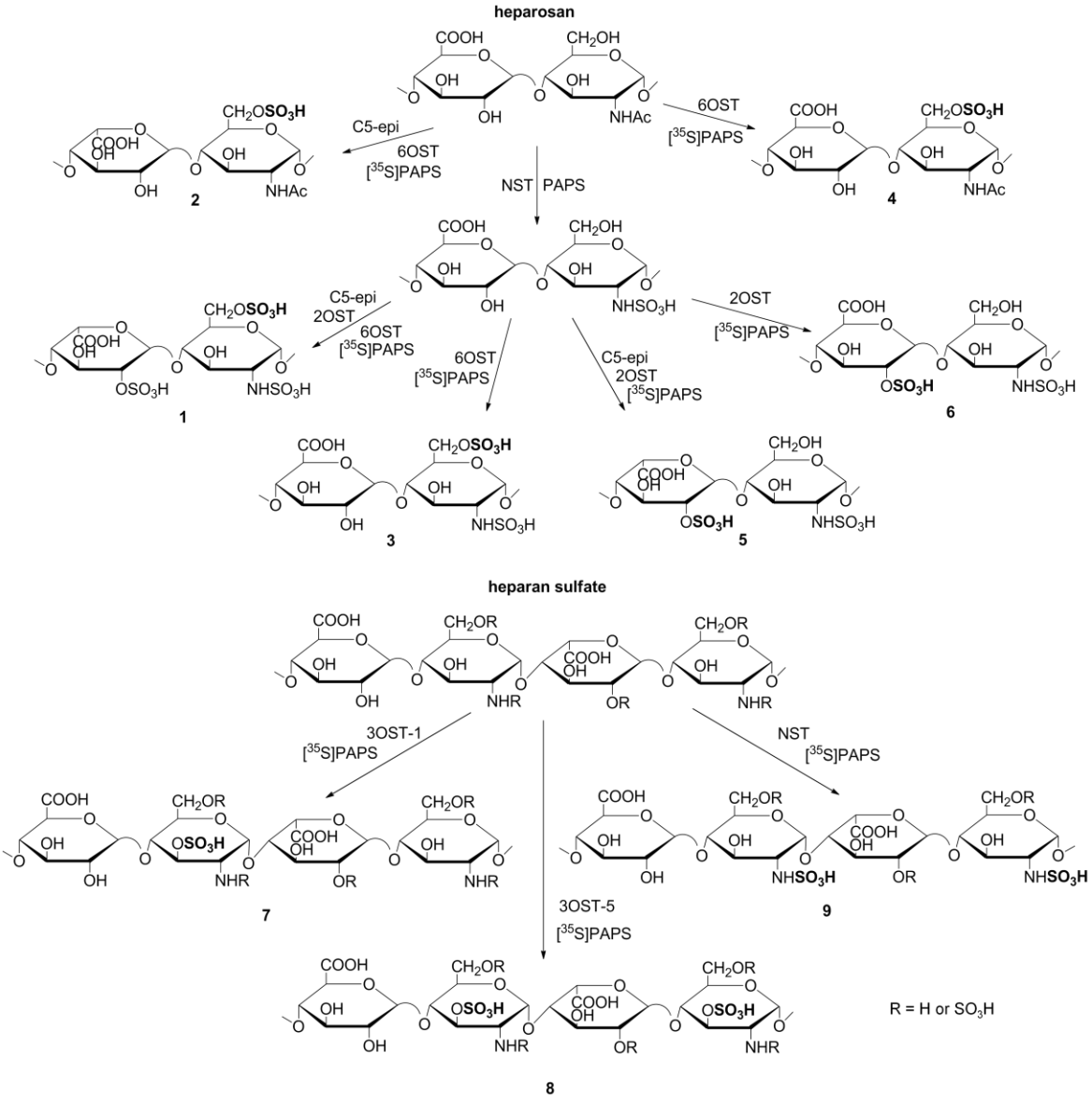

Figure 3.2. Synthetic scheme for the ^{35}S-labeled HS constructs. Heparosan or heparan sulfate were treated with heparan sulfate biosynthetic enzymes and PAPS to achieve the desired sulfation groups and epimerization of the uronic acid. In heparan sulfate, both GlcA and IdoA are present. ^{35}S-labeled groups are shown in bold.

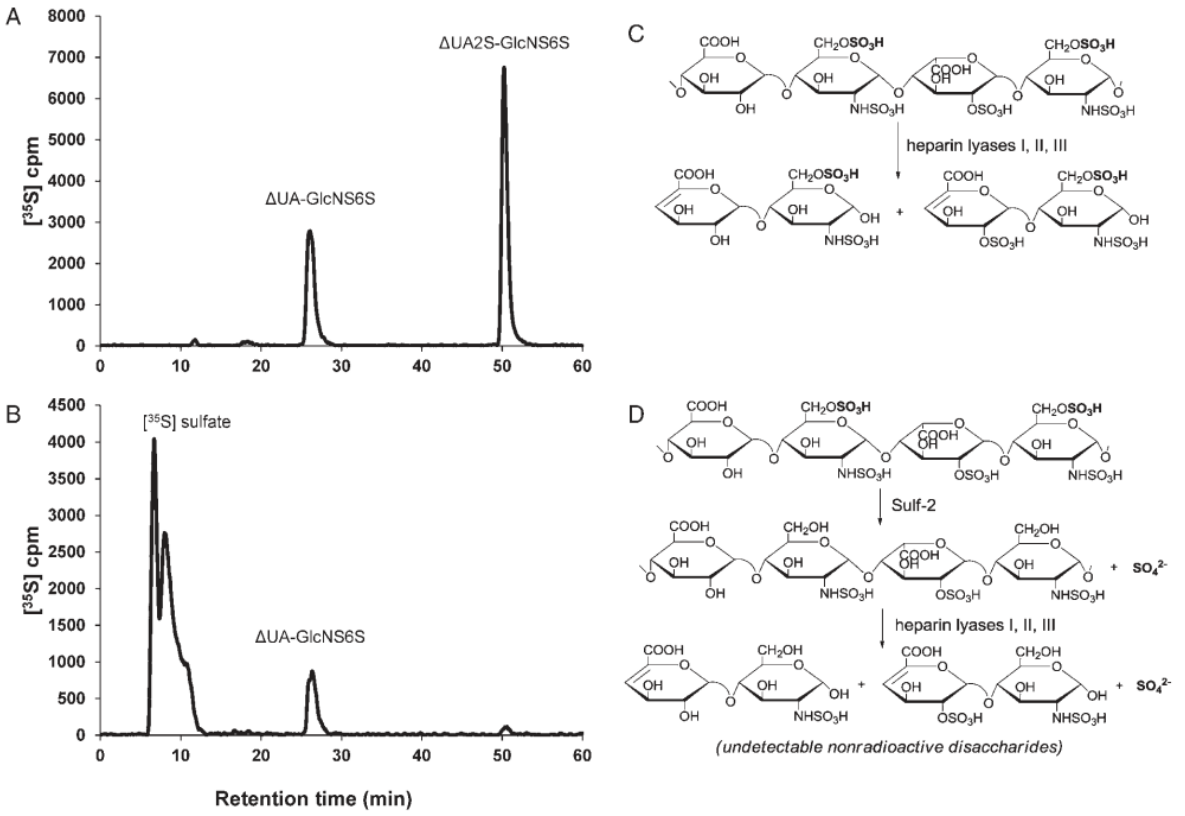

Figure 3.3. Disaccharide analysis of construct 1 before and after Sulf-2 treatment. Construct 1 is IdoUA2S-[6-*O*-^{35}S]GlcNS6S, the best Sulf-2 substrate. **A.** Disaccharide composition of construct 1. **B.** Disaccharide composition of Sulf-2-treated construct 1; disaccharides without ^{35}S-labeled groups are not detected. **C.** Lyase degradation products of construct 1. **D.** Lyase degradation products of Sulf-2-treated construct 1. Cleavable groups are shown in bold.

To quickly quantify the activity of Sulf-2 against the different substrates, spin column assays were performed. Here, the column separates the analytes based on the size of the molecule. We anticipated that the [^{35}S]sulfate would be trapped in the column while the intact polysaccharides would pass through the column without retardation. Substrates were incubated overnight in the presence of Sulf-2 or water as a control, and the samples were purified by QuickSpin column to determine how much ^{35}S-radioactivity had been converted to smaller [^{35}S]sulfate. The results from the spin column assays are shown in Table 3.1. From these assays, it is clear that the best substrate for Sulf-2 is the polysaccharide

containing *N*-, 2-*O*- and 6-*O*-sulfations. Further analysis of the susceptibility of the different sulfated polysaccharides to [^{35}S]sulfate release permitted us to dissect the substrate specificities of Sulf-2.

construct name	**repeating disaccharide structure**	**[^{35}S]sulfation level (nmoles/ug polysaccharide)**	**control [^{35}S] sulfate release (%)**	**Sulf-2-treated [^{35}S] sulfate release (%)**
1	[-IdoA2S-[6-*O*-^{35}S]GlcNS6S-]$_n$	1.7	2.7 ± 1.0	97.5 ± 0.8
2	[-IdoA-[6-*O*-^{35}S]GlcNS6S-]$_n$	1.9	8.3 ± 0.1	24.3 ± 2.7
3	[-GlcA-[6-*O*-^{35}S]GlcNS6S-]$_n$	1.4	6.6 ± 1.6	43.1 ± 2.4
4	[-GlcA-[6-*O*-^{35}S]GlcNAc6S-]$_n$	0.1	14.2 ± 3.5	28.1 ± 1.3
5	[-[2-*O*-^{35}S]IdoA2S-GlcNS-]$_n$	1.1	10.4 ± 2.6	12.6 ± 1.3
6	[-[-2-*O*-^{35}S]GlcA2S-GlcNS-]$_n$	1.3	6.7 ± 1.9	13.7 ± 3.0
7	3-*O*-[^{35}S]HS (consisting of -GlcA-[3-*O*-^{35}S]GlcNS3S±6S- domains)	1.1	13.6	12.2
8	3-*O*-[^{35}S]HS (consisting of -IdoA2S-[3-*O*-^{35}S]GlcNS3S±6S- and -GlcA-[3-*O*-^{35}S]GlcNS3S±6S- domains)	0.8	10.1	13.9
9	*N*-[^{35}S]sulfated HS	1.6	11.7	13.2

Table 3.1. Substrate specificity of Sulf-2. Synthetic substrates were incubated with or without the Sulf-2 enzyme and isolated from released sulfate groups by QuickSpin column. The remaining [^{35}S]sulfate on the polysaccharide was quantified with a scintillation counter.

The susceptibility of the nine HS constructs to sulfatase activity indicated that in addition to trisulfated disaccharides, Sulf-2 is able to desulfate the 6-*O*-sulfo group on a GlcNS6S disaccharide that is flanked by a nonreducing-end GlcA or IdoA residue (constructs **2** and **3**). Construct **4**, which contained GlcA-GlcNAc6S groups, experienced a slight loss of 6-*O* sulfo groups. The inability of Sulf-2 to remove sulfo groups from **5**-**9** confirms that Sulf-2 cannot desulfate from the *N*-, 2-*O*- or 3-*O* positions.

Effect of Sulf-2 treatment on PF4 and antithrombin binding

To assess whether Sulf-2 could decrease the binding of HS to PF4, [^{35}S]HS prepared from CHO cells was used due to its high specific [^{35}S] radioactivity. A dot blot membrane binding assay was used to compare the PF4 binding capabilities of Sulf-2-treated and untreated HS (Fig. 3.4A). The wells contained 6,000 cpm of Sulf-2-treated or untreated [^{35}S]HS with increasing amounts of PF4. [^{35}S]HS bound to PF4 was captured by the nitrocellulose membrane. The untreated samples reached a maximum binding of 66% with 152 nM PF4, but the Sulf-2-treated samples bound only up to 3.1% with 608 nM PF4. From the two binding curves, it is apparent that Sulf-2 treatment can reduce the binding of HS to PF4 by over ten-fold.

AT-binding HS was prepared by incubating HS from bovine kidney with 3OST-1 and [^{35}S]PAPS. A Sulf-2-treated fraction was prepared by incubating this material with Sulf-2. Concanavalin A (ConA)-Sepharose beads were incubated with AT and HS, and the AT-bound HS fraction was eluted using a 1 M NaCl solution (Fig. 3.4). When the treated and untreated fractions were incubated with ConA-Sepharose and AT, 52% of the untreated fraction and 44% of the Sulf-2-treated fraction were recovered, suggesting that Sulf-2 does not remove critical 6-*O*-sulfo groups from the AT-binding pentasaccharide within the polysaccharide. [*N*-^{35}S]HS, which does not considerably bind AT, was used as a negative control.

For a more quantitative assessment of the effect of Sulf-2 treatment on the binding affinities of HS to AT and PF4, affinity co-electrophoresis was performed. This is an established method for determining the affinity constant of radiolabeled polysaccharide ligands with proteins [85]. The mobility of each lane is determined, and the protein concentration in each lane can be used to determine a K_d value based on the Scatchard equation. For antithrombin, gels containing serial dilutions from 0-3.2 µM AT were prepared

and 50,000 cpm of the AT-binding fraction of 3OST-1-treated [^{35}S]HS from CHO cells was added. The gel was run for 2 h, dried overnight, imaged and analyzed using ImageQuant TL software. For the untreated and treated samples, a plot of R/[AT] vs. R gave linear slopes of y=-0.0949x + 0.048 (R^2=0.87) and y=-0.094 + 0.44 (R^2=0.95), respectively. These correspond to K_d values of 10.5 and 10.6 nM, indicating that the binding affinity of HS to AT is unaffected by treatment with Sulf-2.

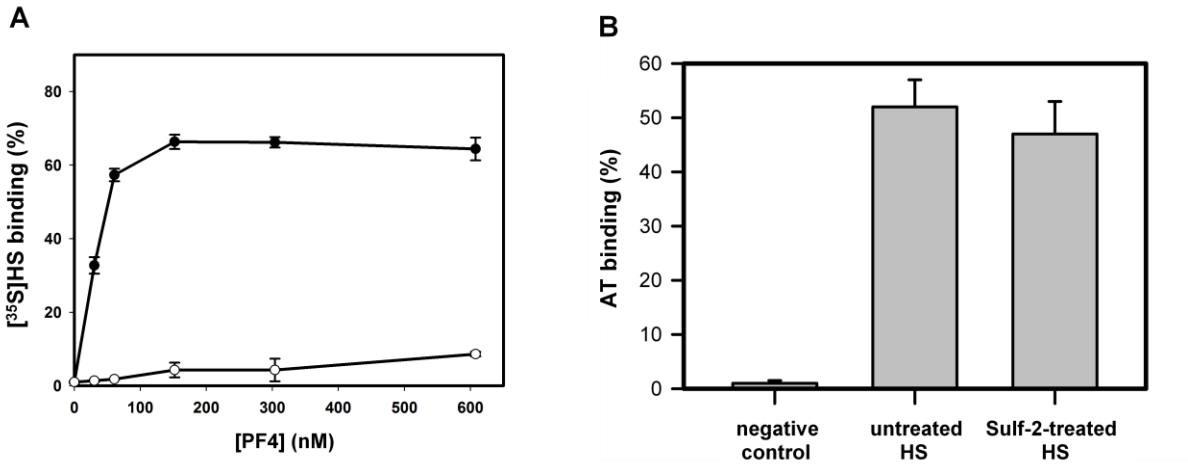

Figure 3.4. Effect of Sulf-2 treatment on PF4 and AT binding. **A.** PF4 binding assay comparing Sulf-2-treated and untreated radiolabeled heparan sulfate. [^{35}S]HS obtained from CHO cells was incubated with varying amounts of PF4, and the solutions were directly applied to a nitrocellulose membrane. The membrane was then washed and subjected to radioactivity analysis using a scintillation counter. Filled circles: untreated HS; open circles: Sulf-2-treated HS. **B.** [^{35}S]HS was incubated with 0.1 mg/mL AT, and the complex of AT and HS was captured using ConA-Sepharose beads. The AT-binding [^{35}S]HS was prepared by incubating HS from bovine kidney with the 3OST-1 enzyme and [^{35}S]PAPS.

For PF4, serial dilutions of 0-1.41 µM PF4 were used, and 50,000 cpm of 3OST-1-treated [^{35}S]HS from CHO cells was added to each gel. The gels were run for 2.5 h and analyzed as above. Linear regression slopes of y=-0.1627x + 0.1238 (R^2=0.77) and y=-0.0085x + 0.0037 (R^2=0.74) were calculated for the untreated and treated substrates,

respectively. These correspond to K_d values of 5.47 and 117.6 nM, showing that the binding affinity of HS for PF4 is decreased approximately 20-fold by treatment with Sulf-2. Taken together, our data suggest that Sulf-2 treatment decreases the binding affinity of HS to PF4 while the affinity to AT remains intact.

	untreated [^{35}S]HS	**Sulf-2-treated [^{35}S]HS**
AT	10.5 nM	10.6 nM
PF4	5.5 nM	118 nM

Table 3.2. Binding affinities of Sulf-2-treated and untreated HS to PF4 and AT. K_d values were determined by affinity co-electrophoresis.

The lack of impact on AT binding led us to question whether the 3-*O*-sulfated glucosamine residue present at the center of the AT-binding pentasaccharide in HS was affected by Sulf-2 [126]. We compared the disaccharide composition of 3-*O*-[^{35}S]sulfated HS with and without Sulf-2 treatment (Fig. 3.5). The disaccharide analysis revealed the presence of three 3-*O*-sulfated disaccharides: Glc-AnMan3S, IdoA2S-AnMan3S and GlcA-AnMan3S6S. We observed that the level of the disaccharide GlcA-AnMan3S6S in the Sulf-2-treated sample was decreased to 38% from 51%, suggesting that Sulf-2 removed a 6-*O*-sulfo group from the 3-*O*-sulfated glucosamine residue. However, the removal of this 6-*O*-sulfo group from the 3-*O*-sulfated glucosamine residue has no impact on the binding affinity to antithrombin. This observation is consistent with the fact that AT-binding HS is composed of a disaccharide unit of GlcA-GlcNS3S (without a 6-*O*-sulfo group in the disaccharide unit) and GlcA-GlcNS3S6S (with a 6-*O*-sulfo group in the disaccharide unit) [127].

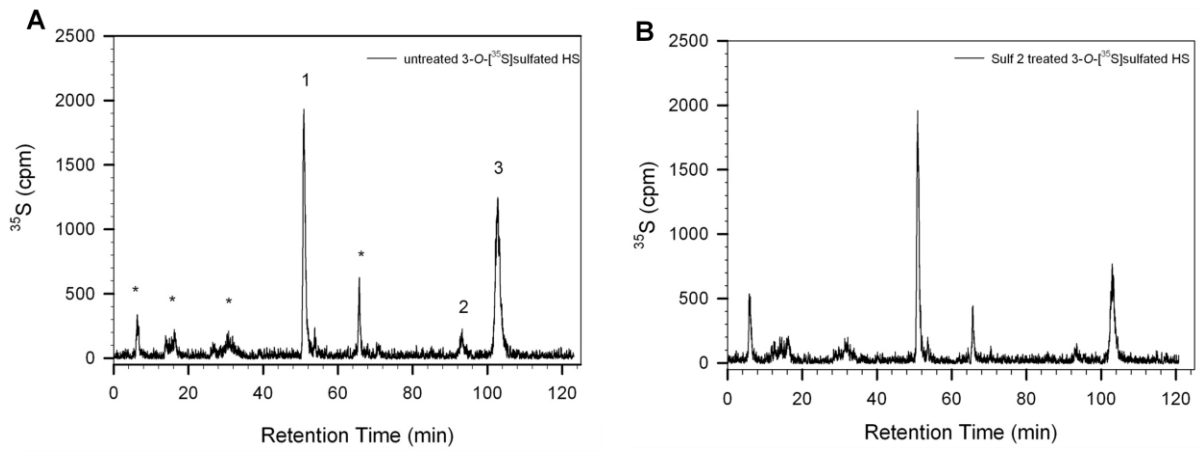

Figure 3.5. Disaccharide analysis of 3-*O*-sulfated HS with and without Sulf-2 treatment. The 3-*O*-[^{35}S]sulfated HS was prepared by incubating HS with purified 3-OST-1 enzyme and [^{35}S]PAPS. A portion of the 3-*O*-[^{35}S]sulfated HS was treated with Sulf-2. Both Sulf-2-treated and untreated HS were subjected to deacetylation with hydrazine followed by nitrous acid degradation at pH 4.5 and 1.5. The resultant disaccharides were analyzed by HPLC. Panel A shows the chromatogram of the analysis of untreated 3-*O*-[^{35}S]sulfated HS. Panel B shows the chromatogram of the analysis of Sulf-2-treated 3-*O*-[^{35}S]sulfated HS. The elution positions were identified by eluting with standards: 1 represents GlcA-AnMan3S, 2 represents IdoA2S-AnMan3S and 3 represents GlcA-AnMan3S6S. * indicates the unidentified components.

PF4 binding of oligosaccharides with anti-IIa activity

A small library of oligosaccharides was prepared by Dr. Yongmei Xu to investigate the relationship between the number of saccharide units and the anti-IIa/-Xa ratio [128]. The synthesis of these oligosaccharides was prepared by a novel method in which a disaccharide starting material (obtained by the degradation of heparosan) is sequentially incubated with HS elongation enzymes (KfiA and pmHS2) and UDP-sugars (UDP-GlcNAc or UDP-GlcNTFA and UDP-GlcA) to add one saccharide unit per step to the HS backbone. The backbone can then be sulfated using HS biosynthetic enzymes as previously described.

The PF4 binding characteristics of four oligosaccharides ranging from a 15-mer to a 21-mer, some showing anti-IIa activity, were examined. The structures of the four oligosaccharides are shown in Table 3.3.

compound	structure	anti-IIa/-Xa
10, 15-mer	GlcNS6S-(IdoA2S-GlcNS6S)$_2$-GlcA-GlcNAc6S-GlcA-GlcNac6S-GlcA-GlcNS6S3S-IdoA2S-GlcNS6S-GlcA-AnMan	N/A
11, 17-mer	GlcNS6S-(IdoA2S-GlcNS6S)$_3$-GlcA-GlcNAc6S-GlcA-GlcNac6S-GlcA-GlcNS6S3S-IdoA2S-GlcNS6S-GlcA-AnMan	N/A
12, 19-mer	GlcNS6S-(IdoA2S-GlcNS6S)$_4$-GlcA-GlcNAc6S-GlcA-GlcNac6S-GlcA-GlcNS6S3S-IdoA2S-GlcNS6S-GlcA-AnMan	1:5
13, 21-mer	GlcNS6S-(IdoA2S-GlcNS6S)$_5$-GlcA-GlcNAc6S-GlcA-GlcNac6S-GlcA-GlcNS6S3S-IdoA2S-GlcNS6S-GlcA-AnMan	1:2

Table 3.3. Chemical structure and anti-IIa/-Xa ratio of synthetic oligosaccharides. The AT-binding domain is shown in red. AnMan,anhydromannitol.

Using the dot blot assay, we determined that all compounds bound to PF4; however, the oligosaccharides bound to PF4 to a lower extent than full-length HS (Fig. 3.6A). It should be noted that ULMW heparin 1 (a 7-mer) did not bind to PF4, consistent with the previous finding indicating that the minimum size of HS oligosaccharides that bind to PF4 is an octasaccharide [129, 130]. Furthermore, the use of fondaparinux, a synthetic ULMW heparin, effectively eliminates the risk of heparin-induced thrombocytopenia [131, 132].

Next, we compared the binding affinity between the oligosaccharides and full-length heparin using a PF4 neutralization assay [129]. In this experiment, heparin and the oligosaccharides were incubated with AT and Xa. Under these conditions, the activity of Xa is low because of the presence of AT-saccharide complexes. Upon the addition of PF4 to

the reaction mixture, PF4 displaced AT by interacting with the oligosaccharides. Consequently, AT lost the ability to inhibit the activity of Xa. As shown in Fig. 3.6B, PF4 effectively neutralized the inhibition effect of heparin at an ED_{50} of ~1.2 μg/mL. In contrast, compound **13** displayed a much higher ED_{50} (3.4 μg/mL), suggesting that the synthesized *21-mer* has reduced binding affinity for PF4. As expected, PF4 was unable to neutralize the anti-Xa activity of ULMW heparin 1 because ULMW heparin 1 does not bind to PF4.

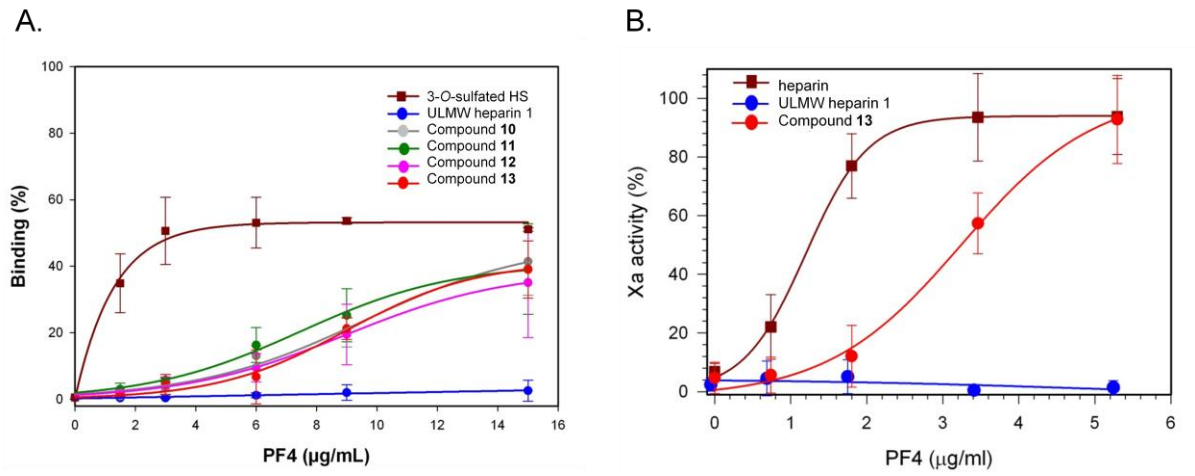

Figure 3.6. Determination of the binding of PF4 to *O*-sulfated oligosaccharides. **A.** Binding between the ^{35}S-labeled oligosaccharides and PF4 using a dot blot assay. ^{35}S-labeled oligosaccharides were incubated with increasing amounts of PF4 and spotted onto a nitrocellulose membrane. Complexes of PF4 and ^{35}S-labeled oligosaccharide were captured by the membrane, excised, and quantified using a scintillation counter. 3-*O*-Sulfated [^{35}S]HS was used as a positive control, and it was prepared by incubating HS from bovine kidney and purified 3-OST-1 enzyme in the presence of [^{35}S]PAPS. **B.** Neutralizing effects of PF4 on the anti-Xa activity of compound **13**, heparin, and ULMW heparin 1. The HS compounds were incubated with AT and varying amounts of PF4 before the addition of Xa. AT inhibited the activity of Xa by binding to HS; PF4 competed with AT for binding to HS and therefore neutralizes the anti-Xa activity of AT. Chromogenic substrate was added to the mixture, and the rate of increase in the absorbance at 405 nm was used to determine Xa activity.

The ability of the compounds to bind AT was confirmed by affinity co-electrophoresis. If a portion of the compound mixture is unable to bind AT, two bands are expected on the gel: an AT-binding portion that is retarded at the top of the lane, and a non-binding portion

that travels partway through the lane. The complete retardation of our compounds at different concentrations of AT indicates that all of the mixture bound AT.

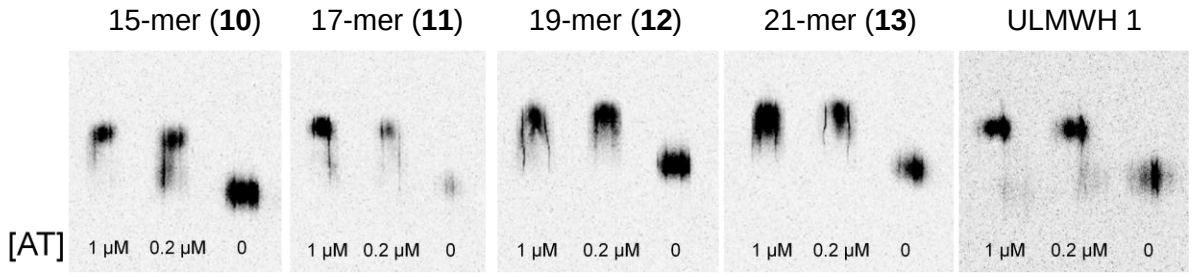

Figure 3.7. Determination of the binding of compounds **10**-**13** to AT using affinity co-electrophoresis. The ^{35}S-labeled compounds were loaded onto the lanes with different concentrations of AT. After performing the electrophoresis, the gels were imaged by phosphoimager. The ^{35}S-labeled compounds were retarded due to the binding of AT and the oligosaccharides. ULMWH-1 represents the ultra-low molecular weight heparin 1, a pure heptasaccharide with a structure of GlcNAc6S-GlcA-GlcNS3S6S-IdoA2S-GlcNS6S-GlcA-AnMan [92]. The ULMWH1 was used as a positive control because it was expected to bind AT completely under this condition.

Conclusions

The results herein present two methods to produce anticoagulant HS with reduced binding to PF4: treatment with Sulf-2 and limited oligosaccharide length. These methods can aid in the design of heparin drugs with a lower incidence of HIT.

Understanding the full substrate specificity of Sulf-2 is of interest due to its involvement in development and cancer and its potential role in preparing HS structures. To address this issue, we synthesized nine HS polysaccharides with unique sulfation patterns and ^{35}S-labeled groups at a specific position. We determined which polysaccharide constructs acted as substrates for Sulf-2 based on their decrease in radioactivity after Sulf-2 treatment. We found that, as previously understood, trisulfated IdoA2S-[6-*O*-^{35}S]GlcNS6S regions served as an excellent substrate for Sulf-2, showing approximately 90% removal of the radiolabeled group. In addition, this study found for the first time that disulfated UA-[6-*O*-

^{35}S]GlcNS6S units experienced hydrolysis of 6-*O*-sulfo groups. Sulfation at positions other than the 6-*O* position was unable to be removed by the enzyme. These results were determined by spin column assay and by HPLC analysis.

We also examined how Sulf-2 treatment affected binding to AT and PF4. Heparin interacts with AT through a specific AT-binding pentasaccharide: GlcNAc/NS6S-GlcA-GlcNS3S6S-IdoA2S-GlcNS6S. It appears from our results that Sulf-2 removes 6-*O*-sulfo groups that are not within the critical AT-binding region, allowing HS to maintain its interaction with AT. It should be noted that the importance of 6-*O*-sulfation for AT-binding is well documented. Atha and colleagues, using a series of synthetic pentasaccharides, demonstrated that a particular 6-*O*-sulfo group on the nonreducing end side of the 3-*O*-sulfated glucosamine residue contributed the AT binding energy nearly equal to that of the 3-*O*-sulfo group [133]. At the polysaccharide level, 6-*O*-sulfation is also important for AT-binding [37, 134]. The unique substrate specificity of Sulf-2 allows the removal of 6-*O*-sulfo groups that are nonessential for AT-binding. In addition, based on a ligand binding assay and affinity co-electrophoresis, we found that Sulf-2 treatment can reduce binding to PF4 on the order of 10- to 20-fold.

The study of oligosaccharides with anti-IIa activity is the first to demonstrate the enzymatic synthesis of HS oligosaccharides up to a 21-mer. These substrates showed that the minimum size requirement for anti-IIa activity is a 19-mer, with a 1:5 anti-IIa/-Xa ratio, and that a 21-mer has a 1:2 ratio. It should be noted that these oligosaccharides, though defined in size, are heterogeneous in their *O*-sulfation patterns; however, they represent a significant step forward in the enzymatic synthesis of HS. All of the oligosaccharides (up to 21 sugars in length) showed decreased binding to PF4 compared to full-length heparin in a dot blot protein binding assay, and the longest was less susceptible to PF4 neutralization than heparin in a chromogenic anti-Xa test. These results provide structural guidelines for new heparins with measurable anti-IIa activity and reduced PF4 interaction.

CHAPTER IV

IDENTIFICATION OF STABILIN-BINDING STRUCTURAL MOTIFS

Although heparin is one of the oldest drugs still in clinical use, its clearance from the body has remained poorly understood. Early studies on the clearance of heparin identified that UFH and LMWH bound and were internalized into lysosomes by human endothelial cells [135, 136], and it was later discovered that liver sinusoidal endothelial cells are the principal site for the clearance of UFH [137]. It is also known that UFH is eliminated via the liver and displays a fast clearance rate, while the pentasaccharide drug Arixtra is not and has a slow clearance rate *in vivo* [138]. Arixtra is instead cleared from the circulation by the kidneys, which makes its use in patients with renal impairment unsafe [79].

Recently, Stabilin-2 (Stab-2) was identified as a systemic clearance receptor for heparins [81]. Stabilin-2, also called HARE (hyaluronic acid receptor for endocytosis), is presented on the cell surface as two isoforms: a 315-kDa version and a 190-kDa version that is the product of proteolytic cleavage (Fig. 4.1.). Both receptors bind to heparin and participate in its clearance. The binding affinity of Stab-2 for UFH is higher than for LWMH, suggesting that the interaction between Stab-2 and heparins is dependent on the length of the carbohydrate chain. Stab-2 is responsible for the clearance of other glycosaminoglycans, such as hyaluronic acid and chondroitin sulfates, although the heparin binding site is known to be distinct from the LINK domain that binds these two substrates [90].

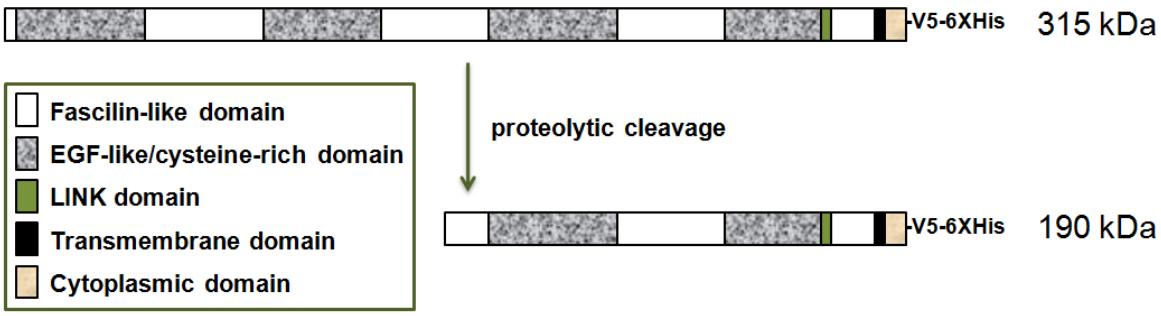

Figure 4.1. Domain structure of Stabilin-2.

Stabilin-1 (Stab-1) is a homolog of Stab-2, with 41% amino acid identity and 56% similarity. It has not been previously reported to bind heparins. Like Stab-2, Stab-1 is expressed in the endothelium of the liver, lymph node and spleen, but it is also uniquely expressed in activated macrophages and continuous endothelial vasculature [139, 140], suggesting that the receptor is immune responsive.

Based on the current understanding of the role of Stabilin-2 in clearing heparin, we hypothesized that the binding affinity between heparin and Stab-2 likely relates to the clearance rate of heparin. We prepared a series of HS poly- and oligosaccharides to probe the structural requirements for binding to Stab-2. In addition, we tested whether the homologous receptor Stabilin-1 is involved in heparin clearance.

Polysaccharide constructs

To investigate how sulfation patterns and IdoA content influenced binding to Stabilin receptors, ten polysaccharide constructs were chemoenzymatically prepared using

heparosan as a starting material. All constructs were *N*-[^{35}S]-labeled using NST and [^{35}S]PAPS. Subsequent sulfo groups were added using nonradiolabeled PAPS; thus, the cpm/µg was equal between the different constructs. The structures of the nine test constructs and the control (3-*O*-sulfo heparin) are shown in Fig. 4.2. Their structures were confirmed using disaccharide analysis.

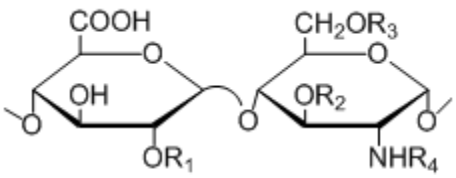

	R_1	R_2	R_3	R_4
14	H	H	H	**SO_3H**
15	H	H	SO_3H	**SO_3H**
17	SO_3H	H	H	**SO_3H**
20	SO_3H	H	SO_3H	**SO_3H**
22	SO_3H	SO_3H	SO_3H	**SO_3H**

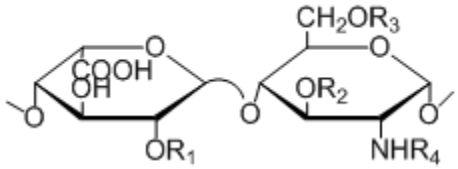

	R_1	R_2	R_3	R_4
16	H	H	SO_3H	**SO_3H**
18	SO_3H	H	H	**SO_3H**
19	SO_3H	H	SO_3H	**SO_3H**
21	SO_3H	SO_3H	SO_3H	**SO_3H**
23	SO_3H	**SO_3H**	SO_3H	SO_3H

Figure 4.2. Chemical structures of the polysaccharide constructs. The top left structure shows the disaccharide structure of constructs without IdoA, and the top right disaccharide represents IdoA-containing structures. The sulfo groups present for each construct are given in the table below. Bold groups indicate a ^{35}S-label.

Cell internalization assays

We tested the Stabilin-mediated cellular internalization of the ten polysaccharide constructs using Flp-In 293 cells. The cell lines were stably transfected with pcDNA5/FRT/V5-6xHIS-TOPO vectors for Stab-1, Stab-2/190-HARE and Stab-2/315-HARE. Transfected cells expressing the Stab-1 or Stab-2 receptors (or empty vector, Hygromycin B

resistant only) were plated in 24-well dishes in DMEM supplemented with 8% FBS and 50 µg/mL Hygromycin B and grown for at least two days prior to experiments. The radiolabeled constructs (2.0 x 10^4 cpm/mL) were added to the cell cultures with fresh medium and incubated for 3 h.

The control construct **23**, 3-*O*-sulfated heparin, was added to the cell lines to assess receptor binding and endocytosis (for structure, see Fig. 4.2). All three cell lines (Stab-1, Stab-2/190-HARE and Stab-2/315-HARE) internalized **23**, as measured by the cpm/µg protein of the cell lysate. The expression level of Stab-2/315-HARE was previously determined to be lower than that of Stab-2/190-HARE; thus, its HS internalization levels tend to be lower. The results of the assay clearly indicated that the cell lines were capable of internalizing radiolabeled heparin (Fig. 4.3).

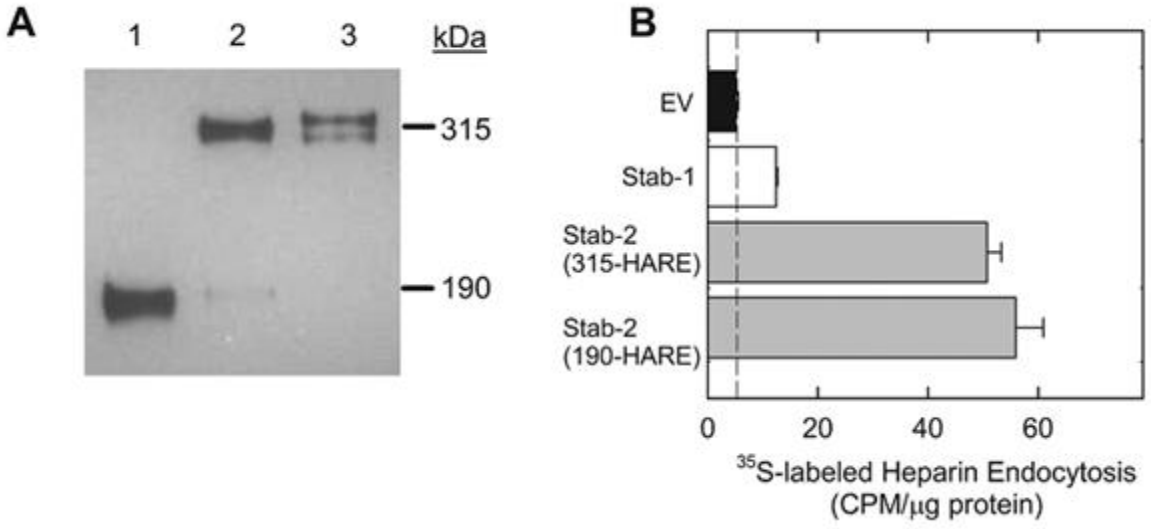

Figure 4.3. Internalization of 3-*O*-sulfated heparin by Stab-1 and -2. **A.** 20 µg of cell lysate was separated by 5% SDS-PAGE, blotted onto nitrocellulose and probed with anti-V5 antibody. Lane 1, Stab-2/190-HARE, 2, Stab-2/315-HARE, 3, Stab-1. **B.** Cell lines expressing Stab-1 (white bar), Stab-2/190-HARE and Stab-2/315-HARE (gray bars) or empty vector (black bar) were incubated with 3-*O*-[^{35}S]-labeled heparin for 3 h. The dotted line represents nonspecific binding. Endocytosis was measured as the cpm/µg cell lysate protein, mean ± s.d., n=3.

Having confirmed the applicability of the cell-based assay, the nine HS constructs were incubated with the three cell lines under the same conditions. In general, constructs with more sulfo groups were more readily internalized. Surprisingly, constructs **21** and **22**, which contained 3-*O*-sulfation, were endocytosed to a much higher extent than the other constructs (Fig. 4.4). Because 3-*O*-sulfation is a rare modification on HS, it is unlikely that the higher internalization was a simply a result of the charge density. Constructs that contained the same sulfo groups but differed in their IdoA content were not appreciably different in the internalization assay. At this time, we cannot conclude that there is any epimerization effect.

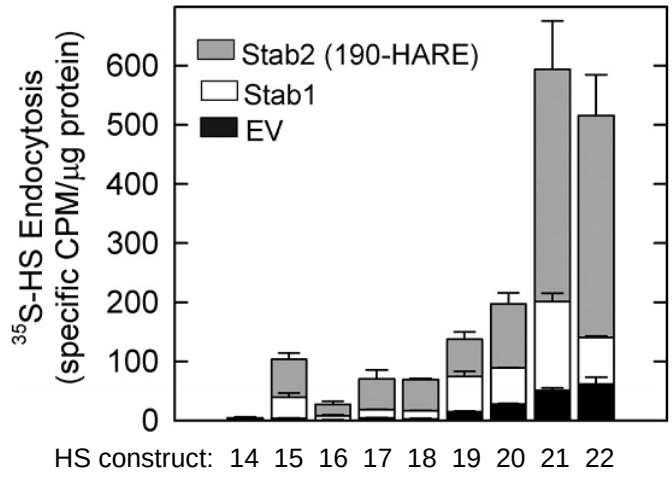

Figure 4.4. Internalization of modified HS polysaccharides. Empty vector, Stab-1 and Stab-2/190-HARE cell lines were incubated with HS constructs for 3 h. The cells were washed, and the [^{35}S] cpm/μg protein cell lysate was determined with scintillation counting. Mean ± s.d., n = 3.

Direct binding assay

The nine polysaccharide constructs were also tested for direct binding to purified Stabilin receptor ectodomains. The Stabilin receptors were isolated from the media of their respective cell lines using anti-V5 antibody coupled to Sepharose resin and were incubated

with the ^{35}S-labeled constructs. An empty vector cell line was used as a baseline for nonspecific binding due to the inherent “stickiness” of highly charged HS.

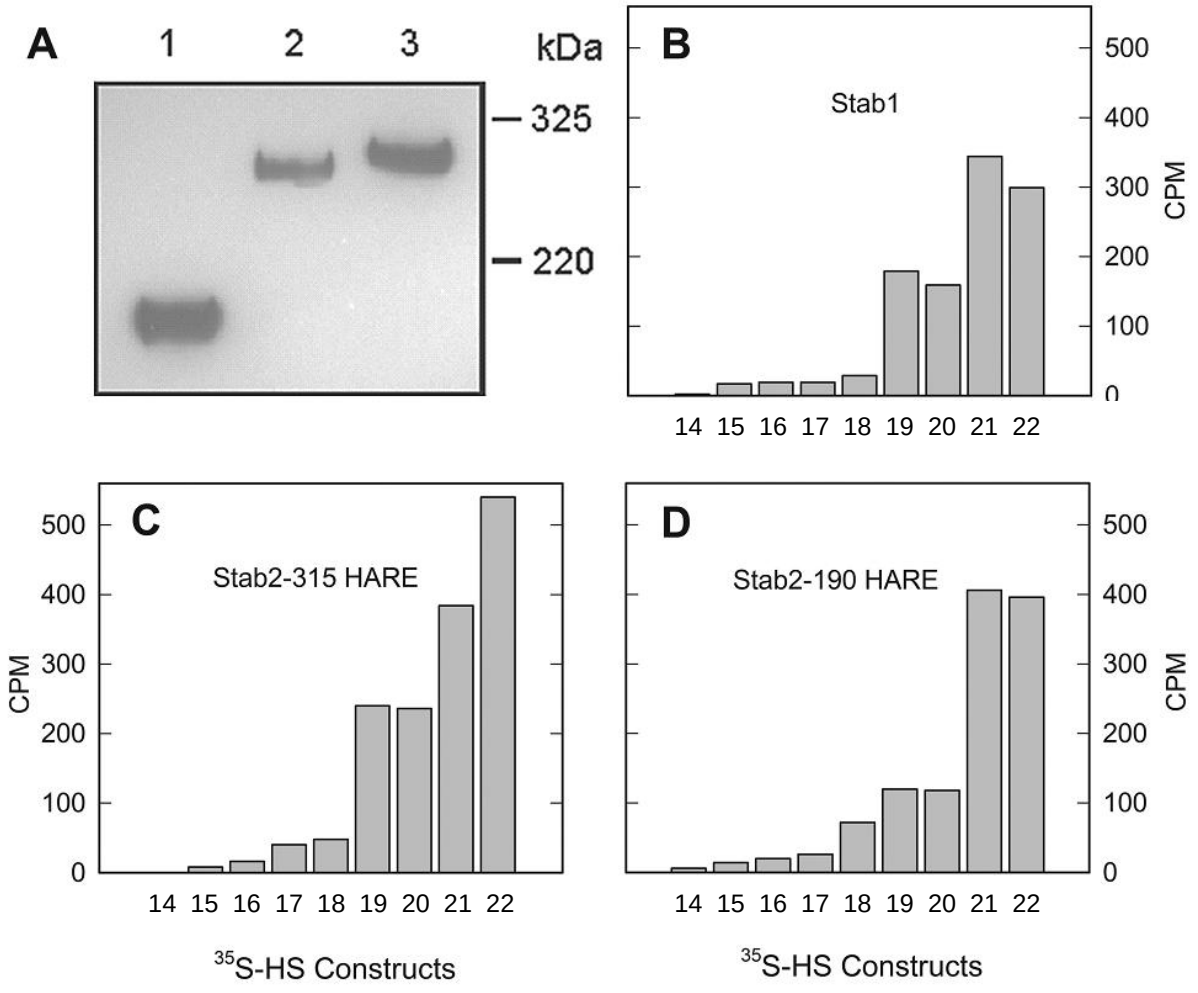

Figure 4.5. Direct binding of HS constructs and Stabilin ectodomains. Secreted ectodomains of each receptor were immunopurified with V5 resin. **A.** Ectodomains were separated by 5% SDS-PAGE, blotted and probed with anti-V5 antibody. Lane 1, Stab-2/190-HARE, 2, Stab-2/315-HARE, 3, Stab-1. **B-D.** Ectodomains bound to V5 resin were incubated with an equal amount of each HS construct for 1.5 h under rotation. The resin was washed three times with Tris-buffered saline and subjected to scintillation counting. Cpm were normalized to the amount of protein on the resin.

The binding between the nine constructs and receptor ectodomains followed a similar pattern to that of the cell internalization assay (Fig. 4.5). Again, constructs **21** and **22** exhibited the highest interaction with the Stabilin receptors, and there was no observed difference between the constructs with IdoA and those without.

Antithrombin competition

We noted that the structural modifications shown to provide the best binding to the Stabilins are the same as those that confer antithrombin binding, namely the presence of 3-O-sulfation. This is a rare modification in HS, but it is critical for antithrombin activity. To discern whether AT and the Stabilins bind HS at the same site, we tested whether antithrombin was able to inhibit the interaction between our constructs and the Stabilin receptors.

First, Stab-1 cells were incubated with [^{35}S]-labeled heparin and increasing concentrations of AT (Fig. 4.6A). Decreased heparin endocytosis with increasing AT indicated that some overlap between the AT-binding sequence and Stabilin-binding sequence does exist. Next, four of our constructs that showed at least partial Stabilin binding (**19**-**22**) were incubated with the three Stabilin-expressing cell lines in the presence and absence of AT. Constructs **19** and **20** do not contain an AT-binding site whereas **21** and **22** do, with **21** being the best substrate for AT due to its IdoA content. Consistent with our previous result, constructs **21** and **22** exhibited decreased endocytosis in the presence of AT, while constructs **19** and **20** were unaffected (Fig. 4.6).

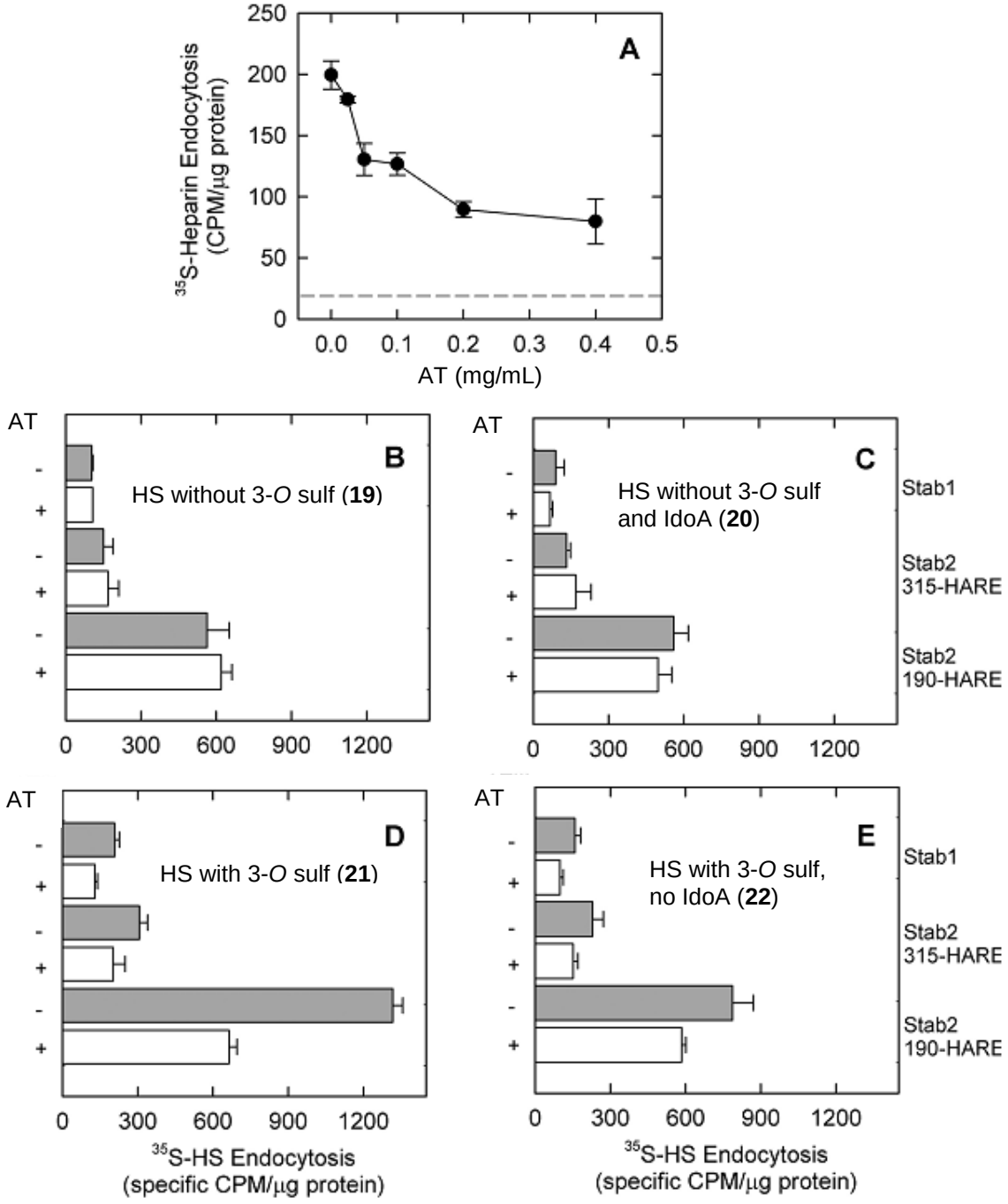

Figure 4.6. Inhibition of Stabilin-mediated endocytosis by antithrombin. **A.** Dose-response curve for AT against radiolabeled heparin. The dotted line represents the threshold for nonspecific binding. **B-E.** Stabilin-binding HS constructs were incubated with the indicated cell lines in the presence or absence of 0.2 mg/mL AT. Constructs **8** and **9** contain an AT-binding site; constructs **6** and **7** do not. Data are the mean ± s.d., n = 4.

Oligosaccharide constructs

Having determined the sulfation patterns necessary for robust Stabilin binding and cell internalization, we sought to determine the minimum oligosaccharide length. The oligosaccharide substrates were elongated (using GlcA-AnMan as a starting material) to the desired length, then treated with recombinant enzymes and PAPS to give the intended structural motifs. A full list of the synthesized HS constructs (including polysaccharides) is given in Table 4.1.

To test the impact of length on endocytosis, oligosaccharides with 3-*O*-sulfation ranging from a 10-mer to a 19-mer (constructs **27**-**36**) were prepared. None of these constructs were internalized by the empty vector cells, but surprisingly, all were taken up by the Stab-1 and Stab-2/315-HARE cells. A 7-mer (**24**) was used as a negative control and showed no internalization. Having determined that the minimum binding structure was between seven and ten sugar units, we synthesized and tested an 8-mer (**25b**) and 9-mer (**26b**). As shown in Fig. 4.7A, the 7-mer and 8-mer exhibit very little internalization. The 9-mer shows a slight increase in internalization, primarily in the Stab-1 cells, while the 10-mer confers a significant increase in the amount of internalized HS. From this point, the amount of HS endocytosis remains steady up to a 19-mer, which was the largest oligosaccharide tested. A similar assay examined the cellular uptake of the 7-mer (not shown) and 19-mer with a 50-fold excess of Arixtra (Fig. 4.7B). The internalization of the 19-mer was unchanged by the addition of Arixtra, suggesting that Arixtra is not cleared by cells expressing Stabilin receptors.

#	disaccharide repeating unit	size of construct
14	(-GlcA-GlcNS-)$_n$	polysaccharide, >6000 Da
15	(-GlcA-GlcNS6S-)$_n$	polysaccharide, >6000 Da
16	(-IdoA-GlcNS6S-)$_n$	polysaccharide, >6000 Da
17	(-GlcA2S-GlcNS-)$_n$	polysaccharide, >6000 Da
18	(-IdoA2S-GlcNS-)$_n$	polysaccharide, >6000 Da
19	(-IdoA2S-GlcNS6S-)$_n$	polysaccharide, >6000 Da
20	(-GlcA2S-GlcNS6S-)$_n$	polysaccharide, >6000 Da
21	(-GlcA-GlcNS±6S±3S-)$_n$ and (-IdoA2S-GlcNS6S-)$_m$	polysaccharide, >6000 Da
22	(-GlcA2S-GlcNS6S-)$_n$ and (-GlcA-GlcNS±6S±3S-)$_m$	polysaccharide, >6000 Da
23	heparin, (-IdoA2S-GlcNS6S-)$_n$ and (-GlcA-GlcNS±6S±3S-)$_m$	polysaccharide, >6000 Da
24	GlcNac6S-GlcA-GlcNS6S3S-IdoA2S-GlcNS6S-GlcA-AnMan	7-mer
25a	GlcA-GlcNS6S-(IdoA±2S-GlcNS6S)$_2$-GlcA-AnMan	8-mer no 3-*O*-sulfation
25b	GlcA-GlcNS6S±3S-(IdoA±2S-GlcNS6S)$_2$-GlcA-AnMan	8-mer with 3-*O*-sulfation
26a	GlcNS6S-GlcA-GlcNS6S-(IdoA±2S-GlcNS6S)$_2$-GlcA-AnMan	9-mer no 3-*O*-sulfation
26b	GlcNS6S-GlcA-GlcNS6S±3S-(IdoA±2S-GlcNS6S)$_2$-GlcA-AnMan	9-mer with 3-*O*-sulfation
27	GlcA-GlcNS6S±3S-(GlcA±2S-GlcNS6S)$_3$-GlcA-AnMan	10-mer no IdoA
28a	GlcA-GlcNS6S-(IdoA±2S-GlcNS6S)$_3$-GlcA-AnMan	10-mer no 3-*O*-sulfation
28b	GlcA-GlcNS6S±3S-(IdoA±2S-GlcNS6S)$_3$-GlcA-AnMan	10-mer with 3-*O*-sulfation
29	GlcA-GlcNS6S±3S-(GlcA±2S-GlcNS6S)$_4$-GlcA-AnMan	12-mer no IdoA
30a	GlcA-GlcNS6S-(IdoA±2S-GlcNS6S)$_4$-GlcA-AnMan	12-mer no 3-*O*-sulfation
30b	GlcA-GlcNS6S±3S-(IdoA±2S-GlcNS6S)$_4$-GlcA-AnMan	12-mer with 3-*O*-sulfation
31	GlcNS6S-(GlcA±2S-GlcNS6S±3S)$_3$-(GlcA-GlcNAc6S)$_2$-GlcA-GlcNS6S-GlcA-AnMan	15-mer no IdoA
32	GlcNS6S-(IdoA±2S-GlcNS6S±3S)$_3$-(GlcA-GlcNAc6S)$_2$-GlcA-GlcNS6S-GlcA-AnMan	15-mer
33	GlcNAc6S-(GlcA±2S-GlcNS6S±3S)$_4$-(GlcA-GlcNAc6S)$_2$-GlcA-GlcNS6S-GlcA-AnMan	17-mer no IdoA
34	GlcNAc6S-(IdoA2S-GlcNS6S±3S)$_4$-(GlcA-GlcNAc6S)$_2$-GlcA-GlcNS6S-GlcA-AnMan	17-mer
35	GlcNS6S-(GlcA±2S-GlcNS6S±3S)$_5$-(GlcA-GlcNAc6S)$_2$-GlcA-GlcNS6S-GlcA-AnMan	19-mer no IdoA
36	GlcNS6S-(IdoA2S-GlcNS6S±3S)$_5$-(GlcA-GlcNAc6S)$_2$-GlcA-GlcNS6S-GlcA-AnMan	19-mer

Table 4.1. Summary of the polysaccharide and oligosaccharide constructs.

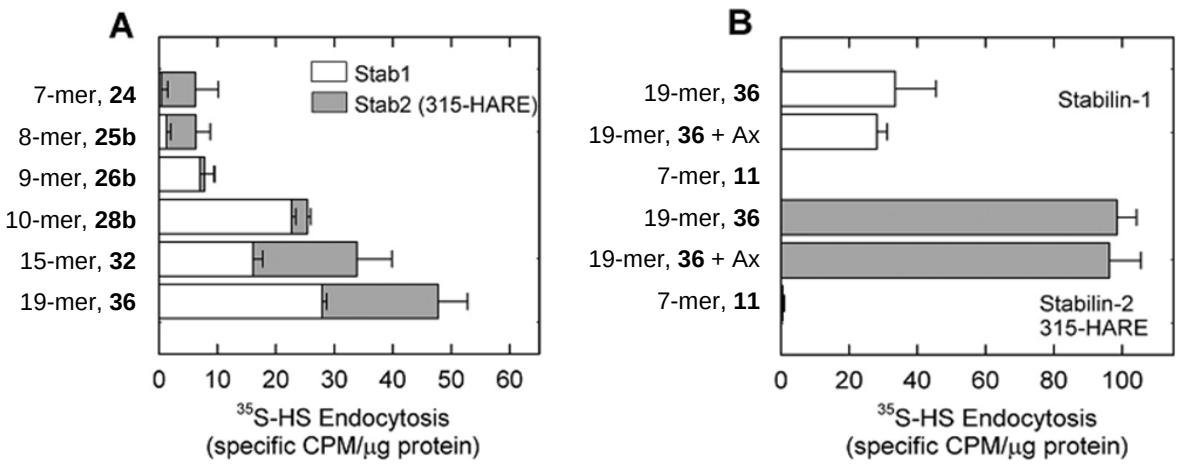

Figure 4.7. Effect of size on endocytosis. **A.** Stab-1 and Stab-2/315-HARE cells were incubated with radiolabeled oligosaccharides for 3 h, washed and quanitified by scintillation counting and Bradford assay. **B.** Radiolabeled 7-mer and 19-mer were incubated for 3 h with Stab-1 and Stab-2/315-HARE cells with a 50-fold excess of Arixtra (Ax), then washed, lysed and quantified. The Stab-2/190-HARE cell line showed similar results. Data are the mean ± s.d., n = 3.

The results up to this point strongly suggested that a 10-mer was the minimum length required for Stabilin binding. To further establish the role of 3-*O*-sulfation near this critical length, we prepared 8-, 9-, 10- and 12-mers without 3-*O*-sulfation (constructs **25a**, **26a**, **28a** and **30a**) and with 3-*O*-sulfation (**25b**, **26b**, **28b** and **30b**). These eight constructs were incubated with Stab-1 and Stab-2/315-HARE cell lines, and heparin and 7-mer were used as positive and negative controls. As seen in Fig. 4.8., the 7-mer, 8-mer and 9-mer showed little to no internalization regardless of whether they contained 3-*O*-sulfation. However, the 10-mer and 12-mer showed much higher internalization when 3-O-sulfation was present; in the Stabilin-1 cells, the levels of endocytosis were similar to those of heparin, and in the Stab-2/315-HARE cells they were about half those of heparin.

Lastly, we were interested to know how Stabilin binding related to the retention of our constructs in the liver. The current understanding is that longer heparin chains are cleared by the liver, while short (non-Stabilin-binding) heparins are processed by the kidneys [138]. Therefore, if the Stabilins are responsible for the bulk of heparin clearance, the size and sulfation parameters for Stabilin binding should lead to their being taken up by the liver.

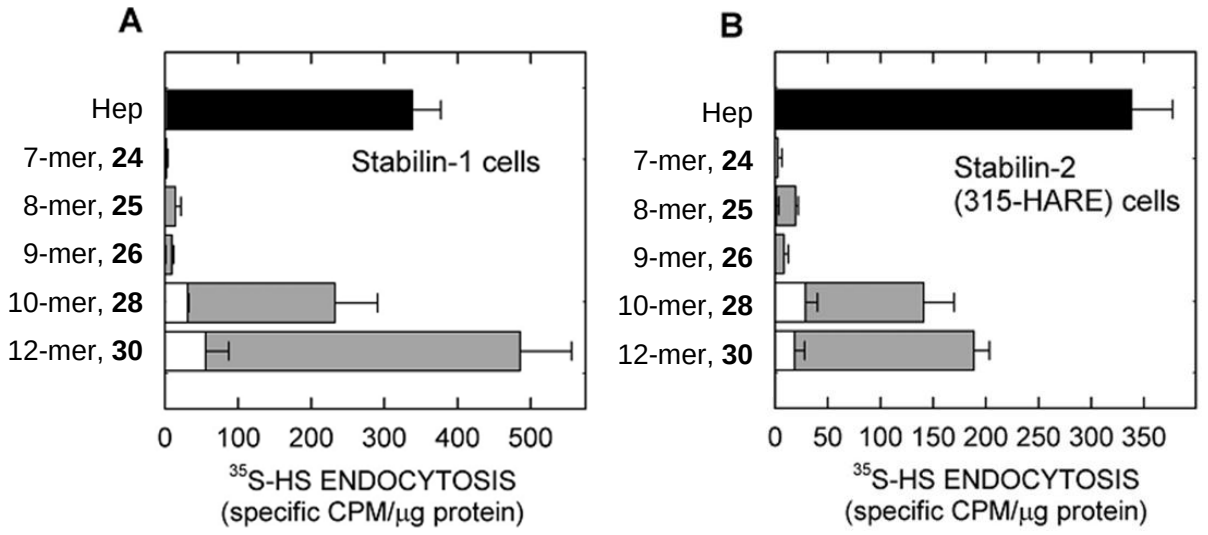

Figure 4.8. A 3-*O*-sulfated decasaccharide is required for binding to Stabilin receptors. Stab-1 (**A**) and Stab-2/315-HARE cells (**B**) were incubated with heparin (positive control, black bars), 7-mer (negative control), 3-*O*-sulfated oligosaccharides (gray bars) and non-3-*O*-sulfated oligosaccharides (white bars) for 3 h. Cells were washed with Hank's buffered saline solution and radioactivity and protein levels were determined, mean ± s.d., n = 3.

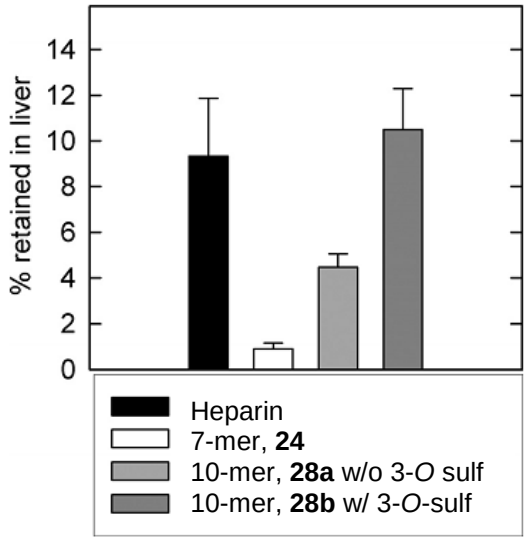

Figure 4.9. 3-*O*-sulfation leads to efficient liver retention. Mice were injected via the tail vein with radiolabeled heparin (black bar), 7-mer (white bar), or a 10-mer with or without 3-*O*-sulfation (**28b**, **28a**). After a short incubation, the livers were collected and processed for scintillation counting. The data presented are the cpm/mass of liver divided by the total cpm injected of at least three liver samples. n = 3 mice.

Mice under general anesthesia were injected via the tail vein with equal amounts of radioactive heparin, 7-mer, **28a** or **28b**, and the compounds were allowed to circulate. The mice were then bled out, and the livers were collected and processed for scintillation counting. The 7-mer was not retained in the liver (Fig. 4.9, white bar), but the 3-*O*-sulfated 10-mer (**28b**) showed retention similar to that of heparin. The non-3-*O*-sulfated 10-mer retention was significantly reduced. Thus, our data suggest that 3-*O*-sulfation indeed contributes to the uptake of heparins by the liver.

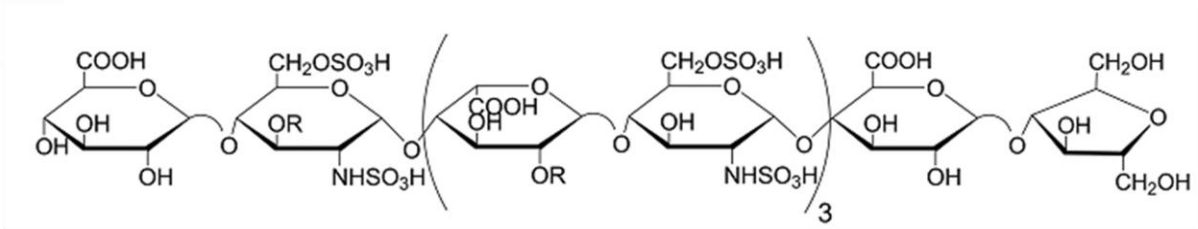

Figure 4.10. The structure of **28b**, the shortest HS construct that displayed robust Stabilin binding.

Conclusions

Understanding the clearance rate of heparin has significant clinical implications for improving the safety of heparin-based drugs. For surgical applications, a fast-clearing heparin drug is preferred, as it would allow the anticoagulant effect to disappear rapidly after the operation and thus reduce the risk of bleeding side effects. In contrast, a slow-clearing heparin is more desirable for patients with that require repeated dosing. Indeed, UFH is widely used in surgical procedures and kidney dialysis, whereas LMWH and fondaparinux are more commonly used as prophylactic agents among high-risk patients prone to thrombosis [141, 142]. Although the size of the heparin chain is known to play a role in the rate of clearance in patients, the precise structural requirements for regulating clearance has remained uncharacterized. Previous studies have demonstrated that a liver endothelial cell receptor, known as Stabilin, is primarily responsible for heparin clearance [81]. By taking advantage of our laboratory's success in synthesizing heparins [91, 92], we investigated the contribution of the sulfation and the size of heparin to the binding to Stab proteins. Our results provide a molecular basis for designing synthetic heparins with desired clearance rates for unique clinical applications.

Our study revealed two binding modes between heparin and Stab proteins. In one binding mode, the heparin polysaccharide binds to Stab-1/-2 nonspecifically; such binding requires a long polysaccharide chain. Another binding mode is specific, in which the Stabilin proteins recognize a saccharide domain containing a 3-*O*-sulfo group. In the specific binding mode, a much shorter oligosaccharide can sufficiently display high affinity to the Stabilins. We also demonstrate that a 3-*O*-sulfated decasaccharide displays higher retention in the liver in mice compared to its counterpart without 3-*O*-sulfation, suggesting that Stabilin binding affinity correlates to the clearance *in vivo.*

Our data also suggest that Stabilin proteins recognize a unique saccharide sequence. Although we do not know the precise saccharide structure recognized by the Stabilin receptors at the present time, some overlaps between the Stab-binding sequence and AT-binding sequence exist. We know that 3-*O*-sulfation is a critical modification for displaying high binding affinity to AT and for carrying anticoagulant activity [143]. Further, competitive binding of the Stabilin receptors and AT to heparins was observed in this study. The mechanistic effect of 3-*O*-sulfation on the binding to the Stabilin receptors is currently unknown. We postulate that this effect is unlikely to be purely attributed to an increase in charge density because 3-*O*-sulfation is a rare modification in HS [144]. A recent study suggests that 3-*O*-sulfation may affect the conformation of neighboring IdoA2S residues to rearrange the positioning of sulfo groups [145]. In addition, previous studies have shown that one natural highly sulfated chondroitin sulfate (CS-D) did not compete with heparin in contrast to other similar chondroitin sulfates (CS-B, CS-E) that demonstrated some degree of competition [90], providing evidence that charge is not the only determinant for heparin binding to the Stabilins.

This is the first report demonstrating the structural selectivity of heparin binding to Stab-1. The Stab-1 receptor is expressed in the liver sinusoidal endothelium as well as in alternatively activated macrophages [146] and other physiological niches [147], and it may play a role in both systemic and localized clearance of heparinoid molecules.

It should be noted that the rate of endocytosis also depends on the concentration of Stab receptors on the cell surface. The Stab-2/190-HARE isoform always showed the highest increase in endocytosis because these cells produce more receptor per microgram of cell lysate than the other two cell lines. Not surprisingly, the liver endothelial cells exhibit a much higher ratio of 190/315-HARE Stab-2 than the recombinant cell lines, which may account for the rapid uptake of heparin within the liver [148]. The consistently lower

internalization rate of heparin in the Stab-1 cells may be reflective of the amount of total surface receptor available to bind and internalize heparin, a lower binding affinity, or the unavailability to bind ligand due to the very short transient time on the cell surface. Others have reported the very short transient time of Stab-1 on the cell surface [146, 149]. In these experiments, we noticed a discrepancy in binding vs. endocytosis. Our *in vitro* binding assays by immunoprecipitation of the ecto-domain of Stab-1 revealed that the binding of the HS oligomers was qualitatively about as high as that of the Stab-2 ecto-domains. This contrasts with the cell-based assays and reveals that a combination of surface availability and rapid turnover, not binding affinity, may be responsible for lower endocytic rates in Stab-1 cells. In addition, the expression of Stabilin receptors can be regulated by other cellular mechanisms. A genetic screen in which human umbilical vein endothelial cells (HUVEC) activated with VEGF revealed an increase of Stab-1 expression reveals that growth factors and cytokines are able to alter endocytosis profiles of tissues [150].

These results provide a molecular basis for designing anticoagulant heparin drugs with controlled clearance rates and advance our understanding of the HS and heparin clearance mechanism.

CHAPTER V

DESIGN OF HOMOGENEOUS HEPARINS WITH CONTROLLED CLEARANCE PATHWAYS

Problems with the heparin drugs available today have underscored the need for structurally pure heparin compounds. Most notable is the recent distribution of contaminated heparin that caused over 80 deaths in the United States and a major drug recall [151]. The heparin supply had been contaminated with oversulfated chondroitin sulfate, a related glycosaminoglycan is difficult to distinguish from heparin by common screening methods but provokes a potentially fatal immune response when administered to patients. Contamination issues of this nature could be avoided by replacing the porcine-derived heparin with a synthetic version that is not dependent on the international (primarily Chinese) pig population and has a shorter, better regulated supply chain.

Other heparin concerns can be addressed by tailoring heparin structures to have improved biological effects and traits desirable for different patient populations. One element of heparin that is essential in surgical applications is the availability of a reversal agent. Protamine sulfate, a highly cationic peptide, is a long-standing heparin antidote. The anticoagulant effect of unfractionated heparin is efficiently reversed by protamine, but protamine is unable to fully neutralize low-molecular-weight heparins. Thus, we investigated the susceptibility of our synthetic heparin compounds to protamine neutralization, with the

goal of designing a low-molecular-weight heparin analog with better protamine reversibility than existing LMWHs like Lovenox.

When assessing new compounds, *in vitro* assays, such as measurements of direct antithrombin binding and anti-Xa activity, give a good indication of the activities of heparin analogs. However, *in vivo* studies are necessary to investigate the biological effects and bioavailability of these compounds.

Most *in vivo* assays of anticoagulants involve taking timed blood samples and measuring a physical parameter, such as clotting, or testing for the activity of components of the coagulation cascade. In human patients, activated partial prothromboplastin time is the standard for unfractionated heparin monitoring, while more complex anti-Xa assays are used for patients on chronic LMWH dosing and for higher risk patients, such as infants, pregnant women and those with renal impairment [152-155]. Other commonly used research models include arterial and venous thrombosis (induced by pharmacologic or mechanical means) and bleeding models (such as rabbit ear bleeding and rat tail bleeding) [156]. Here, we used rodent models to assess anti-Xa activity.

Design and synthesis of 6-, 8-, 10- and 12-mer

With the structural information gathered from previous studies, we set out to design novel anticoagulant heparin structures that were homogenous, reversible by protamine, cleared by the liver and short enough to have reduced PF4 binding. To this end, we designed heparin analogs ranging from a 6-mer to a 12-mer that contained an AT-binding pentasaccharide at the non-reducing end and repeating IdoA2S-GlcNS6S units (which are common in heparin but not heparan sulfate). Commerically available *p*-nitrophenyl β-glucuronide (GlcA-pnp) was used as a starting material because the pnp tag is detectable

by UV at 310 nm, facilitating isolation of the product during the synthetic steps. Based on our previous results, we expected that the 10-mer and 12-mer would be cleared by the liver rather than the kidneys. The molecular weights and AT binding affinities of the constructs are shown in Table 5.1.

compound	molecular mass (Da)	AT affinity (K_d)
6-mer	1791.5	16.2 ± 3.7 nM
8-mer	2368.9	13.1 ± 2.0 nM
10-mer	2946.4	9.9 ± 4.1 nM
12-mer	3485.8	8.5 ± 3.0 nM

Table 5.1. Pure oligosaccharides for *in vivo* studies. All compounds contain an AT-binding motif and repeating IdoA2S-GlcNS6S units. K_d values were determined by affinity co-electrophoresis.

Antithrombin binding affinities

Affinity co-electrophoresis was used to determine the binding affinities (K_d values) of the different constructs to AT. Each oligosaccharide was run through a gel with lanes containing 0-3 µM AT, and the mobility of the oligosaccharide in each lane was used to determine a K_d value. These values are shown in Table 5.1. The four compounds showed comparable binding affinities for antithrombin.

Protamine reversibility

We tested whether protamine could reverse the anti-Xa activity of the four compounds. The assay was similar to that used to test PF4 neutralization (Chapter III); an amount of each compound that was able to inhibit factor Xa by 90% was incubated with increasing concentrations of protamine. The return of Xa activity in the presence of protamine indicated that protamine was inhibiting the ability of the HS compound to bind and antagonize factor Xa.

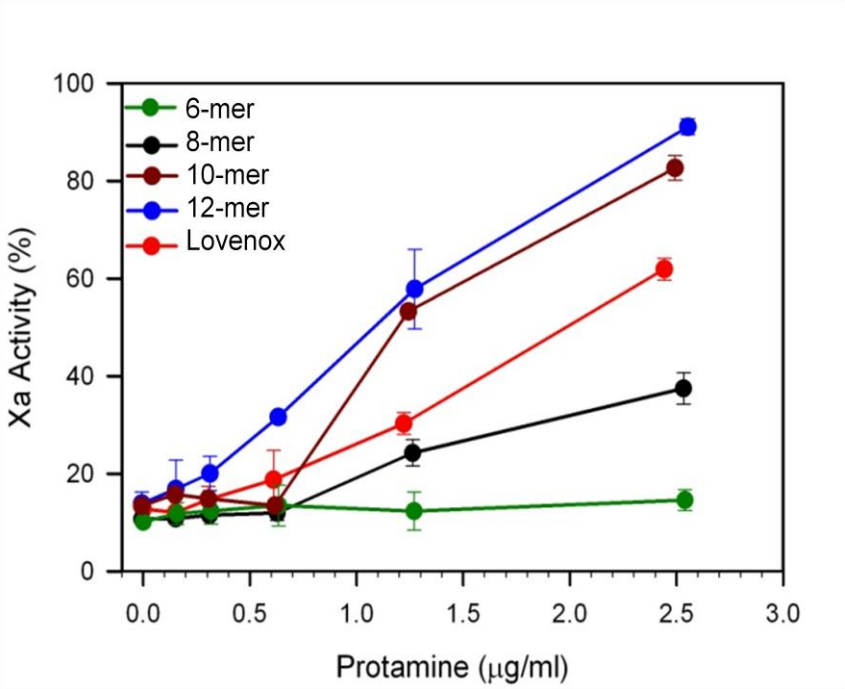

Figure 5.1. Susceptibility of HS oligosaccharides to protamine neutralization. HS constructs expected to display 90% factor Xa inhibition were added to human serum with different amounts of protamine. The Xa activity in the serum was then measured using a chromogenic assay. Lovenox was used as a control.

The experiment indicated that the two longest compounds, a 10-mer and 12-mer, were more susceptible to protamine neutralization than Lovenox, although they were not

completely neutralized. The 6-mer was not reversible by protamine and the 8-mer was reversed less than Lovenox. The result suggests that a pure LMWH that is 10 to 12 sugars long will be reversed by protamine to a greater extent than Lovenox.

Pharmacokinetic profile in rats

Having confirmed the anti-Xa activity of the 6- to 12-mer *in vitro*, we were interested to measure their activity in a living system. Rats and rabbits are used more commonly than mice for anticoagulant testing because multiple blood samples can be taken from a single animal. Because training and facilities for rats were more readily available, we used Sprague-Dawley rats to test the clearance profiles of our compounds.

The existing drugs Lovenox and Arixtra were tested first as controls. Because these drugs have a half-life of 2-6 hours and 17 hours in humans, respectively, we expected that their half-lives in rats would be considerably different from each other and that we could use them as guidelines to judge whether our 6-, 8-, 10- and 12-mer showed fast clearance profiles (close to or shorter than Lovenox) or slow ones (more similar to Arixtra). *In vitro* anti-Xa assays were performed to obtain standard curves for Lovenox and Arixtra and determine an equivalent dosage for the two drugs (Fig. 5.2). The doses chosen were 2.27 mg/kg for Lovenox and 200 µg/kg for Arixtra.

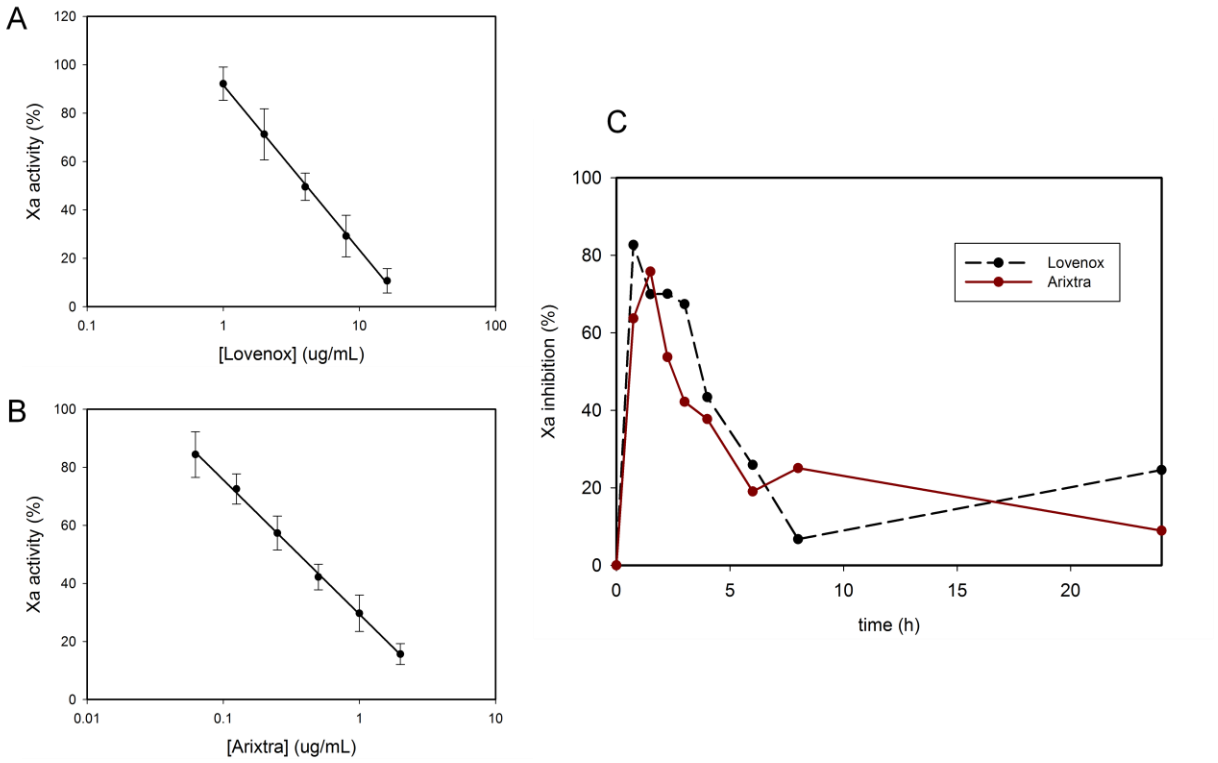

Figure 5.2. Pharmacokinectic profile of Lovenox and Arixtra. Standard curves of the anti-Xa activity of Lovenox (**A**) and Arixtra (**B**) were determined *in vitro* in blank rat serum. **C.** Rats were dosed subcutaneously with heparin drugs, and blood samples were taken by tail clip over a 24-hour period, then centrifuged to isolate plasma and subjected to a chromogenic factor Xa assay. Data points are the average of 2-3 samples.

Male rats (250-350 g) were dosed subcutaneously with approximately 100 µL of Lovenox or Arixtra, and blood was collected by tail clip at 0.75, 1.5, 2.25, 3, 4, 6, 8 and 24 hours. Blood was centrifuged to obtain plasma immediately after collection and was stored at -20°C until use. Rat serum without drugs was used to represent 100% Xa activity (0% inhibition).

When the rat samples were assayed for anti-Xa activity, we were surprised to find that the two drugs exhibited a very similar plasma clearance profile (Fig. 5.2C). Although no published studies have compared the clearance of these two drugs in rats, a review of the

literature confirmed that both Lovenox and Arixtra showed a peak concentration at around 2 hours and a half-life of about 4.5 hours in rats (for examples, see [157-159]). The long half-lives characteristic of pentasaccharide heparin drugs like Arixtra and idraparinux (a fondaparinux analog with a human half-life of 80 hours) are not exhibited in animal studies unless a primate species (commonly baboon) is used [56]. Because we were unlikely to obtain meaningful data on heparin clearance rates in rats and because primate studies were not possible, we abandoned this study and instead investigated how the Stabilin-binding character of our heparin analogs influenced their route of elimination *in vivo*.

Anti-Xa activity and elimination route in mice

BALB/c mice were used to investigate the bioactivity and elimination route of our four compounds. To confirm that the compounds were bioavailable by subcutaneous injection, four mice were injected with each compound (or with PBS as a control), and blood was collected by cardiac puncture after a 30-minute incubation. The samples were spun down to isolate plasma, and the anti-Xa activity of the PBS- and HS-injected mouse samples were compared using a chromogenic assay. The four compounds showed similar activity and did not exhibit a correlation between length and anti-Xa activity. This suggests that pure oligosaccharides ranging from a 6-mer to a 12-mer are equally bioavailable and confirms that they show anti-Xa activity *in vivo*, a common indication of anticoagulant activity.

Having shown that our compounds exhibited anti-Xa activity *in vivo*, we questioned how their Stabilin-binding character would influence their clearance by the liver or by the kidneys. We expected that the 10-mer and 12-mer, which contain Stabilin-binding structures, would be present in the liver after a short incubation time, whereas the 6-mer and

8-mer (which are not Stabilin binding) would be cleared primarily by the kidneys and would be detectable in urine.

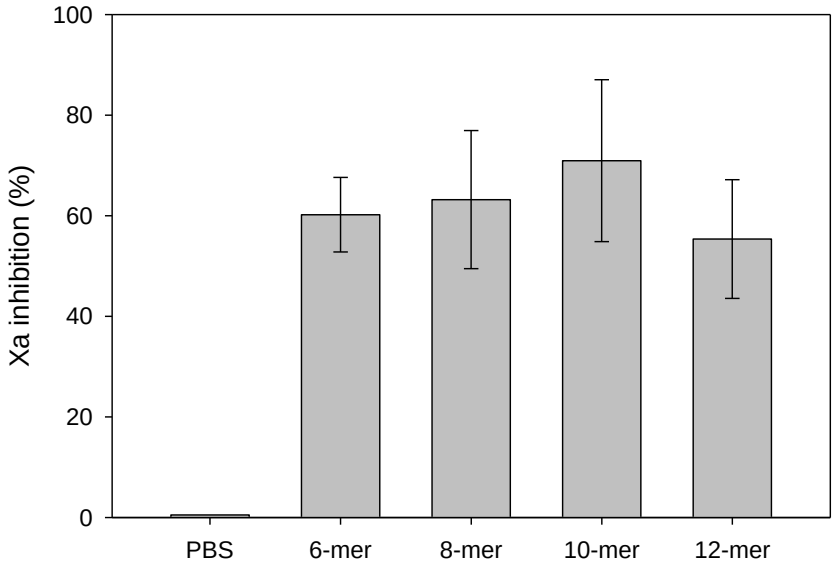

Figure 5.3. Factor Xa inhibition in mice. Male BALB/c mice (16-20 g) were injected subcutaneously with HS at 100 nmoles/kg. After 30 minutes, mice were sacrificed and blood was collected via cardiac puncture. Isolated plasma was tested for Xa activity using a chromogenic assay with plasma from PBS-injected mice as a control. n = 4 mice per compound, 3 assays per sample.

^{35}S-labeled versions of the four compounds were synthesized and injected in mice intravenously. Radiolabeled unfractionated heparin and a 7-mer (an ultra-low-molecular-weight heparin that showed no Stabilin binding) were used as controls. Livers and urine were collected after a ten-minute incubation and were processed for scintillation counting. The percentage of recovered radioactivity (in cpm) out of the amount injected was quantified for each compound.

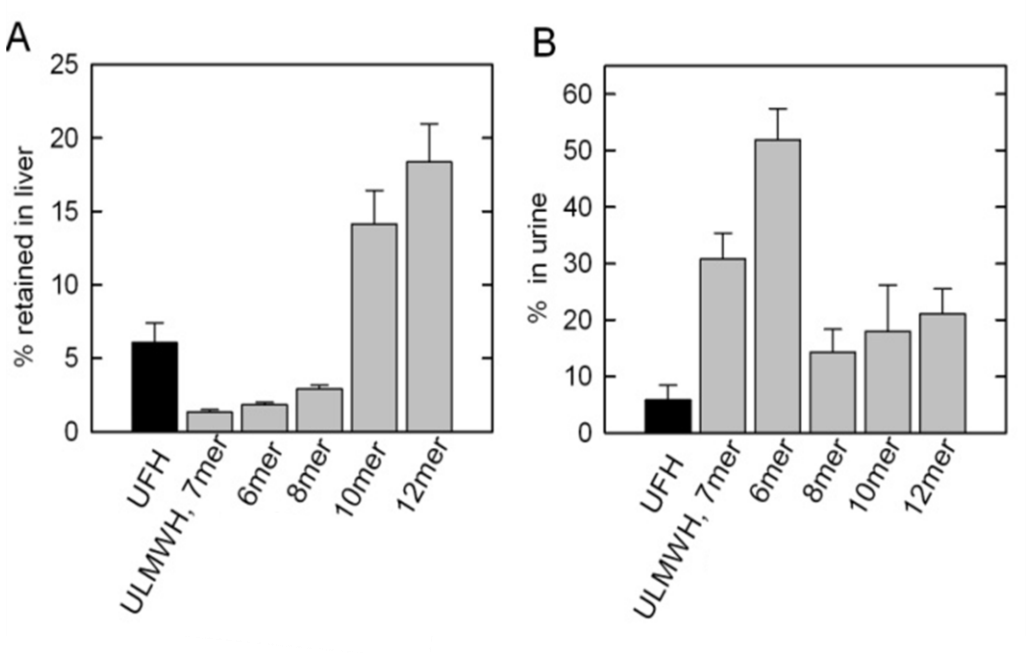

Figure 5.4. Retention of oligosaccharides in mouse liver and urine. Equal amounts of ^{35}S-labeled heparins were injected via the tail vein to male BALB/c mice. After a short incubation, the mice were bled out and the livers were processed for scintillation counting (**A**). ^{35}S-radioactivity in the urine was also determined (**B**). Unfractionated heparin (UFH), which is known to be cleared by the liver, and a 7-mer (ULMWH) that did not show Stabilin binding were used as controls. n = 4 mice.

The study found that the 7-mer control, 6-mer and 8-mer were retained at a very low level, whereas the 10-mer and 12-mer showed greater retention in the liver than UFH. In the urine, the 6-mer and 7-mer were present to a much higher extent than the other compounds. These data support the hypothesis that Stabilin-binding oligosaccharides are primarily cleared by the liver and that non-Stabilin-binding ones are cleared by the kidneys and excreted in urine. This information could be useful in the future design of heparins for patients with renal impairment and suggests different clinical applications for the four compounds designed in this study.

Conclusions

These studies present the first synthesis of structurally homogenous heparin oligosaccharides with anticoagulant activity. Four heparan sulfate constructs, a 6-, 8-, 10- and 12-mer, were prepared by sulfating the sugars concurrently with saccharide chain elongation. As a result, C_5-epimerase exhibited its irreversible reaction mode and IdoA residues were locked in place, allowing the formation of repeating IdoA2S-GlcNS6S regions.

When compared to an existing low-molecular-weight heparin, Lovenox, the 10-mer and 12-mer were more reversible by protamine in an *in vitro* assay. The 10-mer and 12-mer were also retained in the liver, not the kidneys, to a greater extent than the 6-mer and 8-mer, which is consistent with our data on Stabilin binding. Avoiding heparin kidney clearance would be highly advantageous for renally impaired patients and for elderly patients, who experience reduced clearance of drugs eliminated by the kidneys due to physiological changes in old age [160]. All four compounds exhibited similar anti-Xa activity in mice, suggesting that bioavailability does not change within this oligosaccharide size range.

Despite the passage of nearly a century since its discovery, the chemical structure of the drug heparin has gone largely unchanged. The first decades of its use saw the development of depolymerized low-molecular-weight heparins and later, the synthesis of the AT-binding pentasaccharide region by both chemical and enzymatic methods. After the development of Arixtra, innovations in the heparin field have primarily focused on extending the half-life of the drugs. This has been achieved by adding tags such as biotin and by replacing sulfo groups with less reactive methyl groups. Despite these advances, there has been no targeted development of heparin analogs that have specific biological functions or meet the needs of specific patient populations.

Breakthroughs in the field of heparan sulfate synthesis and in understanding heparan sulfate biochemistry have facilitated the production of heparan sulfate constructs that have desirable biological activities. We hope that these innovations will enable the development of new heparin drugs that better serve patients requiring anticoagulant therapy.

CHAPTER VI

CONCLUSIONS

Heparan sulfate is a ubiquitous carbohydrate that regulates many physiological events. A special highly-sulfated form of heparan sulfate, heparin, has been exploited for its anticoagulant activity and used as a drug for over 70 years. Due to the abundance of electronegative sulfo groups on the sugar backbone of heparin, it engages in both specific and nonspecific interactions with many proteins. A chemoenzymatic method was employed to prepare many heparan sulfate compounds having different sulfation patterns; in some cases, oligosaccharides of different lengths were also utilized.

First, the substrate specificity of the Sulf-2 enzyme and its effect on HS-PF4 binding was examined. Sulf-2 removes sulfo groups from HS, and we hypothesized that treatment with Sulf-2 would affect binding between HS and platelet factor 4. Sulf-2 was previously shown to remove a 6-*O*-sulfo group from trisulfated disaccharides [101]; in addition, we found that 6-*O*-sulfo groups were removed from disaccharides carrying *N*- and 6-*O*-sulfation but not 2-*O*-sulfation. These studies were completed using HS polysaccharides prepared with a ^{35}S-label at a specific sulfo group. By comparing Sulf-2-treated and untreated HS, we also confirmed that treatment with the Sulf-2 enzyme will reduce binding between HS and PF4 by approximately 10 to 20-fold but will not affect binding to antithrombin.

The PF4 binding character of size-defined oligosaccharides was also examined. HS oligosaccharides having 15, 17, 19 and 21 sugar units were synthesized to investigate the

effect of size on the ratio of anti-IIa to anti-Xa activity. The 19-mer and 21-mer had 1:5 and 1:2 anti-IIa/Xa ratios, respectively, and the 15-mer and 17-mer were too short to have anti-IIa activity. All four oligosaccharides bound to PF4 in a dot blot assay; however, they bound to a much lower extent than unfractionated heparin. The anti-Xa activity of the 21-mer, which had the highest anti-IIa activity, was compared to an ultralow-molecular-weight heparin (7-mer) and full-length heparin. PF4 had no effect on the 7-mer and was able to fully neutralize the anti-Xa activity of full-length heparin; the 21-mer showed significantly reduced neutralization by PF4. Thus, Sulf-2 treatment and reduced length are proposed as methods to reduce binding between heparin and PF4.

Stabilin-2, a scavenger receptor located on sinusoidal endothelial cells, was identified recently as a clearance receptor for heparins [81]. It had been determined that Arixtra (which is cleared by the kidneys) does not bind Stabilin-2, while unfractionated heparin (which is cleared primarily by the liver) does bind. We hypothesized that HS sulfation and length would control binding to Stabilin-2 and that binding to Stabilin-2 would result in liver clearance. First, by synthesizing HS polysaccharides and testing them for internalization by Stabilin-expressing cells, we found that Stabilin binding appeared to be somewhat charge-dependent but that the addition of 3-*O*-sulfation led to much greater internalization. This finding was confirmed by direct binding assays between the HS constructs and purified Stabilin ectodomains. Incubation of Stabilin-binding constructs with antithrombin in the cell internalization assay indicated that there is some overlap between the Stabilin and AT binding sites on HS.

With the structural information gathered from the polysaccharide studies, a series of oligosaccharides were prepared that contained the Stabilin-binding motifs but varied in length. We found that a 10-mer was required for robust binding to Stabilin-1 and Stabilin-2, and that removing the 3-*O*-sulfation nearly eliminated the internalization of a 10-mer and 12-

mer. Additionally, we found that the 3-*O*-sulfated 10-mer was retained in the liver to the same extent as heparin after administration to mice, indicating that a Stabilin-binding LMWH should avoid clearance by the kidneys. This would be beneficial for kidney-impaired and elderly patients, and it would have a shorter half-life than small heparins like Arixtra.

Later studies focused on the bioactivity of four new pure compounds that were 6-12 sugars in length. All compounds contained an AT-binding domain and repeating IdoA2S-GlcNS6S units, which are commonly found in heparin but not HS. The compounds had similar binding affinities for antithrombin in affinity co-electrophoresis assays. In anti-Xa activity assays, the activities of the 10-mer and 12-mer were more effectively reversed by protamine than Lovenox, a common LMWH, suggesting that a pure heparin compound 10-12 sugars long could be more reversible that the low-molecular-weight mixtures that are currently available.

In vivo studies in rats proved incapable of distinguishing the different half-lives of the drugs, but the subcutaneous bioavailability of the compounds was confirmed by administration to mice and anti-Xa testing. As anticipated after the cell-based assays, additional mouse experiments showed that the 10-mer and 12-mer were retained in the liver, not in urine, to a much higher extent than the 6-mer and 8-mer.

When considering strategies for improved heparins, the research presented in this dissertation provides several pieces of new information that could be beneficial to the design of new anticoagulants. First, two methods are proposed to reduce binding to PF4 and potentially heparin-induced thrombocytopenia: removal of 6-*O*-sulfation by treatment with Sulf-2 and limiting the size of the oligosaccharide. In our studies, HS constructs up to a 21-mer had reduced binding to PF4 compared to full-length heparin. Next, we demonstrated that binding to Stabilin receptors can be achieved with HS that is at least 10 sugars in length

and contains *N*-, 2-*O*-, 6-*O*- and especially 3-*O*-sulfation. This finding should allow the design of short heparins with either short half-lives and liver clearance or long half-lives and kidney clearance. In addition, HS constructs up to a 12-mer were found to be available by subcutaneous injection. While we did not investigate the maximum length for this administration route, this shows that pure synthetic compounds in the size range of LMWHs will not need to be given intravenously. We hope that these findings will be useful in the synthesis of new heparin drugs that are safe, effective and well suited for different patient populations.

APPENDIX I

Curriculum Vitae

Elizabeth Pempe Chappell

2708 Farthing St., Durham, NC 27704 · (919) 309-6721 · pempe@email.unc.edu

Education

Ph.D. candidate, Pharmaceutical Sciences 2008-present
Division of Chemical Biology and Medicinal Chemistry
University of North Carolina at Chapel Hill

B.S., Chemistry *(cum laude)* GPA: 3.7 2003-2007
Biochemistry track
Whitworth University, Spokane, WA

Research Experience

Doctoral Candidate, Dr. Jian Liu laboratory, UNC-Chapel Hill 01/2009-present
Synthesized heparan sulfate poly- and oligosaccharides using a novel chemoenzymatic method; used these constructs to test substrate specificities for heparin clearance, 6-O-endosulfatase and anti-Xa/IIa activity.

Rotation Student, Dr. Scott Singleton laboratory, UNC-Chapel Hill 08/2008-12/2008
Synthesized small molecules and screened them for inhibition of RecA, a bacterial DNA repair enzyme, with the goal of identifying leads for antibiotic therapy.

Development Associate, AlphaVax Human Vaccines, RTP, NC 09/2007-01/2008
Prepared experimental vaccine formulations and performed long-term stability studies using immunofluorescence assays of virus-like replicon particles.

Summer Research Fellow, Whitworth University, Spokane, WA 05/2006-07/2006
Created a GST-fusion protein of subunit d from yeast V-ATPase and attempted expression in E. coli; developed structural homology model using Modeller program.

Laboratory Intern, Hope Heart Institute, Seattle, WA 06/2004-08/2004
Performed basic microbiology procedures in a lab studying perlecan expression during vascular injury.

Publications

1. **Elizabeth P. Chappell**, Jian Liu. Use of biosynthetic enzymes in heparin and heparan sulfate synthesis. *Bioorg Med Chem*. Epub 2012 Dec 12. Review.

2. Yongmei Xu, **Elizabeth H. Pempe**, Jian Liu. Chemoenzymatic synthesis of heparin oligosaccharides with both anti-Xa and anti-IIa activities. *J Biol Chem*. 2012 Aug 17;287(34):29054-61. Epub 2012 Jul 6.

3. **Elizabeth H. Pempe**, Tanya C. Burch, Courtney J. Law, Jian Liu. Substrate specificity of 6-O-endosulfatase (Sulf-2) and its implications in synthesizing anticoagulant heparan sulfate. *Glycobiology*. 2012 Oct;22(10):1353-62. Epub 2012 Jun 12.

4. **Elizabeth H. Pempe**, Yongmei Xu, Sandhya Gopalakrishnan, Jian Liu, Edward N. Harris. Probing structural selectivity of synthetic heparin binding to stabilin protein receptors. *J Biol Chem*. 2012 Jun 15;287(25):20774-83. Epub 2012 Apr 30.

5. Manali Joglekar, Pedro M. Quintana Diez, Stephen Marcus, Rui Qi, Benjamin Espinasse, Mark R. Wiesner, **Elizabeth Pempe**, Jian Liu, Dougald M. Monroe, Gowthami M. Arepally. Disruption of PF4/H multimolecular complex formation with a minimally anticoagulant heparin (ODSH). *Thromb Haemost.* 2012 Apr;107(4):717-25. Epub 2012 Feb 8.

Fellowships and Awards

The North Carolina Translational and Clinical Sciences (NC TraCS) Institute $2K grant for clinical and translational research projects — 2012

Graduate Education Advancement Board Impact Award — 2012

National Institutes of Health Predoctoral Ruth L. Kirschstein National Research Service Award Fellowship #1F31AG040927-01 ($28,951/year for 3 years) — 2011

American Heart Association Mid-Atlantic Affiliate Predoctoral Fellowship #11PRE7240031 ($23,000/year for 2 years) *(declined)* — 2011

Professional Experience

Adviser, Pre-graduate Education Advising Program, UNC-CH — 08/2012-present
Advised undergraduates applying to graduate and professional programs.

Laboratory Animal Coordinator, Jian Liu lab — 11/2011-present
Completed training and paperwork to commence animal studies in the Liu laboratory, attended lectures.

Radiation and Laboratory Safety Officer, Jian Liu lab — 05/2011-present
Performed monthly radiation checks, trained personnel, ordered and inventoried radioactive reagents, managed radioactive and chemical waste.

Contract Editor, American Journal Experts — 03/2010-present
Edited over 200 scientific manuscripts in a variety of fields for publication in English-language journals.

Graduate Student Organization Division Representative, UNC-CH 08/2010-05/2011
Organized social and fundraising activities for graduate students in the School of Pharmacy.

Graduate TA, Biochemistry I-II and Pharmacodynamics, UNC-CH 08/2008-05/2010
Led review sessions, held weekly office hours, wrote and graded exams, maintained grades and course materials using Blackboard.

Program Volunteer, Sexual and Reproductive Health, SPW Uganda 01/2008-08/2008
Taught weekly health classes to primary and secondary school students at eight schools and organized community events such as clinic visits and HIV testing in rural Uganda.

Chemistry Tutor, Whitworth University 09/2006-05/2007
Tutored lower-division chemistry students for four hours per week.

Teaching Assistant, Organic Chemistry labs, Whitworth University 09/2005-12/2005
Prepared lab reagents, disposed of chemical waste and assisted students in lab experiments.

Poster Presentations

Elizabeth H. Pempe, Yongmei Xu, Sandhya Gopalakrishnan, Jian Liu, Edward N. Harris. Structural Requirements for Synthetic Heparin Binding to the Stabilin-1/-2 Receptors. Gordon Research Conference on Proteoglycans, Andover, NH. 2012.

Tanya C. Burch, **Elizabeth H. Pempe**, Courtney L. Jones, Jian Liu. Characterization of Heparan Sulfate 6-O-endosulfatase Substrate Specificity: potential for a safer heparin drug. International Carbohydrate Symposium, Tokyo, Japan. 2010.

Elizabeth H. Pempe, Deanna D. Ojennus. Creating a structural model of subunit d of yeast V-ATPase. Murdock Undergraduate Research Conference, Salem, OR, and Spokane Intercollegiate Research Conference, Spokane, WA. 2007.

REFERENCES

1. Esko, J. D., Kimata, K. and Lindahl, U. (2009) Proteoglycans and Sulfated Glycosaminoglycans.

2. Bernfield, M., Gotte, M., Park, P. W., Reizes, O., Fitzgerald, M. L., Lincecum, J. and Zako, M. (1999) Functions of cell surface heparan sulfate proteoglycans. Annu Rev Biochem. **68**, 729-777

3. Park, P. W., Reizes, O. and Bernfield, M. (2000) Cell surface heparan sulfate proteoglycans: selective regulators of ligand-receptor encounters. J Biol Chem. **275**, 29923-29926

4. Iozzo, R. V. (1998) Matrix proteoglycans: from molecular design to cellular function. Annu Rev Biochem. **67**, 609-652

5. McCormick, C., Duncan, G., Goutsos, K. T. and Tufaro, F. (2000) The putative tumor suppressors EXT1 and EXT2 form a stable complex that accumulates in the Golgi apparatus and catalyzes the synthesis of heparan sulfate. Proc Natl Acad Sci U S A. **97**, 668-673

6. Chen, M., Bridges, A. and Liu, J. (2006) Determination of the substrate specificities of N-acetyl-d-glucosaminyltransferase. Biochemistry. **45**, 12358-12365

7. Sismey-Ragatz, A. E., Green, D. E., Otto, N. J., Rejzek, M., Field, R. A. and DeAngelis, P. L. (2007) Chemoenzymatic synthesis with distinct Pasteurella heparosan synthases: monodisperse polymers and unnatural structures. J Biol Chem. **282**, 28321-28327

8. Liu, R., Xu, Y., Chen, M., Weiwer, M., Zhou, X., Bridges, A. S., DeAngelis, P. L., Zhang, Q., Linhardt, R. J. and Liu, J. (2010) Chemoenzymatic design of heparan sulfate oligosaccharides. J Biol Chem. **285**, 34240-34249

9. Peterson, S., Frick, A. and Liu, J. (2009) Design of biologically active heparan sulfate and heparin using an enzyme-based approach. Nat Prod Rep. **26**, 610-627

10. Sueyoshi, T., Kakuta, Y., Pedersen, L. C., Wall, F. E., Pedersen, L. G. and Negishi, M. (1998) A role of Lys614 in the sulfotransferase activity of human heparan sulfate N-deacetylase/N-sulfotransferase. FEBS Lett. **433**, 211-214

11. Saribas, A. S., Mobasseri, A., Pristatsky, P., Chen, X., Barthelson, R., Hakes, D. and Wang, J. (2004) Production of N-sulfated polysaccharides using yeast-expressed N-deacetylase/N-sulfotransferase-1 (NDST-1). Glycobiology. **14**, 1217-1228

12. Sheng, J., Liu, R., Xu, Y. and Liu, J. (2011) The dominating role of N-deacetylase/N-sulfotransferase 1 in forming domain structures in heparan sulfate. J Biol Chem. **286**, 19768-19776

13. de Paz, J. L., Noti, C. and Seeberger, P. H. (2006) Microarrays of synthetic heparin oligosaccharides. J Am Chem Soc. **128**, 2766-2767

14. Forsberg, E., Pejler, G., Ringvall, M., Lunderius, C., Tomasini-Johansson, B., Kusche-Gullberg, M., Eriksson, I., Ledin, J., Hellman, L. and Kjellen, L. (1999) Abnormal mast cells in mice deficient in a heparin-synthesizing enzyme. Nature. **400**, 773-776

15. Aikawa, J., Grobe, K., Tsujimoto, M. and Esko, J. D. (2001) Multiple isozymes of heparan sulfate/heparin GlcNAc N-deacetylase/GlcN N-sulfotransferase. Structure and activity of the fourth member, NDST4. J Biol Chem. **276**, 5876-5882

16. Hagner-McWhirter, A., Hannesson, H. H., Campbell, P., Westley, J., Roden, L., Lindahl, U. and Li, J. P. (2000) Biosynthesis of heparin/heparan sulfate: kinetic studies of the glucuronyl C5-epimerase with N-sulfated derivatives of the Escherichia coli K5 capsular polysaccharide as substrates. Glycobiology. **10**, 159-171

17. Sheng, J., Xu, Y., Dulaney, S. B., Huang, X. and Liu, J. (2012) Uncovering biphasic catalytic mode of C5-epimerase in heparan sulfate biosynthesis. J Biol Chem. **287**, 20996-21002

18. Rong, J., Habuchi, H., Kimata, K., Lindahl, U. and Kusche-Gullberg, M. (2001) Substrate specificity of the heparan sulfate hexuronic acid 2-O-sulfotransferase. Biochemistry. **40**, 5548-5555

19. Bethea, H. N., Xu, D., Liu, J. and Pedersen, L. C. (2008) Redirecting the substrate specificity of heparan sulfate 2-O-sulfotransferase by structurally guided mutagenesis. Proc Natl Acad Sci U S A. **105**, 18724-18729

20. Smeds, E., Habuchi, H., Do, A. T., Hjertson, E., Grundberg, H., Kimata, K., Lindahl, U. and Kusche-Gullberg, M. (2003) Substrate specificities of mouse heparan sulphate glucosaminyl 6-O-sulphotransferases. Biochem J. **372**, 371-380

21. Liu, R. and Liu, J. (2011) Enzymatic placement of 6-O-sulfo groups in heparan sulfate. Biochemistry. **50**, 4382-4391

22. Jemth, P., Smeds, E., Do, A. T., Habuchi, H., Kimata, K., Lindahl, U. and Kusche-Gullberg, M. (2003) Oligosaccharide library-based assessment of heparan sulfate 6-O-sulfotransferase substrate specificity. J Biol Chem. **278**, 24371-24376

23. Esko, J. D. and Lindahl, U. (2001) Molecular diversity of heparan sulfate. J Clin Invest. **108**, 169-173

24. Shukla, D., Liu, J., Blaiklock, P., Shworak, N. W., Bai, X., Esko, J. D., Cohen, G. H., Eisenberg, R. J., Rosenberg, R. D. and Spear, P. G. (1999) A novel role for 3-O-sulfated heparan sulfate in herpes simplex virus 1 entry. Cell. **99**, 13-22

25. Pempe, E. H., Xu, Y., Gopalakrishnan, S., Liu, J. and Harris, E. N. (2012) Probing structural selectivity of synthetic heparin binding to Stabilin protein receptors. J Biol Chem. **287**, 20774-20783

26. Nader, H. B., Chavante, S. F., dos-Santos, E. A., Oliveira, T. W., de-Paiva, J. F., Jeronimo, S. M., Medeiros, G. F., de-Abreu, L. R., Leite, E. L., de-Sousa-Filho, J. F., Castro, R. A., Toma, L., Tersariol, I. L., Porcionatto, M. A. and Dietrich, C. P. (1999) Heparan sulfates and heparins: similar compounds performing the same functions in vertebrates and invertebrates? Braz J Med Biol Res. **32**, 529-538

27. Gomes, P. B. and Dietrich, C. P. (1982) Distribution of heparin and other sulfated glycosaminoglycans in vertebrates. Comp Biochem Physiol B. **73**, 857-863

28. Sarras, M. P., Jr., Madden, M. E., Zhang, X. M., Gunwar, S., Huff, J. K. and Hudson, B. G. (1991) Extracellular matrix (mesoglea) of Hydra vulgaris. I. Isolation and characterization. Dev Biol. **148**, 481-494

29. Selleck, S. B. (2001) Genetic dissection of proteoglycan function in Drosophila and C. elegans. Semin Cell Dev Biol. **12**, 127-134

30. Kakuta, Y., Sueyoshi, T., Negishi, M. and Pedersen, L. C. (1999) Crystal structure of the sulfotransferase domain of human heparan sulfate N-deacetylase/ N-sulfotransferase 1. J Biol Chem. **274**, 10673-10676

31. Duncan, M. B., Liu, M., Fox, C. and Liu, J. (2006) Characterization of the N-deacetylase domain from the heparan sulfate N-deacetylase/N-sulfotransferase 2. Biochem Biophys Res Commun. **339**, 1232-1237

32. Kuberan, B., Lech, M. Z., Beeler, D. L., Wu, Z. L. and Rosenberg, R. D. (2003) Enzymatic synthesis of antithrombin III-binding heparan sulfate pentasaccharide. Nat Biotechnol. **21**, 1343-1346

33. Zhou, X., Chandarajoti, K., Pham, T. Q., Liu, R. and Liu, J. (2011) Expression of heparan sulfate sulfotransferases in Kluyveromyces lactis and preparation of 3'-phosphoadenosine-5'-phosphosulfate. Glycobiology. **21**, 771-780

34. Munoz, E., Xu, D., Avci, F., Kemp, M., Liu, J. and Linhardt, R. J. (2006) Enzymatic synthesis of heparin related polysaccharides on sensor chips: rapid screening of heparin-protein interactions. Biochem Biophys Res Commun. **339**, 597-602

35. Kuberan, B., Beeler, D. L., Lech, M., Wu, Z. L. and Rosenberg, R. D. (2003) Chemoenzymatic synthesis of classical and non-classical anticoagulant heparan sulfate polysaccharides. J Biol Chem. **278**, 52613-52621

36. Chen, J., Avci, F. Y., Munoz, E. M., McDowell, L. M., Chen, M., Pedersen, L. C., Zhang, L., Linhardt, R. J. and Liu, J. (2005) Enzymatic redesigning of biologically active heparan sulfate. J Biol Chem. **280**, 42817-42825

37. Chen, J., Jones, C. L. and Liu, J. (2007) Using an enzymatic combinatorial approach to identify anticoagulant heparan sulfate structures. Chem Biol. **14**, 986-993

38. Edavettal, S. C., Lee, K. A., Negishi, M., Linhardt, R. J., Liu, J. and Pedersen, L. C. (2004) Crystal structure and mutational analysis of heparan sulfate 3-O-sulfotransferase isoform 1. J Biol Chem. **279**, 25789-25797

39. Myette, J. R., Shriver, Z., Liu, J., Venkataraman, G., Rosenberg, R. and Sasisekharan, R. (2002) Expression in Escherichia coli, purification and kinetic characterization of human heparan sulfate 3-O-sulfotransferase-1. Biochem Biophys Res Commun. **290**, 1206-1213

40. Mochizuki, H., Yoshida, K., Shibata, Y. and Kimata, K. (2008) Tetrasulfated disaccharide unit in heparan sulfate: enzymatic formation and tissue distribution. J Biol Chem. **283**, 31237-31245

41. Moon, A. F., Edavettal, S. C., Krahn, J. M., Munoz, E. M., Negishi, M., Linhardt, R. J., Liu, J. and Pedersen, L. C. (2004) Structural analysis of the sulfotransferase (3-o-sulfotransferase isoform 3) involved in the biosynthesis of an entry receptor for herpes simplex virus 1. J Biol Chem. **279**, 45185-45193

42. Liu, J., Shriver, Z., Blaiklock, P., Yoshida, K., Sasisekharan, R. and Rosenberg, R. D. (1999) Heparan sulfate D-glucosaminyl 3-O-sulfotransferase-3A sulfates N-unsubstituted glucosamine residues. J Biol Chem. **274**, 38155-38162

43. Xu, D., Moon, A. F., Song, D., Pedersen, L. C. and Liu, J. (2008) Engineering sulfotransferases to modify heparan sulfate. Nat Chem Biol. **4**, 200-202

44. Chen, J., Duncan, M. B., Carrick, K., Pope, R. M. and Liu, J. (2003) Biosynthesis of 3-O-sulfated heparan sulfate: unique substrate specificity of heparan sulfate 3-O-sulfotransferase isoform 5. Glycobiology. **13**, 785-794

45. Dietrich, C. P., Tersariol, I. L., Toma, L., Moraes, C. T., Porcionatto, M. A., Oliveira, F. W. and Nader, H. B. (1998) Structure of heparan sulfate: identification of variable and constant oligosaccharide domains in eight heparan sulfates of different origins. Cell Mol Biol (Noisy-le-grand). **44**, 417-429

46. Medeiros, G. F., Mendes, A., Castro, R. A., Bau, E. C., Nader, H. B. and Dietrich, C. P. (2000) Distribution of sulfated glycosaminoglycans in the animal kingdom: widespread occurrence of heparin-like compounds in invertebrates. Biochim Biophys Acta. **1475**, 287-294

47. Cassaro, C. M. and Dietrich, C. P. (1977) Distribution of sulfated mucopolysaccharides in invertebrates. J Biol Chem. **252**, 2254-2261

48. Rahemtulla, F. and Lovtrup, S. (1976) The comparative biochemistry of invertebrate mucopolysaccharides-VI. Crustacea. Comp Biochem Physiol B. **53**, 15-18

49. Bianchini, P., Osima, B., Parma, B., Dietrich, C. P., Takahashi, H. K. and Nader, H. B. (1985) Structural studies and "in vivo" and "in vitro" pharmacological activities of heparin fractions and fragments prepared by chemical and enzymic depolimerization. Thromb Res. **40**, 49-58

50. Paiva, J. F., Santos, E. A., Jeske, W., Fareed, J., Nader, H. B. and Dietrich, C. P. (1995) A comparative study on the mechanism of the anticoagulant action of mollusc and mammalian heparins. Comp Biochem Physiol A Physiol. **111**, 495-499

51. Gomez-Outes, A., Suarez-Gea, M. L., Calvo-Rojas, G., Lecumberri, R., Rocha, E., Pozo-Hernandez, C., Terleira-Fernandez, A. I. and Vargas-Castrillon, E. (2012) Discovery of anticoagulant drugs: a historical perspective. Curr Drug Discov Technol. **9**, 83-104

52. Loke, C., Ali, S. S. and Johari, V. (2012) Pharmacology of anticoagulants. Dis Mon. **58**, 424-430

53. Hirsh, J., Fuster, V., Ansell, J. and Halperin, J. L. (2003) American Heart Association/American College of Cardiology Foundation guide to warfarin therapy. J Am Coll Cardiol. **41**, 1633-1652

54. Hedlund, K., Coyne, D., Sanford, D. and Huddelson, J. (2013) The heparin recall of 2008. Perfusion. **28**, 61-65

55. Mousa, S. A. (2010) Novel anticoagulant therapy: principle and practice. Methods Mol Biol. **663**, 157-179

56. Herbert, J. M., Herault, J. P., Bernat, A., van Amsterdam, R. G., Lormeau, J. C., Petitou, M., van Boeckel, C., Hoffmann, P. and Meuleman, D. G. (1998) Biochemical and pharmacological properties of SANORG 34006, a potent and long-acting synthetic pentasaccharide. Blood. **91**, 4197-4205

57. Buller, H. R., Cohen, A. T., Davidson, B., Decousus, H., Gallus, A. S., Gent, M., Pillion, G., Piovella, F., Prins, M. H. and Raskob, G. E. (2007) Idraparinux versus standard therapy for venous thromboembolic disease. N Engl J Med. **357**, 1094-1104

58. Buller, H. R., Cohen, A. T., Davidson, B., Decousus, H., Gallus, A. S., Gent, M., Pillion, G., Piovella, F., Prins, M. H. and Raskob, G. E. (2007) Extended prophylaxis of venous thromboembolism with idraparinux. N Engl J Med. **357**, 1105-1112

59. Eriksson, B. I., Dahl, O. E., Rosencher, N., Kurth, A. A., van Dijk, C. N., Frostick, S. P., Prins, M. H., Hettiarachchi, R., Hantel, S., Schnee, J. and Buller, H. R. (2007) Dabigatran etexilate versus enoxaparin for prevention of venous thromboembolism after total hip replacement: a randomised, double-blind, non-inferiority trial. Lancet. **370**, 949-956

60. Jacobson, B. C., Ferris, T. G., Shea, T. L., Mahlis, E. M., Lee, T. H. and Wang, T. C. (2003) Who is using chronic acid suppression therapy and why? Am J Gastroenterol. **98**, 51-58

61. Hiebert, L. M. (2002) Oral heparins. Clin Lab. **48**, 111-116

62. Paliwal, R., Paliwal, S. R., Agrawal, G. P. and Vyas, S. P. (2012) Recent advances in search of oral heparin therapeutics. Med Res Rev. **32**, 388-409

63. Rivera, T. M., Leone-Bay, A., Paton, D. R., Leipold, H. R. and Baughman, R. A. (1997) Oral delivery of heparin in combination with sodium N-[8-(2-hydroxybenzoyl)amino]caprylate: pharmacological considerations. Pharm Res. **14**, 1830-1834

64. Hoffart, V., Lamprecht, A., Maincent, P., Lecompte, T., Vigneron, C. and Ubrich, N. (2006) Oral bioavailability of a low molecular weight heparin using a polymeric delivery system. J Control Release. **113**, 38-42

65. Kim, S. K., Lee, E. H., Vaishali, B., Lee, S., Lee, Y. K., Kim, C. Y., Moon, H. T. and Byun, Y. (2005) Tricaprylin microemulsion for oral delivery of low molecular weight heparin conjugates. J Control Release. **105**, 32-42

66. Chandy, T., Rao, G. H., Wilson, R. F. and Das, G. S. (2002) Delivery of LMW heparin via surface coated chitosan/peg-alginate microspheres prevents thrombosis. Drug Deliv. **9**, 87-96

67. Bara, L., Billaud, E., Gramond, G., Kher, A. and Samama, M. (1985) Comparative pharmacokinetics of a low molecular weight heparin (PK 10 169) and unfractionated heparin after intravenous and subcutaneous administration. Thromb Res. **39**, 631-636

68. Dawes, J., Bara, L., Billaud, E. and Samama, M. (1986) Relationship between biological activity and concentration of a low-molecular-weight heparin (PK 10169) and unfractionated heparin after intravenous and subcutaneous administration. Haemostasis. **16**, 116-122

69. Petitou, M., Herault, J. P., Bernat, A., Driguez, P. A., Duchaussoy, P., Lormeau, J. C. and Herbert, J. M. (1999) Synthesis of thrombin-inhibiting heparin mimetics without side effects. Nature. **398**, 417-422

70. Levine, M. N. and Hirsh, J. (1986) Hemorrhagic complications of anticoagulant therapy. Semin Thromb Hemost. **12**, 39-57

71. Hirsh, J. (1991) Heparin. N Engl J Med. **324**, 1565-1574

72. Bick, R. L. and Frenkel, E. P. (1999) Clinical aspects of heparin-induced thrombocytopenia and thrombosis and other side effects of heparin therapy. Clin Appl Thromb Hemost. **5 Suppl 1**, S7-15

73. Warkentin, T. E. and Greinacher, A. (2009) Heparin-induced anaphylactic and anaphylactoid reactions: two distinct but overlapping syndromes. Expert Opin Drug Saf. **8**, 129-144

74. Mannucci, P. M. and Levi, M. (2007) Prevention and treatment of major blood loss. N Engl J Med. **356**, 2301-2311

75. Hartman, S. K. and Teruya, J. (2012) Practice guidelines for reversal of new and old anticoagulants. Dis Mon. **58**, 448-461

76. Levi, M., Eerenberg, E. and Kamphuisen, P. W. (2011) Bleeding risk and reversal strategies for old and new anticoagulants and antiplatelet agents. J Thromb Haemost. **9**, 1705-1712

77. Simpson, E., Lin, Y., Stanworth, S., Birchall, J., Doree, C. and Hyde, C. (2012) Recombinant factor VIIa for the prevention and treatment of bleeding in patients without haemophilia. Cochrane Database Syst Rev. **3**, CD005011

78. Yukizawa, Y., Inaba, Y., Watanabe, S., Yajima, S., Kobayashi, N., Ishida, T., Iwamoto, N., Hyonmin, C., Nakamura, M. and Saito, T. (2012) Plasma accumulation of fondaparinux 2.5 mg in patients after total hip arthroplasty. J Thromb Thrombolysis. **34**, 526-532

79. Grand'Maison, A., Charest, A. F. and Geerts, W. H. (2005) Anticoagulant use in patients with chronic renal impairment. Am J Cardiovasc Drugs. **5**, 291-305

80. Chappell, E. P. and Liu, J. (2012) Use of biosynthetic enzymes in heparin and heparan sulfate synthesis. Bioorg Med Chem

81. Harris, E. N., Weigel, J. A. and Weigel, P. H. (2008) The human hyaluronan receptor for endocytosis (HARE/Stabilin-2) is a systemic clearance receptor for heparin. J Biol Chem. **283**, 17341-17350

82. Liu, R., Xu, Y., Chen, M., Weïwer, M., Zhou, X., Bridges, A. S., DeAngelis, P. L., Zhang, Q., Linhardt, R. J. and Liu, J. (2010) Chemoenzymatic design of heparan sulfate oligosaccharides. J Biol Chem. **285**, 34240-34249

83. Vann, W. F., Schmidt, M. A., Jann, B. and Jann, K. (1981) The structure of the capsular polysaccharide (K5 antigen) of urinary-tract-infective Escherichia coli 010:K5:H4. A polymer similar to desulfo-heparin. Eur J Biochem. **116**, 359-364

84. Mikhailov, D., Young, H. C., Linhardt, R. J. and Mayo, K. H. (1999) Heparin dodecasaccharide binding to platelet factor-4 and growth-related protein-alpha. Induction of a partially folded state and implications for heparin-induced thrombocytopenia. J Biol Chem. **274**, 25317-25329

85. Lee, M. K. and Lander, A. D. (1991) Analysis of affinity and structural selectivity in the binding of proteins to glycosaminoglycans: development of a sensitive electrophoretic approach. Proc Natl Acad Sci U S A. **88**, 2768-2772

86. Zhao, G., Guan, W., Cai, L. and Wang, P. G. (2010) Enzymatic route to preparative-scale synthesis of UDP-GlcNAc/GalNAc, their analogues and GDP-fucose. Nat. Protoc. **5**, 636-646

87. Zhang, L., Beeler, D. L., Lawrence, R., Lech, M., Liu, J., Davis, J. C., Shriver, Z., Sasisekharan, R. and Rosenberg, R. D. (2001) 6-O-sulfotransferase-1 represents a critical enzyme in the anticoagulant heparan sulfate biosynthetic pathway. J. Biol. Chem. **276**, 42311-42321

88. Duncan, M. B., Chen, J., Krise, J. P. and Liu, J. (2004) The biosynthesis of anticoagulant heparan sulphate by the heparan sulphate 3-O-sulphotransferase isoform 5. Biochim Biophys Acta. **1671**, 34-43

89. Shively, J. E. and Conrad, H. E. (1976) Formation of anhydrosugars in the chemical depolymerization of heparin. Biochemistry. **15**, 3932-3942

90. Harris, E. N. and Weigel, P. H. (2008) The ligand-binding profile of HARE: hyaluronan and chondroitin sulfates A, C, and D bind to overlapping sites distinct from the sites for heparin, acetylated low-density lipoprotein, dermatan sulfate, and CS-E. Glycobiology. **18**, 638-648

91. Chen, J., Jones, C. L. and Liu, J. (2007) Using an enzymatic combinatorial approach to identify anticoagulant heparan sulfate structures. Chem Biol. **14**, 986-993

92. Xu, Y., Masuko, S., Takieddin, M., Xu, H., Liu, R., Jing, J., Mousa, S. A., Linhardt , R. J. and Liu, J. (2011) Chemoenzymatic synthesis of homogeneous ultra-low molecular weight heparin. Science. **334**, 498-501

93. Xia, G., Chen, J., Tiwari, V., Ju, W., Li, J.-P., Malmström, A., Shukla, D. and Liu, J. (2002) Heparan sulfate 3-O-sulfotransferase isoform 5 generates both an antithrombin-binding site and an entry receptor for herpes simplex virus, type 1. J. Biol. Chem. **277**, 37912-37919

94. Zhou, X., Chandarajoti, K., Pham, T. Q., Liu, R. and Liu, J. (2011) Expression of heparan sulfate sulfotransferases in Kluyveromyces lactis and preparation of PAPS Glycobiology. **21**, 771-780

95. Harris, E. N., Weigel, J. A. and Weigel, P. H. (2004) Endocytic function, glycosaminoglycan specificity, and antibody sensitivity of the recombinant human 190-kDa hyaluronan receptor for endocytosis (HARE). J. Biol. Chem. **279**, 36201-36209

96. Harris, E. N., Kyosseva, S. V., Weigel, J. A. and Weigel, P. H. (2007) Expression, processing, and glycosaminoglycan binding activity of the recombinant human 315-kDa hyaluronic acid receptor for endocytosis (HARE). J. Biol. Chem. **282**, 2785-2797

97. Jaax, M. E. and Greinacher, A. (2012) Management of heparin-induced thrombocytopenia. Expert Opin Pharmacother. **13**, 987-1006

98. Greinacher, A., Amiral, J., Dummel, V., Vissac, A., Kiefel, V. and Mueller-Eckhardt, C. (1994) Laboratory diagnosis of heparin-associated thrombocytopenia and comparison of platelet aggregation test, heparin-induced platelet activation test, and platelet factor 4/heparin enzyme-linked immunosorbent assay. Transfusion. **34**, 381-385

99. Zucker, M. B. and Katz, I. R. (1991) Platelet factor 4: production, structure, and physiologic and immunologic action. Proc Soc Exp Biol Med. **198**, 693-702

100. Dhoot, G. K., Gustafsson, M. K., Ai, X., Sun, W., Standiford, D. M. and Emerson, C. P., Jr. (2001) Regulation of Wnt signaling and embryo patterning by an extracellular sulfatase. Science. **293**, 1663-1666

101. Morimoto-Tomita, M., Uchimura, K., Werb, Z., Hemmerich, S. and Rosen, S. D. (2002) Cloning and characterization of two extracellular heparin-degrading endosulfatases in mice and humans. J Biol Chem. **277**, 49175-49185

102. Ai, X., Do, A. T., Kusche-Gullberg, M., Lindahl, U., Lu, K. and Emerson, C. P., Jr. (2006) Substrate specificity and domain functions of extracellular heparan sulfate 6-O-endosulfatases, QSulf1 and QSulf2. J Biol Chem. **281**, 4969-4976

103. Nagamine, S., Koike, S., Keino-Masu, K. and Masu, M. (2005) Expression of a heparan sulfate remodeling enzyme, heparan sulfate 6-O-endosulfatase sulfatase FP2, in the rat nervous system. Brain Res Dev Brain Res. **159**, 135-143

104. Ohto, T., Uchida, H., Yamazaki, H., Keino-Masu, K., Matsui, A. and Masu, M. (2002) Identification of a novel nonlysosomal sulphatase expressed in the floor plate, choroid plexus and cartilage. Genes Cells. **7**, 173-185

105. Ai, X., Do, A. T., Lozynska, O., Kusche-Gullberg, M., Lindahl, U. and Emerson, C. P., Jr. (2003) QSulf1 remodels the 6-O sulfation states of cell surface heparan sulfate proteoglycans to promote Wnt signaling. J Cell Biol. **162**, 341-351

106. Tang, R. and Rosen, S. D. (2009) Functional consequences of the subdomain organization of the sulfs. J Biol Chem. **284**, 21505-21514

107. Viviano, B. L., Paine-Saunders, S., Gasiunas, N., Gallagher, J. and Saunders, S. (2004) Domain-specific modification of heparan sulfate by Qsulf1 modulates the binding of the bone morphogenetic protein antagonist Noggin. J Biol Chem. **279**, 5604-5611

108. Ai, X., Kitazawa, T., Do, A. T., Kusche-Gullberg, M., Labosky, P. A. and Emerson, C. P., Jr. (2007) SULF1 and SULF2 regulate heparan sulfate-mediated GDNF signaling for esophageal innervation. Development. **134**, 3327-3338

109. Lamanna, W. C., Frese, M. A., Balleininger, M. and Dierks, T. (2008) Sulf loss influences N-, 2-O-, and 6-O-sulfation of multiple heparan sulfate proteoglycans and modulates fibroblast growth factor signaling. J Biol Chem. **283**, 27724-27735

110. Dai, Y., Yang, Y., MacLeod, V., Yue, X., Rapraeger, A. C., Shriver, Z., Venkataraman, G., Sasisekharan, R. and Sanderson, R. D. (2005) HSulf-1 and HSulf-2 are potent inhibitors of myeloma tumor growth in vivo. J Biol Chem. **280**, 40066-40073

111. Yue, X., Li, X., Nguyen, H. T., Chin, D. R., Sullivan, D. E. and Lasky, J. A. (2008) Transforming growth factor-beta1 induces heparan sulfate 6-O-endosulfatase 1 expression in vitro and in vivo. J Biol Chem. **283**, 20397-20407

112. Holst, C. R., Bou-Reslan, H., Gore, B. B., Wong, K., Grant, D., Chalasani, S., Carano, R. A., Frantz, G. D., Tessier-Lavigne, M., Bolon, B., French, D. M. and Ashkenazi, A. (2007) Secreted sulfatases Sulf1 and Sulf2 have overlapping yet essential roles in mouse neonatal survival. PLoS One. **2**, e575

113. Lum, D. H., Tan, J., Rosen, S. D. and Werb, Z. (2007) Gene trap disruption of the mouse heparan sulfate 6-O-endosulfatase gene, Sulf2. Mol Cell Biol. **27**, 678-688

114. Ratzka, A., Kalus, I., Moser, M., Dierks, T., Mundlos, S. and Vortkamp, A. (2008) Redundant function of the heparan sulfate 6-O-endosulfatases Sulf1 and Sulf2 during skeletal development. Dev Dyn. **237**, 339-353

115. Lai, J. P., Sandhu, D. S., Yu, C., Han, T., Moser, C. D., Jackson, K. K., Guerrero, R. B., Aderca, I., Isomoto, H., Garrity-Park, M. M., Zou, H., Shire, A. M., Nagorney, D. M., Sanderson, S. O., Adjei, A. A., Lee, J. S., Thorgeirsson, S. S. and Roberts, L. R. (2008) Sulfatase 2 up-regulates glypican 3, promotes fibroblast growth factor signaling, and decreases survival in hepatocellular carcinoma. Hepatology. **47**, 1211-1222

116. Morimoto-Tomita, M., Uchimura, K., Bistrup, A., Lum, D. H., Egeblad, M., Boudreau, N., Werb, Z. and Rosen, S. D. (2005) Sulf-2, a proangiogenic heparan sulfate endosulfatase, is upregulated in breast cancer. Neoplasia. **7**, 1001-1010

117. Nawroth, R., van Zante, A., Cervantes, S., McManus, M., Hebrok, M. and Rosen, S. D. (2007) Extracellular sulfatases, elements of the Wnt signaling pathway, positively regulate growth and tumorigenicity of human pancreatic cancer cells. PLoS One. **2**, e392

118. Lai, J. P., Chien, J. R., Moser, D. R., Staub, J. K., Aderca, I., Montoya, D. P., Matthews, T. A., Nagorney, D. M., Cunningham, J. M., Smith, D. I., Greene, E. L., Shridhar, V. and Roberts, L. R. (2004) hSulf1 Sulfatase promotes apoptosis of hepatocellular cancer cells by decreasing heparin-binding growth factor signaling. Gastroenterology. **126**, 231-248

119. Lai, J., Chien, J., Staub, J., Avula, R., Greene, E. L., Matthews, T. A., Smith, D. I., Kaufmann, S. H., Roberts, L. R. and Shridhar, V. (2003) Loss of HSulf-1 up-regulates heparin-binding growth factor signaling in cancer. J Biol Chem. **278**, 23107-23117

120. Lemjabbar-Alaoui, H., van Zante, A., Singer, M. S., Xue, Q., Wang, Y. Q., Tsay, D., He, B., Jablons, D. M. and Rosen, S. D. (2010) Sulf-2, a heparan sulfate endosulfatase, promotes human lung carcinogenesis. Oncogene. **29**, 635-646

121. Rosen, S. D. and Lemjabbar-Alaoui, H. (2010) Sulf-2: an extracellular modulator of cell signaling and a cancer target candidate. Expert Opin Ther Targets. **14**, 935-949

122. Phillips, J. J., Huillard, E., Robinson, A. E., Ward, A., Lum, D. H., Polley, M. Y., Rosen, S. D., Rowitch, D. H. and Werb, Z. (2012) Heparan sulfate sulfatase SULF2 regulates PDGFRalpha signaling and growth in human and mouse malignant glioma. J Clin Invest. **122**, 911-922

123. Saad, O. M., Ebel, H., Uchimura, K., Rosen, S. D., Bertozzi, C. R. and Leary, J. A. (2005) Compositional profiling of heparin/heparan sulfate using mass spectrometry: assay for specificity of a novel extracellular human endosulfatase. Glycobiology. **15**, 818-826

124. Javot, L., Sapin, A., Scala-Bertola, J., Vigneron, C., Lecompte, T. and Maincent, P. (2010) Oral administration of a microencapsulated low-molecular-weight heparin to rabbits: anti-Xa and anti-IIa profiles. Thromb Haemost. **103**, 1254-1267

125. Peterson, S. B. and Liu, J. (2010) Unraveling the specificity of heparanase utilizing synthetic substrates. J Biol Chem. **285**, 14504-14513

126. Liu, J., Shworak, N. W., Fritze, L. M. S., Edelberg, J. M. and Rosenberg, R. D. (1996) Purification of heparan sulfate D-glucosaminyl 3-*O*-sulfotransferase. J. Biol. Chem. **271**, 27072-27082

127. Colliec-Jouault, S., Shworak, N. W., Liu, J., De Agostini, A. I. and Rosenberg, R. D. (1994) Characterization of a cell mutant specifically defective in the synthesis of anticoagulantly active heparan sulfate. J. Biol. Chem. **271**, 24953-24958

128. Xu, Y., Pempe, E. H. and Liu, J. (2012) Chemoenzymatic Synthesis of Heparin Oligosaccharides with both Anti-factor Xa and Anti-factor IIa Activities. J Biol Chem. **287**, 29054-29061

129. Lane, D. A., Denton, J., Flynn, A. M., Thunberg, L. and Lindahl, U. (1984) Anticoagulant activities of heparin oligosaccharides and their neutralization by platelet factor 4. Biochem J. **218**, 725-732

130. Maccarana, M. and Lindahl, U. (1993) Mode of interaction between platelet factor 4 and heparin. Glycobiology. **3**, 271-277

131. Spinler, S. A. (2006) New concepts in heparin-induced thrombocytopenia: diagnosis and management. J Thromb Thrombolysis. **21**, 17-21

132. Corbett, T. L., Elher, K. S. and Garwood, C. L. (2010) Successful use of fondaparinux in a patient with a mechanical heart valve replacement and a history of heparin-induced thrombocytopenia. J Thromb Thrombolysis. **30**, 375-377

133. Atha, D. H., Lormeau, J. C., Petitou, M., Rosenberg, R. D. and Choay, J. (1985) Contribution of monosaccharide residues in heparin binding to antithrombin III. Biochemistry. **24**, 6723-6729

134. Zhang, L., Beeler, D. L., Lawrence, R., Lech, M., Liu, J., Davis, J. C., Shriver, Z., Sasisekharan, R. and Rosenberg, R. D. (2001) 6-O-sulfotransferase-1 represents a critical enzyme in the anticoagulant heparan sulfate biosynthetic pathway. J Biol Chem. **276**, 42311-42321

135. Barzu, T., Molho, P., Tobelem, G., Petitou, M. and Caen, J. (1985) Binding and endocytosis of heparin by human endothelial cells in culture. Biochim Biophys Acta. **845**, 196-203

136. Trindade, E. S., Boucas, R. I., Rocha, H. A., Dominato, J. A., Paredes-Gamero, E. J., Franco, C. R., Oliver, C., Jamur, M. C., Dietrich, C. P. and Nader, H. B. (2008) Internalization and degradation of heparin is not required for stimulus of heparan sulfate proteoglycan synthesis. J Cell Physiol. **217**, 360-366

137. Oie, C. I., Olsen, R., Smedsrod, B. and Hansen, J. B. (2008) Liver sinusoidal endothelial cells are the principal site for elimination of unfractionated heparin from the circulation. Am J Physiol Gastrointest Liver Physiol. **294**, G520-528

138. Hirsh, J., O'Donnell, M. and Eikelboom, J. W. (2007) Beyond unfractionated heparin and warfarin: current and future advances. Circulation. **116**, 552-560

139. Goerdt, S., Bhardwaj, R. and Sorg, C. (1993) Inducible expression of MS-1 high-molecular-weight protein by endothelial cells of continuous origin and by dendritic cells/macrophages in vivo and in vitro. Am J Pathol. **142**, 1409-1422

140. Kzhyshkowska, J., Gratchev, A. and Goerdt, S. (2006) Stabilin-1, a homeostatic scavenger receptor with multiple functions. J Cell Mol Med. **10**, 635-649

141. Tohu, M., Iqbal, O., Hoppensteadt, D., Neville, B., Messmore, H. L. and Fareed, J. (2004) Anti-Xa and anti-IIa drugs after international normalized ratio measurements: Potential problems in the monitoring of oral anticoagulants. Clin Appl Thrombos Hemostas. **10**, 301-309

142. Weitz, J. I. (2010) Potential of new anticoagulants in patients with cancer. Thromb. Res. **125 (Suppl 2)**, S30-S35

143. Atha, D. H., Lormeau, J.-C., Petitou, M., Rosenberg, R. D. and Choay, J. (1985) Contribution of monosaccharide residues in heparin binding to antithrombin III. Biochemistry. **24**, 6723-6729

144. Rosenberg, R. D., Showrak, N. W., Liu, J., Schwartz, J. J. and Zhang, L. (1997) Heparan sulfate proteoglycans of the cardiovascular system: specific structures emerge but how is synthesis regulated? J. Clin. Invest. **99**, 2062-2070

145. Moon, A. F., Xu, Y., Woody, S., Krahn, J. M., Linhardt , R. J., Liu, J. and Pedersen, L. C. (2012) Dissecting substrate recognition mode of heparan sulfate 3-O-sulfotransferases for the biosynthesis of anticoagulant heparin. Proc. Natl. Acad. Sci. USA, in press

146. Kzhyshkowska, J., Gratchev, A. and Goerdt, S. (2006) Stabilin-1, a homeostatic scavenger receptor with multiple functions. J. Cell Mol. Med. **10**, 635-649

147. Falkowski, M., Schledzewski, K., Hansen, B. and Goerdt, S. (2003) Expression of stabilin-2, a novel fasciclin-like hyaluronan receptor protein, in murine sinusoidal endothelia, avascular tissues, and at solid/liquid interfaces. Histochem. Cell Biol. **120**, 361-369

148. Zhou, B., Weigel, J. A., Fauss, L. and Weigel, P. H. (2000) Identification of the Hyaluronan Receptor for Endocytosis (HARE). J. Biol. Chem. **275**, 37733-37741

149. Prevo, R., Banerji, S., Ni, J. and Jackson, D. G. (2004) Rapid plasma membrane-endosomal trafficking of the lymph node sinus and high endothelial venule scavenger receptor/homing receptor stabilin-1 (FEEL-1/CLEVER-1). J. Biol. Chem. **279**, 52580-52592

150. Wary, K. K., Thakker, G. D., Humtsoe, J. O. and Yang, J. (2003) Analysis of VEGF-responsive genes involved in the activation of endothelial cells. Mol. Cancer. **2**, 25

151. Harris, G. (2008) U.S. Identifies Tainted Heparin in 11 Countries. The New York Times.

152. Hirsh, J. and Raschke, R. (2004) Heparin and low-molecular-weight heparin: the Seventh ACCP Conference on Antithrombotic and Thrombolytic Therapy. Chest. **126**, 188S-203S

153. Garcia, D. A., Baglin, T. P., Weitz, J. I. and Samama, M. M. (2012) Parenteral anticoagulants: Antithrombotic Therapy and Prevention of Thrombosis, 9th ed: American College of Chest Physicians Evidence-Based Clinical Practice Guidelines. Chest. **141**, e24S-43S

154. Boneu, B. and de Moerloose, P. (2001) How and when to monitor a patient treated with low molecular weight heparin. Semin Thromb Hemost. **27**, 519-522

155. Samama, M. M. and Guinet, C. (2011) Laboratory assessment of new anticoagulants. Clin Chem Lab Med. **49**, 761-772

156. Mousa, S. A. (2010) In vivo models for the evaluation of antithrombotics and thrombolytics. Methods Mol Biol. **663**, 29-107

157. Vetter, A., Perera, G., Leithner, K., Klima, G. and Bernkop-Schnurch, A. (2010) Development and in vivo bioavailability study of an oral fondaparinux delivery system. Eur J Pharm Sci. **41**, 489-497

158. Herbert, J. M., Herault, J. P., Bernat, A., van Amsterdam, R. G., Vogel, G. M., Lormeau, J. C., Petitou, M. and Meuleman, D. G. (1996) Biochemical and pharmacological properties of SANORG 32701. Comparison with the "synthetic pentasaccharide' (SR 90107/ORG 31540) and standard heparin. Circ Res. **79**, 590-600

159. Herault, J. P., Bernat, A., Roye, F., Michaux, C., Schaeffer, P., Bono, F., Petitou, M. and Herbert, J. M. (2002) Pharmacokinetics of new synthetic heparin mimetics. Thromb Haemost. **87**, 985-989

160. Turnheim, K. (2003) When drug therapy gets old: pharmacokinetics and pharmacodynamics in the elderly. Exp Gerontol. **38**, 843-853